JPRS L/10530

19 May 1982

Translation

NONCONTACT METHODS OF MEASURING OCEANOGRAPHIC PARAMETERS

Ed. by

S.V. Viktorov

FBIS FOREIGN BROADCAST INFORMATION SERVICE

NOTE

JPRS publications contain information primarily from foreign newspapers, periodicals and books, but also from news agency transmissions and broadcasts. Materials from foreign-language sources are translated; those from English-language sources are transcribed or reprinted, with the original phrasing and other characteristics retained.

Headlines, editorial reports, and material enclosed in brackets [] are supplied by JPRS. Processing indicators such as [Text] or [Excerpt] in the first line of each item, or following the last line of a brief, indicate how the original information was processed. Where no processing indicator is given, the information was summarized or extracted.

Unfamiliar names rendered phonetically or transliterated are enclosed in parentheses. Words or names preceded by a question mark and enclosed in parentheses were not clear in the original but have been supplied as appropriate in context. Other unattributed parenthetical notes within the body of an item originate with the source. Times within items are as given by source.

The contents of this publication in no way represent the policies, views or attitudes of the U.S. Government.

APPROVED FOR RELEASE: 2007/02/09: CIA-RDP82-00850R000500060043-3

JPRS L/10530

19 May 1982

NONCONTACT METHODS OF MEASURING OCEANOGRAPHIC PARAMETERS

Moscow NEKONTAKTNYYE METODY IZMERENIYA OKEANOGRAFICHESKIKH PARAMETROV in Russian 1981 pp 1-119

[Annotation, foreword and selected passages from book "Noncontact Methods of Measuring Oceanographic Parameters," a collection of reports of the Third All-Union Seminar, Leningrad, 17-19 January 1978, edited by S. V. Viktorov, candidate of physical and mathematical sciences, Leningrad Division of the State Oceanographic Institute, Moscow Division of Gidrometeoizdat]

CONTENTS

FOR OFFICIAL USE ONLY

APPROVED FOR RELEASE: 2007/02/09: CIA-RDP82-00850R000500060043-3

UDC 551.46

NONCONTACT METHODS OF MEASURING OCEANOGRAPHIC PARAMETERS

Moscow NEKONTAKTNYYE METODY IZMERENIYA OKEANOGRAFICHESKIKH PARAMETROV in Russian 1981 pp 2-5

[Annotation and foreword from book "Noncontact Methods of Measuring Oceanographic Parameters," a collection of reports of the Third All-Union Seminar, Leningrad, 17-19 January 1978, edited by S. V. Viktorov, candidate of physical and mathematical sciences, Leningrad Division of the State Oceanographic Institute, Moscow Division of Gidrometeoizdat]

[Text] Annotation

A study is made of the results of theoretical and experimental research aimed at creating noncontact methods and means of measuring oceanographic parameters.

The problems of using instruments installed on board aircraft and spacecraft to measure the characteristics of sea waves, ice, the surface temperature of the sea and pollution of the sea surface with petroleum products are discussed in the greatest detail. The collection contains the following sections:

1. Active Microwave Methods.
2. Passive Microwave Methods.
3. Measurements in the Infrared Range.
4. Laser Methods.
5. Space and Aerial Surveying in the Optical Range.
6. Ultrasonic Methods.
7. Procedural Problems of Noncontact Measurements.

The collection is designed for a broad class of scientific workers and engineers studying the natural resources of the earth and the world ocean and also students in the advanced courses of the corresponding specialties.

Editor's Foreword

In the program document "Basic Areas of Development of the National Economy of the USSR in 1976-1980" adopted by the 25th CPSU Congress, along with other highly important goals, the goal has been set for Soviet science "to expand comprehensive studies of the world ocean." This far-reaching endeavor requires significant expenditures, the creation of special hardware, and the involvement of highly qualified specialists. The necessity for reinforcing and developing scientific research organizations engaged in ocean research and the study of the possibilities of efficient use of the resources of the sea is entirely obvious, for with every year the ocean is becoming to an ever greater degree a province of scientific and production activity, an arena for the application of the forces of many countries. The ocean is the "hydrocosmos"; the study of the ocean is a no less difficult matter than the study of outer space.

The classical methods of studying the world ocean by instruments carried by ships and buoys do not fully correspond to modern requirements, they do not provide a complete picture of processes occurring in the ocean. The growing practical requirements of science and the national economy require the application of qualitatively new measurement techniques which will provide regularly available information about the basic oceanographic parameters from the entire body of water making up the world ocean.

The possibility of a new approach to the solution of this problem can to a significant degree be supported by the use of noncontact methods of measuring oceanographic parameters with the help of instruments installed on spacecraft and aircraft.

In the above-mentioned document the goal was set "to expand research in the application of space hardware to study the earth's natural resources, in meteorology, oceanology, navigation, communications and for other needs of the national economy." Attaching great significance to the development of noncontact methods and the creation of modern measuring devices based on these methods, for a number of years the State Oceanographic Institute (GOIN) has promoted the coordination of various forms of activity of the numerous scientific research and design-development organizations and institutions of higher learning working in this field. One form of such coordination is the holding of all-union seminars on the problem of "noncontact measurements of oceanographic parameters."

The first seminar was held on 4-7 September 1973, in Sevastopol, and it was primarily devoted to noncontact methods of measuring the parameters of sea waves. The Second All-Union Seminar on "Noncontact Methods of Measuring Oceanographic Parameters," held on 18-20 November 1975, in Sevastopol, summed up the results of the work in this field by a number of scientific research and design organizations of the country in the ninth 5-year period.

The third all-union seminar, held on 17-19 January 1978 in Leningrad, was the largest and most representative gathering of specialists in noncontact oceanographic measurements. Opening the seminar, chairman of the Presidium of the

USSR Geographic Society, corresponding member of the USSR Academy of Sciences A. F. Treshnikov emphasized the urgency of the development and introduction of noncontact methods into oceanographic research practice, and he called on the participants in the seminar for "active discussion of reports, heated, but not malevolent creative discussion."

The work of the third all-union seminar was participated in by about 150 representatives of 62 institutions of the Main Administration of the Hydrometeorological Service, the USSR Academy of Sciences and union republics, the USSR and RSFSR ministries of the institutions of higher learning, the Ministry of the Fishing Industry and other ministries and departments of the country. About 60 original reports were heard and discussed during the seminar.

In order to improve the effectiveness of the third seminar, the following format was introduced in the practice of holding all-union seminars on noncontact methods of measuring oceanographic parameters. Along with plenary sessions, there were five parallel sections on basic research areas. Reports of the section chairmen were heard in the concluding plenary session. These reports discussed the course and results of the section discussions, they singled out the most interesting reports, they characterized the general state of the art and level of performed research. Thus, along with the possibility of entering into detailed discussions of his own basic topic in the section, each seminar participant was able to obtain a compactly formulated view of the state of the art of work in adjacent fields. A new format for holding an all-union seminar was greeted with interest by the participants, and it was approved.

In the seminar resolution adopted at the concluding plenary session on 19 January 1978, it was noted that during the time since holding the second all-union seminar, definite progress had been made in the development of noncontact methods and the creation of hardware for measuring oceanographic parameters based on them. Nevertheless, difficulties were also noted in connection with the organization and coordination of scientific research work, the production of new types of equipment, and the introduction of the results of theoretical and experimental work into practice. (Resolutions of the Third Seminar on "Noncontact Methods of Measuring Oceanographic Parameters" published for discussion in "Automation of Hydrometeorological Data Gathering and Processing," EKSPRESS-INFORMATSII VNIIGMI-MTsD, No 4 (58), 1978)

When compiling the present collection, it was recognized as expedient to group the reports presented for publication in the following areas:

1. Active Microwave Methods.
2. Passive Microwave Methods.
3. Measurements in the Infrared Range.
4. Laser Methods.
5. Space and Aerial Surveying in the Optical Range.

6. Ultrasonic Methods.

7. Procedural Problems of Noncontact Measurements.

It must be noted that regrets that in view of the limited size of the collection, a number of reports are only represented by annotations, and some of the reports are not reflected in the collection at all.

I consider it my duty in the name of all the seminar participants to express appreciation to the directors of the USSR Geographic Society for setting up conditions under which the plenary and section meetings were held.

In conclusion, I should like to note with gratitude the efforts of many co-workers of the Division of Space Oceanography and Aerial Techniques of the Leningrad Division of the GOIN with respect to the preparation for and holding of the seminar. I thank B. A. Pomytkin and M. D. Latkin, who participated directly in the preparation of this collection for publication.

10845
CSO: 8144/1010

ACTIVE MICROWAVE METHODS

UDC 551.501.81:502.55:665.2(260)

STUDY OF OIL SLICKS AT SEA BY SIDE-LOOKING RADAR

Moscow NEKONTAKTNYYE METODY IZMERENIYA OKEANOGRAFICHESKIKH PARAMETROV in Russian 1981 pp 6-8

[Report by K. I. Volyak, R. M. Glushkov, Yu. N. Yemel'yanov, V. B. Komarov, S. Ye. Kontorov, E. M. Mudrova, A. Ye. Popov and V. A. Starostin]

[Text] Annotation. Results are presented from studies of petroleum pollution of the sea over large areas using bipolarization side-looking radar. It is demonstrated that this type of radar is a highly efficient means of operational monitoring of pollution.

The primary goals of the study and monitoring of petroleum pollution of the sea surface are as follows: 1) determination of the pollution sources; 2) determination of the surface area covered by the petroleum; 3) estimation of the thickness of the petroleum layer; 4) indication of speed and direction of drift of the oil slick. Prospective means of remote sounding permitting comprehensive solution of these problems include side-looking radar (RLS BO). Using this type of radar installed on board an aircraft, it is possible in a comparatively short time to measure the distribution of the specific backscattering cross section over a quite significant area of the underlying surface. By comparison with optical methods of indicating pollution, side-looking radar has important advantages: it is possible to make the radar survey at night and through a cloud cover.

In the centimeter wavelength band, the primary mechanism of the backscattering of electromagnetic waves by the sea surface is the resonant Bragg effect, where the scatterer is the small-scale ripple with Bragg wavelength [1]:

$$\Lambda_B = \lambda_0/2 \sin \theta_0,$$

the wave vector of which is parallel to the plane of incidence (λ_0 is the incident radio wavelength, θ_0 is the angle of incidence reckoned from the vertical). For large angles $\theta_0 \geq 60$ to 70° where $\Lambda_B \approx \lambda_0/2$, reflection from large

gravity waves before breaking also becomes significant in the horizontal polarization [2].

The specific effective scattering cross section σ_0 is proportional to the spectral plane $S(\Lambda_B)$ of the Bragg component of the wave action. It is known [2] that the presence of a thin film on the surface of the water greatly increases the damping decrement of small-scale ripple, which leads to a significant decrease in the backscattering cross section σ_0. According to the data of [4], a film about 0.1 micron thick on a wavelength of λ_0 = 3 cm at large angles $\Theta_0 \sim 87°$ leads to a drop in the level of the received vertically polarized signal by more than 20 decibels by comparison with a smooth sea surface.

Remote observations of petroleum pollution were made in November 1976 in the Caspian Sea in an area of intense oil production (Neftyanyye Kamni) using an experimental model of a bipolarization centimeter-band side-looking radar installed on board an aircraft. A special electronic camera (EFRU) recorded the distribution of the scattering cross section σ_0 in a side-looking strip 15 km wide on photographic film. The near edge of the scanning strip lay 4 to 6 km from the flight path.

The short-wave suppression effect of the oil slick was observed clearly on both polarizations. However, the image contrast between the clean and polluted sections, as should be expected according to the calculation of [4] based on the Bragg scattering model, was significantly better in the vertical polarization, for the average signal level on the horizontal polarization in the given range of angle $\Theta_0 \approx 70$ to 86° is 20 to 30 decibels less than on vertical polarization. In addition, the contrast on horizontal polarization is worse as a result of the signal spikes connected with large breaking waves, inasmuch as large waves are much less subject to the damping effect of an oil slick.

The dynamics of an oil slick over a 24-hour period were easily traced as a function of meteorological conditions with the help of side-looking radar. Thus, according to the observations on 26 November, with a northeasterly wind at 5 to 8 m/sec, the leeward part of the continuous slick was seriously broken up in 1 hour, as a result of which the slick diminished by several times in size (only the southwestern part of it was left). During the next 4 hours the wind intensified to 12 m/sec without changing direction, and the solid slick in practice ceased to exist.

The dynamics of the development of oil slicks in the open sea were observed analogously. Radar images of fresh oil slicks in the Black Sea (in the vicinity of the port of Batumi) permit estimation of the rate of spread of the slick, its rate of drift under the effect of wind and also simultaneous detection of the source of the pollution.

The results of the performed research shows that by using side-looking radar installed on board an aircraft, sources of petroleum pollution are completely reliably detected, the area and outlines of the oil slick and also the dynamics of its development are determined. The determination of the thickness of the slick obviously requires the application of other procedures, for example,

combination of centimeter-band side-looking radar with a meter- or decimeter-band scatterometer or with passive instruments.

BIBLIOGRAPHY

1. Bass, F. G., and Fuchs, I. M., "Rasseyaniye voln na statisticheski nerovnoy poverkhnosti" [Wave Scattering on a Statistically Uneven Surface], Moscow, Nauka, 1972.

2. Long, M. W., IEEE TRANS., Ap-22, No 5, 1974, p 667.

3. Phillips, O. M., "Dinamika verkhnego sloya okeana" [Dynamics of the Upper Layer of the Ocean], Moscow, Mir, 1969.

4. Galayev, Yu. M., Kalmykov, A. I., Kurekin, A. S., et al., IZV. AN. SSSR, FIZIKA ATM. I OKEANA, Vol 13, No 4, 1977, p 406.

10845
CSO: 8144/1010

UDC 551.46:621.396.969

RADIO ALTIMETER STUDY OF SURFACE SEA WAVES

Moscow NEKONTAKTNYYE METODY IZMERENIYA OKEANOGRAFICHESKIKH PARAMETROV in Russian 1981 pp 9-12

[Report by A. Ye. Basharinov (deceased), A. I. Baskakov and A. A. Kalinkevich]

[Text] Annotation. It is demonstrated that by recording the average shape of an echo it is possible to evaluate the disturbed state of the sea surface. Calculations are presented for two types of sounding signals: a simple radio pulse and LFM pulse.

In the vertical sounding mode, the data on the degree of disturbance of the sea can be obtained from analysis of the average shape of a pulse reflected from the sea surface. Let us find the expression for the average shape of echo and let us investigate its dependence on the intensity of the disturbance and characteristics of the radar.

Let us use a phenomenological model of the sea surface [1], which is a set of independent elementary reflectors. The echo is a superposition of partial signals with respect to the irradiated region having random, independent and uniformly distributed phases in the 0 to 2π interval. Let the transmitting and receiving antennas of the radar be matched, and let the receiver consist of a filter matched with the sounding signal and an envelope detector. Then the signal at the filter exit

$$u(t) \sim \left| \sum_{n=1}^{N} \sqrt{\frac{2P_0^2 G_0^2 \sigma_n}{(4\pi)^3}} F(\theta_n, \varphi_n, t) \frac{\rho\left(t - \frac{2R_n}{c}\right)}{R_n^2(\theta_n, \varphi_n, t)} e^{i(\omega_0 + \omega_{dn})\left(t - \frac{2R_n}{c}\right)} \right|, \quad (1)$$

where σ_n is the effective reflection area of the elementary reflector oriented normal to the direction of incidence of the radio wave; θ_n, ϕ_n are the coordinates of the n-th reflector; $F(\theta_n, \phi_n, t)$ is the normalized coefficient de-defined by the antenna radiation pattern (DNA) and the surface backscattering pattern (DOR); $R_n(\theta_n, \phi_n, t)$ is the distance from the radar to the n-th reflector; $\rho(t)$ is the autocorrelation function of the sounding signal; ω_{dp} is the Doppler frequency shift. The dependence of the echo on the Doppler frequency and the dependence of $F(\theta, \phi, t)$, $R(\theta, \phi, t)$ on time can be neglected, for in practice the relation $VT_u \sin\theta < 0.25\lambda$ is always satisfied, where V is the radar velocity, T_u is the sounding pulse duration ($T_u \leq 10^{-7}$ sec).

Here let us consider that the 0.5 power radiation pattern width does not exceed $\theta_0 < 30°$, and its axis is oriented almost normal to the average surface level. The echo is characterized by its autocorrelation function

$$R(t_1, t_2) = Re\left\{P_1 \int_S \frac{F^2(\theta,\varphi)}{R^4(\theta,\varphi)} \int_{-\infty}^{\infty} W(\eta)\dot{p}(t_1 - T - \eta)\dot{p}^*(t_2 - T - \eta)\,d\eta\,dS \times e^{i\omega_0(t_1 - t_2)}\right\}, \quad (2)$$

where $P_1 = \frac{P_0 \lambda^2 G_0^2 K_0^2}{512\pi^3 a_\omega^2}$; $\eta = 2z/c$; $T = \tau_0 + 2r/cH$, $\tau_0 = \frac{2H}{c}$. The altitude (H) of the radar above the sea surface is appreciably greater than the zone irradiated on the surface (r). K_0 is the Fresnel coefficient, a_ω is the roughness parameter [1].

The averaging in (2) is realized by a set of random reflectors arranged along the Z-axis with probability density described by a normalized distribution law.

The radiation pattern is approximated by a Gaussian curve, and the expression for the DOR is taken from [1]. The angle of deflection of the radiation pattern axis from the normal to the average surface level will be denoted by θ_s; the axis of the radiation pattern is projected on the coordinate X-axis, and the angle ϕ is reckoned from the X-axis (the plane XOY is matched with the average level of the sea surface).

1. Let, for example, a short radio pulse with Gaussian envelope $v(t) = \exp(-g^2t^2)$ be emitted, where $g = \sqrt{\pi}/T_u$, T_u is the pulse duration at the 0.46 level. The expression for the average power characterizing the average shape of the pulse reflected from the sea surface will be obtained from (2), setting $t_1 = t_2$:

$$P(t) = \frac{P_0 \lambda^2 \theta_0^2 K_0^2 C T_u}{64\pi^2 H^3 a_\omega^2} \exp\left(-5{,}55\frac{\theta_s^2}{\theta_0^2} \cdot \frac{\beta^2\mu^2}{4} - bt\right)\left[\frac{1}{2} - \Phi\left(\frac{\beta\mu}{2} - \frac{t}{\mu}\right)\right], \quad (3)$$

where $b = \frac{c[5{,}55 a_\omega^2(1 - 5{,}55\theta_s^2/\theta_0^2) \cdot \Omega^2 + 1}{H\theta_0^2 a_\omega^2}$, $\mu = \sqrt{\frac{1}{\pi} \cdot 2\sigma^2}$ is a parameter taking into account the influence of the sea wave height on the shape of the reflected echo, $\Phi(t)$ is the probability integral. From (5) it follows that in order to increase the sensitivity of the averaged shape of the echo to the intensity of the wave action, it is necessary to use shorter sounding pulses, but this will lead to a decrease in the energy of the echo. The solution can be found by using complex signals.

2. Now let a signal with envelope of Gaussian form and intrapulse linear frequency modulation (LFM) $v(t) = \exp[-(g^2 - jk)t^2]$ be emitted, where $k = \Delta\omega_M/2T_u$, $D = \sqrt{1 + k^2/g^4} \approx \Delta f_M T_u$ is the compression factor; $gD = \sqrt{\pi}\Delta f_M$. Let us find the expression for the averaged form of the echo:

$$P(t) = \frac{P_0 \lambda^2 G_0^2 K_0^2 C D}{64\pi^2 H^3 \Delta f_M a_\omega^2} \exp\left(-\frac{5{,}55\theta_s^2}{\theta_0^2} \cdot \frac{\beta^2\gamma^2}{4} - bt\right)\left[\frac{1}{2} - \Phi\left(\frac{\beta\gamma}{2} - \frac{t}{\gamma}\right)\right], \quad (4)$$

where $\gamma = \sqrt{1/\pi\Delta f_M^2 + 2\sigma^2}$. From a comparison of (3) and (4) it is obvious that for identical band width of the sounding signals and peak transmitter power, the energy of the echo with LFM is greater than the energy of the reflected radio pulse by the compression factor (D) times. For solution of the problem of measuring sea wave height by the form of the reflected pulse, the operating conditions of the radar with a restriction with respect to pulse duration $\theta_0 >$ arctg (2 to $3\sqrt{cT_u/H}$) is preferable from the point of view of acceptable antenna sizes and simplicity of stabilization in the nadir. The dependence of the average form of the echo on the radar characteristics and intensity of the wave action is presented in Figure 1 (T = 20 nanoseconds, H = 600 km, σ_z = 1 to 4 meters, θ_0 = 0.5 to 5°, θ_S = 0 to 0.8°). Thus, recording the leading edge of the echo, it is possible to estimate the mean square height of the sea waves. The processing of the echo is constructed by the following principle. Let us approximate the leading edge of the echo by the exponential polynomial

$$Q(t) = a_0 + a_1 t + a_2 t^2 + a_3 t^3 \qquad (5)$$

The numbers of the node points of the approximation will be denoted by j = -2, -1, 0, +1, +2, where the central point corresponds to t = 0. The readings will be considered independent, taken after an interval $\Delta t = T_u$ (Figure 1). The approximating polynomial is selected by the least squares method. The dependence of $a_1 = 12\Delta t a_1$ and $a_3 = 12\Delta t^3 a_3$ on the sea wave height as presented in Figure 2, that is, by the value of these coefficients it is possible to estimate the intensity; here

$$a_1 = \frac{P_2 - 8P_1 + 8P_{-1} - P_{-2}}{12\Delta t}; \quad a_3 = \frac{-P_2 + 2P_1 - 2P_{-1} + P_{-2}}{12\Delta t^3}, \qquad (6)$$

where P_j is the value of the readings P(t) at the node points of the approximation.

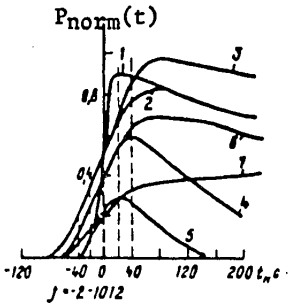

Figure 1. Average form of the echo as a function of the radar characteristics and sea wave intensity: 1--θ_0 = 2°, σ_z = 1 meter; 2--θ_0 = 2°, σ_z = 4 meters; 3--θ_0 = 5°, σ_z = 4 meters; 4--θ_0 = 1°, σ_z = 4 meters; 5--θ_0 = 0.5°, σ_z = 4 meters; 6--θ_0 = 0.33°, σ_z = 4 meters; 7--θ_0 = 0.8°, σ_z = 4 meters.

For measurement of the sea wave height, each arriving echo is gated by a ridge of 5 nanosecond gate pulses with corresponding weights, and then a_3 (or a_1) is

calculated by the algorithm (6). The ridge of gates is started by a pulse from the tracking system of the radio altimeter. After averaging by the known function $a'_{3(1)} = f(\sigma_z)$, an estimate is made of the mean square height of the sea wave in the investigated region. The required number of averaged echoes is presented to obtain measurement accuracy of $\sigma_z = 0.25$ meter with a signal/noise ratio in the receiver of 10 decibels; $T_u = 20$ nanoseconds; $\theta_0 = 2°$; $\theta_S = 0$; H = 600 nm.

σ_z(M)	0.5	1.0	2.0	3.0	4.0
N	8,354	2,530	814	1,150	5,000

The given method of measuring sea wave height by the shape of the echo offers the possibility of resolving five to six intensity gradations.

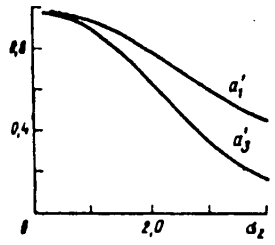

Figure 2. Coefficients of the approximating polynomial a as a function of the mean square wave height.

BIBLIOGRAPHY

1. Zubnovich, S. G., "Statisticheskiye kharakteristiki radiosignalov, otrazhennykh ot zemnoy poverkhnosti" [Statistical Characteristics of Radio Signals Reflected From the Earth's Surface], Moscow, Sov. radio, 1968.

10845
CSO: 8144/1010

UDC 551.46:621.396.969

STUDY OF POSSIBILITY OF DETERMINING SEA WAVE HEIGHT BY MULTIFREQUENCY CORRELATION METHOD USING SATELLITE RADIO ALTIMETERS

Moscow NEKONTAKTNYYE METODY IZMERENIYA OKEANOGRAFICHESKIKH PARAMETROV in Russian 1981 p 13

[Annotation from report by A. Ye. Basharinov (deceased), A. A. Kalinkevich and A. I. Baskakov]

[Text] Annotation. A study is made of the correlation method of determining sea wave height from an aircraft or spacecraft with vertical sounding by short microwave pulses. The correlation coefficient is found between the signals corresponding to the signal bands, the width of which is comparable to the width of the sounding signal, and the central frequencies of which are separated by ΔF. The correlation processing algorithm is defined. An analysis is performed for sounding by pulses with τ_{pulse} = 20 nanoseconds with a height = 600 nm.

10854
CSO: 8144/1010

UDC 621.396.969:551.46

VARIATIONS OF CHARACTERISTICS OF TWO-DIMENSIONAL SPECTRUM OF RADAR IMAGES OF SEA SURFACE DERIVED FROM METER MOVEMENT

Moscow NEKONTAKTNYYE METODY IZMERENIYA OKEANOGRAFICHESKIKH PARAMETROV in Russian 1981 pp 14-17

[Report by A. A. Zagorodnikov, K. B. Chelyshev and V. M. Chegrenets]

[Text] Annotation. Results are presented from theoretical and experimental studies of errors in determining the parameters of the two-dimensional energy spectrum of waves obtained by a radar wave meter with respect to projections and cross sections on board a flight vehicle.

The three-dimensional time-space random field of the z-coordinates of the relief of a disturbed sea surface in the linear approximation can be represented by a superposition of a set of moving planar harmonic components [1] with different wave numbers, directions of propagation and amplitudes. As a result of their ergodicity, normalness and existence of a functional relation (dispersion relation) between the time and space frequencies, the complete statistical characteristic of the wave field is given by the two-dimensional energy spectrum or correlation function. For determination of the spectrum, full-sized realizations of the wave relief field over a significant area of the sea and for a prolonged observation period are needed.

Under flight conditions, as a result of the limited measurement time and noncoincidence of the dimensionalities of the analyzing remote sensor and the wave field on board the flight vehicle it is possible to obtain only undersized realizations of this field (projection and cross section). The determination of the space and time characteristics of the wave action by these realizations (projections and cross sections distorted as a result of movement of the measuring instrument carrier) is accompanied by significant errors.

For geometric representation of an arbitrary moving plane wave (out of the entire set) in an affine space $\{x, y, t\}$ by a set of surfaces of constant phase of the wave characteristic, the fields determined by an arbitrary moving point meter with respect to cross sections are found as projections of a segment of the trajectory of motion of the meter truncated by the average planes of the constant phases, on the time axis and on the plane of the space coordinates. The wave period and length are determined here, respectively.

Recently, remote on-board meters [2], coupled to side-looking radar, have found application in studying the wave field. In the direction transverse to the motion, the radar information about the wave field arrives with half the speed of light and is in the form of an image line on the display. In the longitudinal direction the information arrives with the speed of movement of the analyzing sensor carrier. These sensors are categorized as linear with respect to the method of forming the image. It is convenient to investigate the obtained image by arbitrary cross sections. For analysis of the errors in measuring the wave characteristics, in this case it is convenient to use coordinate transformation, as a result of which one of the coordinate axes coincides with the trajectory of motion of the point sensor or with the direction of the cross section with respect to the radar image in the case of a linear sensor.

For performance of these transformations, a study was made of the transition from an affine space {x, y, t} to metric space {x, y, t} by introducing the provisional time coordinate $z = c_0 t$ (c_0 = 1 m/sec). Applying the corresponding linear coordinate transformation in matrix form to obtain the expression for the uniform spectrum of the space cross section of the image and using the approximation of Yu. M. Krylov for a two-dimensional wave spectrum, we find the expression for the average sea wave length along an arbitrary cross section of the radar image of the sea surface obtained by the moving linear sensor:

$$\bar{\Lambda}_u(\gamma,\psi,W)=\frac{\bar{\Lambda}_0(\gamma+\psi)}{\sqrt{1-1{,}5\,K_1 K_2'\cos(\gamma+\psi)\cos\psi\,\frac{c}{W}+0{,}63\,K_2'\cos^2\psi\left(\frac{c}{W}\right)^2}}= \tag{1}$$
$$=\chi_\Lambda\,\bar{\Lambda}_0(\gamma+\psi).$$

Here

$$K_1=\frac{\Gamma^2(m/2+1)}{\Gamma[(m+1)/2]\,\Gamma[(m+3)/2]};\quad K_2'=\frac{m+2}{1+m\cos^2(\gamma+\psi)};$$

χ_Λ is the deformation coefficient; $\bar{\Lambda}_0(\gamma + \psi)$ is the average wave length of the frozen relief (two-dimensional spatial cross section) of the sea surface in the direction $\gamma + \psi$ with respect to the primary direction. The deformation coefficient characterizes the systematic error in measuring the average sea wave length as a function of the magnitude of the velocity W and the direction of motion of the sensor with respect to the primary path of the wave γ, the average phase velocity of the wave ($\bar{c}$), the width coefficient of the angular spectrum of the wave m. The analysis of the relation obtained indicates stretching of the measured wave length during movement of the sensor in the sector of azimuthal angles ±60 along the direction of the wave path and compression in the sector 120 to 240°. When moving along the line of the crests the distortions are minimal.

The expression for the width coefficient of the angular spectrum (the three-dimensionality coefficient) of the wave m_u defined by the ratio of the average wave lengths in the direction of the crest line $\bar{\Lambda}_{crest} = \bar{\Lambda}_{max}$ and in the primary direction $\bar{\Lambda}_0 = \bar{\Lambda}_{min}$, is obtained in the form

$$m_u = \left[\frac{\bar{\lambda}_v(\beta - \pi/2)}{\bar{\lambda}_u(\beta - 0)}\right]^2 - 1 = \frac{m(1 - 1{,}5K_1\bar{c}/v) - 3K_1\bar{c}/v}{1 + 0{,}63(m+2)(\bar{c}/v)^2}. \quad (2)$$

With an increase in the speed of the carrier (more precisely, the ratio $w/\bar{c}$) the measured three-dimensionality coefficients of the wave action, just as the average wave length, approach their true values. At low speeds, such large distortions are possible that the spectrum obtained by the measurement results turns out to be isotropic with significant anisotropy of the real wave action. The absolute measurement errors of the coefficient of the angular spectrum increase with an increase in the true value, and the relative errors decrease.

The angular displacement of the measured direction of the primary path of the waves with respect to the true direction is determined by the function

$$\Delta\theta = \pi/2 - \arccos(0{,}42\,K_1^{-1}\,\bar{c}/w). \quad (3)$$

For checking the assumptions and the approximations during the calculations, an experiment was run to determine the distortions in the measured average wave lengths $\bar{\lambda}_u$, the coefficients of the angular spectra m_u and the directions of the primary path of the waves as a function of the flight azimuth of the carrier. As the sensor of the information on the wave structure, the "Toros" side-looking radar was used. The flight path was a series of rectangular tacks (Г1, Г2, ..., with radiation from the left side and the right side), ensuring that radar images with four directions of irradiation differing by 90° were obtained for one segment of the sea surface [2]. The obtained images were processed under laboratory conditions on an experimental two-dimensional harmonic analysis setup. By the transparencies of the obtained spatial two-dimensional wave spectra, relations were constructed for the average wave length (Figure 1) and the three-dimensionality coefficient (Figure 2) of the waves as a function of the number of the flight tack. The analysis of the results demonstrated that the maximum errors occur when moving along or opposite to the main direction of the sea wave travel. For the two wave systems existing during the measurements, these errors reach the following magnitudes, respectively:

a. for the sea wave length 20 to 25 percent (theoretically expected 15 to 20 percent);

b. for the angular spectrum coefficient 25 to 40 percent (theoretically expected 30 to 45 percent);

c. for the directions of primary travel of the waves 20 to 25° (theoretically expected 20 to 30°).

Minimum distortions of the results were observed when moving along the crest line of the waves. Thus, the theoretical conclusions regarding the magnitudes and nature of the distortions of the wave measurement results caused by movement of the information sensor were confirmed experimentally.

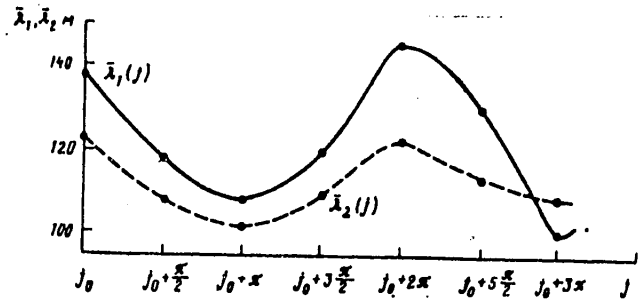

Figure 1. Experimental dependence of the average sea wave length on the direction of motion of the meter.

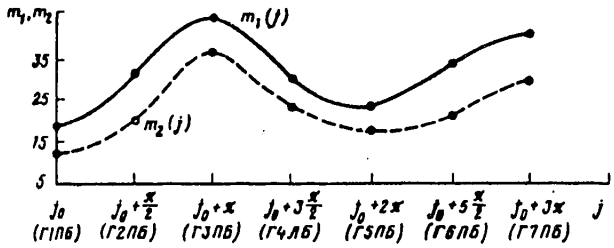

Figure 2. Experimental dependence of the angular spectrum width coefficient of wave action on the direction of motion of the meter.

BIBLIOGRAPHY

1. Krylov, Yu. M., "Spektral'nyye metody issledovaniya i rascheta vetrovykh voln" [Spectral Method of Investigation and Calculation of Wind-Driven Waves], Leningrad, Gidrometeoizdat, 1966.

2. Belousov, P. S., et al., "Study of Sea Wave Parameters by Side-Looking Radar," "Trudy simpoziuma po sovetsko-amerikanskomu eksperimentu 'Bering'" [Works of the Symposium on the Soviet-American "Bering" Experiment], Leningrad, Gidrometeoizdat, 1975.

10845
CSO: 8144/1010

UDC 621.396.969:551.46

ANGULAR SPECTRA OF SEA WAVES ACCORDING TO REMOTE MEASUREMENT DATA

Moscow NEKONTAKTNYYE METODY IZMERENIYA OKEANOGRAFICHESKIKH PARAMETROV in Russian 1981 pp 18-20

[Report by Ye. O. Zhilko, A. A. Zagorodnikov and K. B. Chelyshev]

[Text] Annotation. The results of experiments in measuring the width of the angular spectrum of waves are discussed.

A small number of papers are known in which the angular spectrum of sea waves $S(\theta)$, characterizing the wave energy distribution by directions was studied [1-4]. The most widespread approximation of the integral angular spectrum is a function of the type

$$S(\theta)=N\cos^m\theta, \quad (1)$$

where N is the normalizing factor, θ is the direction of propagation of the spectral components. The first hypothetical information about the value of the coefficient m characterizing the width of the angular spectrum of sea waves is contained in the papers by R. Arthur, V. Pearson and I. N. Davidan [1-3]. These studies demonstrated that individual narrow bands of the frequency spectra have different values of the coefficient m. In [4] it is considered that the low-frequency components have m = 3, for frequencies in the vicinity of the maximum m = 2, and high-frequency components from the equilibrium interval m = 1.

There is also information about more significant scattering of the values of the coefficients m = 2 to 10. This scattering is explained by the following:

a. there are insufficiently substantiated theoretical prerequisites about the value of m;

b. the stereophotographic survey used as the basic tool in determining $S(\theta)$ cannot give high measurement precision as a result of limited size of the plots (no more than 0.5 x 0.5 km);

c. the accuracy of contact sensors recording the integral picture without separation into individual wave systems is also inadequate.

In order to obtain reliable data on the values of the width of the integral angular spectrum it is necessary to have a realization of the image of the sea wave relief with large dimensions (5 x 5 km, 10 x 10 km). Such realizations can be obtained, for example, using side-looking radar or ordinary aerial photographic surveying.

The procedure for measuring the angular spectrum function by radar images and aerial photographs is discussed in [5]. Their essence consists in the fact that the method of two-dimensional harmonic analysis permits determination of both the angular spectrum of each system of waves individually and the angular spectrum of a narrow band of spatial frequencies and vicinities of the wave number.

After obtaining the function $S(\theta)$ its width can be determined at the 0.5 level of the maximum value by the formula

$$m = \frac{\lg 2}{\lg \cos \theta_{0.5}}. \qquad (2)$$

In a number of cases, by the energies of sea waves it is possible to determine the value of the coefficient m with respect to the average crest length, $\bar{\Lambda}_{crest}$, and the average wave length, $\bar{\Lambda}$, in the general direction of propagation of the wave energy.

$$m = \left(\frac{\bar{\Lambda}_{cr}}{\bar{\Lambda}}\right)^2 - 1. \qquad (3)$$

The authors had at their disposal a large quantity of experimental data in the form of radar and aerial photographic images obtained in 1970 to 1974 in the Bering, Baltic, Kara and Black Seas.

The values of the coefficient m were determined by two methods (see expressions (2), (3)).

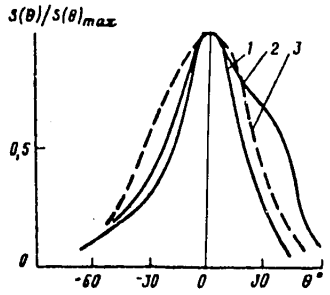

Figure 1. Realization of angular spectra.

The realizations of the angular integral spectra are presented in Figure 1 for an example. Curves 1, 2, 3 were obtained for aerial photographic images taken

after small time intervals at distances of 100, 50 and 25 km from the shore. Analysis of these spectra permits the dynamics of the development of sea waves to be traced; thus, 100 km from the shore (Curve 1) the angular spectrum is more narrow.

In Figure 2 the function m(k) is presented which was obtained by analysis of one wave system. From the graph it is obvious that the low-frequency components have a more narrow spectrum (larger value of m).

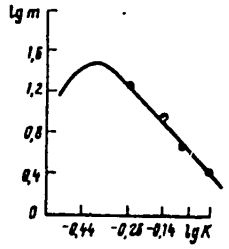

Figure 2. Angular coefficient as a function of the spatial frequency of one wave system.

An analysis of the results permits the following conclusions to be drawn:

1. The coefficient m for individual wave systems varies within broad limits from 2 to 45, which permits us to talk about the presence of narrowly directional, narrow-band angular spectra.

2. The results of the calculations by formulas (2), (3) are quite close.

3. The width of the angular spectrum varies as a function of the spatial frequency on which the measurements are performed.

BIBLIOGRAPHY

1. Arthur, R., "Difference in Direction of Propagation of Waves Caused by a Constant Wind," "Osnovy predskazaniya vetrovykh voln, zybi i priboya" [Fundamentals of Predicting Wind-Driven Waves, Swell and Breaking Waves], collection of translations edited by V. B. Shtokman, Moscow, Izd-vo inostr. lit-ry, 1951.

2. "Vetrovyye volny" [Wind-Driven Waves], collection of translations edited by Yu. M. Krylov, Moscow, Izd-vo inostr. lit-ry, 1962.

3. Zagorodnikov, A. A., and Chelyshev, K. B., "Application of Optical Processing for Wave Measurements by Remote Methods," TRUDY GOIN, No 117, 1973.

4. Krylov, Yu. M., "Vetrovyye volny i ikh vozdeystviya na sooruzheniya" [Wind Waves and Their Effect on Structures], Leningrad, Gidrometeoizdat, 1976.

10845
CSO: 8144/1010

UDC 621.396.969:551.46

RESULTS OF MEASURING SEA WAVE PARAMETERS AND ATMOSPHERIC TURBULENCE BY GROUND INCOHERENT RADAR

Moscow NEKONTAKTNYYE METODY IZMERENIYA OKEANOGRAFICHESKIKH PARAMETROV in Russian 1981 p 21

[Annotation from report by Yu. B. Gagarin, G. I. Dyatlov, Ye. O. Zhilko and Ye. M. Meshcheryakov]

[Text] Annotation. Results are presented and discussed from an experimental determination of the parameters of sea waves and atmospheric turbulence during radar sounding of the sea surface and cloud formations by incoherent radar.

The results of the experimental studies permit the following conclusions to be drawn:

1. Synchronous measurements of the current sea wave height using a radar meter and contact wave recorder at the same point on the sea surface demonstrated practical coincidence.

2. Accuracy of measuring the sea wave parameters is higher, the more intense the wave action.

3. When measuring the parameters of atmospheric turbulence, low reliability of the amplitude methods for quantitative determination of the turbulence intensity was confirmed.

4. The possibility of using a mean frequency meter of the interperiod fluctuations of the echo intensity to determine sea wave and atmospheric turbulence parameters, which permits expansion of data obtained from shore and ground stations to improve the quality of hydrometeorological forecasts, was demonstrated.

10845
CSO: 8144/1010

UDC 621.396.969:551.46

MEASURING SEA WAVE PARAMETERS BY A DOPPLER METER FOR VARIOUS AIRCRAFT FLIGHT CONDITIONS

Moscow NEKONTAKTNYYE METODY IZMERENIYA OKEANOGRAFICHESKIKH PARAMETROV in Russian 1981 pp 22-25

[Report by Yu. V. Baytsur, Yu. B. Gagarin, Ye. O. Zhilko and S. I. Miroshnichenko]

[Text] Annotation. A study is made of the results of measuring sea wave height by an aircraft radar wave meter for various carrier flight conditions and ways to improve the meter.

The degree of informativeness of the meter is determined by the possibility of encompassing large sea surfaces by simultaneous measurements. The aircraft meters of sea surface parameters on this level have significant advantages over ship or shore measurements. However, measurements from an aircraft have a number of peculiarities which can prevent reliable data from being obtained.

The purpose of this experiment was to study the peculiarities of the functioning of an aviation Doppler meter for measuring sea wave parameters under various aircraft flight conditions and ways to further improve the meter to increase the reliability of the results.

The operating principle of the meter is based on using the linear dependence of the Doppler frequency shift of the signal reflected by each elementary reflector of the sea surface on its radial velocity with respect to the radar [1].

The experimental flight studies were performed in the Black and Caspian Seas.

On the basis of the studies, relations were constructed for the readings of the sea wave parameter meter as a function of various aircraft flight conditions and evolutions.

Figure 1 shows the measurements of sea wave height as a function of aircraft flight speed during horizontal flight. An analysis of the graph shows that with an increase in horizontal flight speed of the aircraft, no stable trend toward increased instrument error in determining the sea wave height is observed.

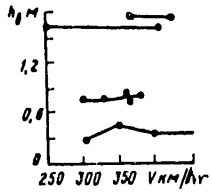

Figure 1. Measurements of sea wave heights as a function of aircraft speed during horizontal flight.

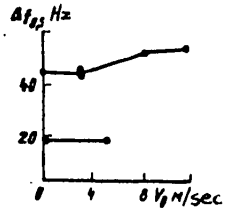

Figure 2. Readings during flights losing altitude.

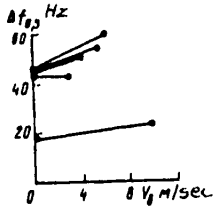

Figure 3. Readings during flights gaining altitude.

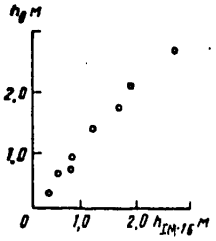

Figure 4. Comparative readings of aircraft and contact wave recorders.

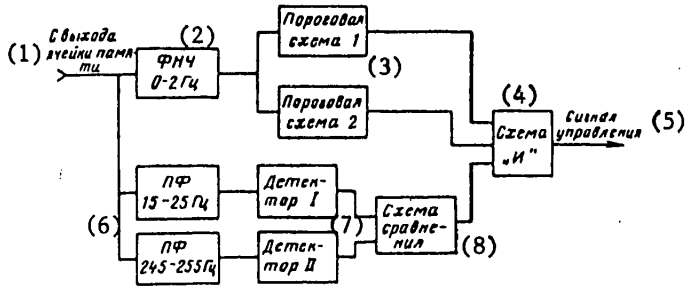

Figure 5. Functional diagram of the automatic control unit for the operation of an aircraft wave recorder.

Key:
1. From the memory cell output
2. Low-frequency filter 0-2 Hz
3. Threshold circuit ...
4. AND circuit
5. Control signal
6. Band pass filter ... Hz
7. Detector ...
8. Comparison circuit

Figures 2 and 3 present the functions for the instrument readings during flights losing and gaining altitude. The analysis of these graphs shows that with an increase in vertical velocity V_V of the aircraft, the instrument errors increase. The average amplitudes of the sea wave envelopes h_{wave} recorded by the wave meter are presented in Figure 4 (the y-axis). The measurement of the results obtained using the IM-16 marine wave recorder at the same time are plotted on the x-axis.

During operation of the wave meter under conditions of evolution of motion of the flight vehicle, the amplitude of the reflected signal varied from large values going beyond the linear part of the amplitude characteristic of the receiver, to inadmissibly small values. Similar signal variations were traced with a period of 1.0 to 10 seconds. In both cases the wave meter readings contained significant errors. In addition, significant errors arose in the case of a small ratio of the signal voltage to the effective value of the noise voltage of the receiver.

The noted deficiencies require observation of the amplitude of the reflected signal with respect to the receiver noise, which complicates the work of the operator and requires high qualifications of him. For simplification of working with the instrument and to improve the reliability of the obtained results, on occurrence of the above-noted situations the wave meter must be automatically switched off and a signal sent that exact measurement of the wave parameters is impossible.

The functional diagram (Figure 5) of a control unit for the operation of a wave meter contains three channels. The first two of them monitor the level variation of the lowest-frequency components of the signal (from 0 to 2 Hz). When the amplitude of the low-frequency components exceeds the value of U_{max}, the threshold circuit 1 responds, and when the amplitude drops below U_{min}, threshold circuit 2 responds. The values of U_{max} and U_{min} are determined for each type of radar by their amplitude characteristics.

The third channel of the automatic control unit monitors the signal/noise ratio. The functional diagram of the channel is constructed under the assumption that a signal reflected from a disturbed sea surface has a narrower spectrum than the spectrum of the noise samplings of the receiver. Actually, for the 3-cm radar wave range the frequency band of the echo does not exceed 150 Hz, at the same time as the spectrum of the noise sampling of the receiver is in practice uniform in the range from 0 to 1/2T Hz, where T is the radar sounding pulse repetition period.

The third channel consists of a low-frequency filter with pass band from 15 to 25 Hz and a filter with band from 245 to 255 Hz, signal detectors at the filter outputs and comparison circuit which monitors the voltage ratio at the detector output.

A signal from the third channel output, halting the operation of the wave meter, arrives if the voltage at the output of detector I does not exceed the voltage at the output of detector II by a given number of times. The required signal to noise level ratio is selected beginning with the required accuracy of the measurements.

At the output of the control unit there is an AND circuit, which sends the signal to operate only when favorable conditions have been met with respect to all channels.

Checking the serviceability of such a control unit produced positive results.

On the basis of the results obtained it is possible to draw the following conclusions:

1. The deviation of heights measured by a multichannel Doppler meter compared to data obtained by contact wave recorders used abroad is 3 to 17 percent. The observed wave heights of 3 percent guarantee are 2.7 meters in this case.

2. The variation in flight speed of the aircraft from 250 to 500 km/hr during scanning of the radar antenna in the ±30° sector with respect to the ground speed vector, is in practice not felt in the operating errors of the instrument.

3. Losing and gaining altitude by the aircraft with a vertical velocity of 3 m/sec does not introduce additional errors when measuring the wave height. Increasing the vertical rate of descent of the aircraft to 10 m/sec increases the wave height measurement error to 15 to 25 percent.

4. For simplification of working with the instrument and in order to improve the reliability of the obtained results, automation of the wave recorder control is necessary.

BIBLIOGRAPHY

1. Zagorodnikov, A. A., "Use of the Doppler Spectrum of a Radar Signal To Measure Some Sea Wave Parameters," METEOROLOGIYA I GIDROLOGIYA, No 1, 1971.

10845
CSO: 8144/1010

UDC 621.396.96:551.466

ENERGY CHARACTERISTICS OF RADAR SIGNALS ENVELOPE AND THEIR RELATION TO WAVE PARAMETERS

Moscow NEKONTAKTNYYE METODY IZMERENIYA OKEANOGRAFICHESKIKH PARAMETROV in Russian 1981 pp 26-30

[Report by V. G. Vazhenin, A. A. Kalmykov and N. M. Kharlova]

[Text] Annotation. Results are presented in this paper from experimental studies of the energy characteristics of an echo (normalized autocorrelation function and spectrum) during vertical irradiation of the sea surface and with commensurate dimensions of the irradiated area and the average sea wave lengths.

The possibility of using radar with LFM for measuring the sea wave profile and estimating the basic oceanographic parameters is demonstrated in [1].

The peculiarities of using radar (small heights, vertical irradiation) are giving rise to significant dependence of the energy characteristics of the echo not only on the irradiation conditions, wave length and intensity, but also the ratio of the dimensions of the irradiated area and the geometric dimensions of the sea waves and the state of the sea surface [2].

Fluctuations of the echo envelope with small dimensions of the reflecting area vary in accordance with variation of the slopes of long sea waves passing through the irradiated area [3] which permits use of the spectrum of the echo envelope to measure the slope spectrum of the sea surface and, correspondingly, the spectrum of the sea wave height. In [4] the presence of a relation of the spectra of the echo envelope and the fluctuation spectrum of the sea surface for the irradiated areas, the dimensions of which are appreciably less than the average sea wave length, is demonstrated.

In the given paper results are presented from experimental studies of the characteristic of the echo envelope (correlation function and spectrum) when using antennas with wide radiation patterns and commensurate dimensions of the irradiated area and the sea wave lengths.

In the experiment a 7-cm-band LFM radar was used. The block diagram of the experiment is presented in Figure 1.

In the figure ГЛЧМ is the LFM generator, СМ is the mixer, Ф is the beat signal filter, ЧД is the frequency discriminator, АД is the amplitude detector.

Experimental studies were performed for vertical irradiation from stationary scaffolding (H = 12 meters) of a disturbed sea surface (wave height to 2 to 3 meters). The ratio of the dimensions of the irradiated area and the average sea wave length in the given experiments was 0.4 with a radiation pattern width of the antennas of $\theta = 40°$ and 0.8 for $\theta = 80°$. The remaining radar parameters, the experimental conditions and also the procedure are described in [1].

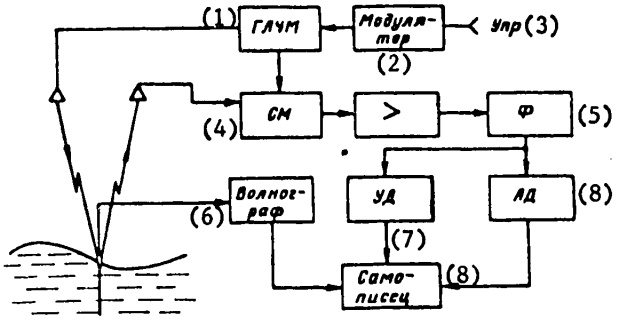

Figure 1. Block diagram of the experiment.

Key:
1. LFM generator
2. Modulator
3. Control
4. Mixer
5. Filter
6. Wave recorder
7. Frequency discriminator
8. Amplitude detector
9. Pen recorder

Figure 2 shows the normalized correlation function (a) and the spectrum (b, c, d) of the echo envelope (2) and the sea surface (1) for $\theta = 40°$ (a, b) and $\theta = 80°$ (c) for linear polarization and $\theta = 40°$ for circular polarization (d).

Discussion of the results:

1. The obtained results indicate the presence of a relation of the characteristics of the echo envelope to the sea wave parameters. This permits their use for estimation of the wave parameters and the reflected signal envelope characteristics.

2. With vertical irradiation of the sea surface from low altitudes, the fluctuations of the echo envelope can be divided into two components:

a) low-frequency, caused by large gravity waves,

b) low-frequency, caused by fine structure superposed on large waves.

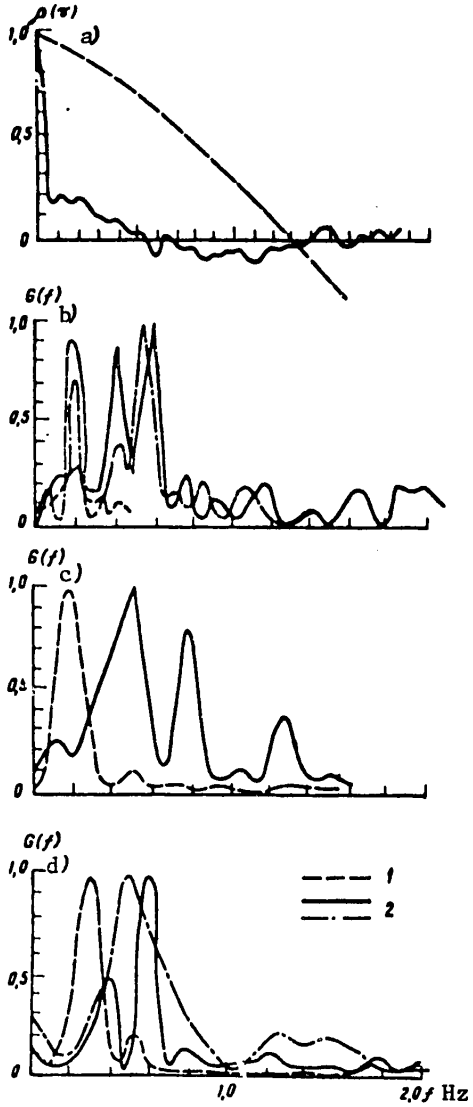

Figure 2

3. For commensurate dimensions of the irradiated area and sea wave lengths, the spectrum of the echo envelope can contain one or several peaks on frequencies approximately corresponding to the harmonics of the main energy carrying component of the sea waves.

The obtained spectra of the envelope and also the qualitative analysis of synchronous recordings of the echo envelope and the sea wave action indicate that in the wave slope spectrum observed during the experiments, peaks occur at frequencies close to the harmonics of the basic wave component.

4. Under conditions under which the experiment was run, the correlation interval of the high-frequency component of the echo envelope fluctuation is on the order of 0.1 to 0.2 second, and it is primarily determined by the frequency properties of the small waves.

5. A variation in the ratio of the diameter of the irradiated area and the average sea wave length from 0.4 to 0.8 and also changing of the emitted and received polarization of the microwave signal from linear to circular under the conditions under which the experiment was run does not lead to significant changes in the frequency and time characteristics of the echo envelope.

6. The results of the experimental studies presented in the given paper, just as in [1], indicate that at low altitudes and with vertical sounding the LFM radar, which has wide antenna radiation patterns, can be used to measure the basic parameters of sea waves.

BIBLIOGRAPHY

1. Vazhenin, V. G., and Kalmykov, A. A., "Use of Continuous Emission Radar To Measure Wave Heights and Sea Level," "Nekontaktnyye metody izmereniya okeanograficheskikh parametrov" [Noncontact Methods of Measuring Oceanographic Parameters], Moscow, Gidrometeoizdat, 1977, pp 125-128.

2. Zagorodnikov, A. A., "Dependence of the Spectrum of a Radar Signal Scattered by the Sea Surface, on the Dimensions of the Irradiated Section and Intensity of the Sea Waves," RADIOTEKHNIKA I ELEKTRONIKA, No 3, 1972, pp 477-487.

3. Zamarayev, B. D., and Kalmykov, A. I., "Possibility of Determining the Spatial Structure of the Disturbed Sea Surface," IZV. AN SSSR, FIZIKA ATMOSFERY I OKEANA, Vol 5, No 8, 1969, pp 724-729.

4. Parfent'yev, V. N., and Prakhov, V. P., "Correlation Functions of the Envelope of a Radar Signal Reflected From Real Earth Surfaces," "Nekontaktnyye metody izmereniya okeanograficheskikh parametrov," Moscow, Gidrometeoizdat, 1977, pp 165-167.

10845
CSO: 8144/1010

PASSIVE MICROWAVE METHODS

UDC 551.46.09

ESTIMATES OF STATE AND PHYSICOCHEMICAL SURFACE PROPERTIES OF BODIES OF WATER BY THE DATA FROM SPECTRAL MEASUREMENTS OF MICROWAVE RADIATION

Moscow NEKONTAKTNYYE METODY IZMERENIYA OKEANOGRAFICHESKIKH PARAMETROV in Russian 1981 pp 31-34

[Article by A. M. Shutko]

[Text] Annotation. An analysis is made of the effectiveness of determining hydrophysical parameters by the data from spectral measurements of microwave radiation.

The sensitivity of the microwave radiation field to variations of the temperature T, the chemical composition of the water medium S, the intensity of the waves γ, the packing of floating ice P, the oil slick thickness α, and atmospheric parameters differ significantly with respect to spectrum (Figure 1).

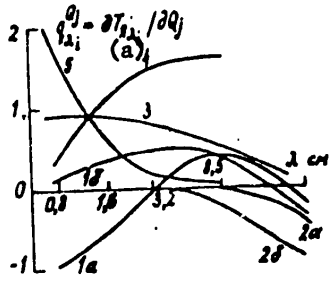

Figure 1. Spectral sensitivity of radiation field:
1 -- $\partial T_{bright}/\partial T$, K/°C; 2a -- $\partial T_{bright}/\partial S$, K/°/oo at 40°/oo and °C; 2b -- $\partial T_{bright}/\partial S$, K/°/oo at 40°/oo and 30°C;
3 -- $\partial T_{bright}/\partial \gamma$, K/(m-sec^{-1}) at θ=0°, $\gamma \geq$7m/sec;
4 -- $\partial T_{bright}/\partial P$, K/°/o; 5 -- $\partial T_{bright}/\partial \alpha \cdot 10^2$, K/micron

Key:
a. bright

These differences are the basis for methods of determining the hydrophysical parameters Q_j under complex meteorological conditions according to the data from simultaneous measurements of the radioemission $T_{\lambda 1}^{bright},\ldots,T_{\lambda i}^{bright}$ on waves of

$\lambda_1,\ldots,\lambda_i$ [1, 2]. In order to obtain reliable hydrophysical information, the solution with respect to Q_j must be stable in all intervals $Q_{j\ max} \leq Q_j \leq Q_{j\ min}$ for some ambiguity of the radiation-hydrophysical relations and errors in measuring the brightness. This problem is solved by selecting sections of the spectrum maximizing the determinant of the system of radiation-hydrophysical equations or minimizing the measurement errors. In order to solve this problem, a broken linear approximation of the functions $\Delta T_{\lambda i}^{bright}(Q_j)=T_{\lambda i}^{bright}(Q_j)-T_{\lambda i}^{bright}(Q_{j\ min})$, (Figure 2a)

$$\Delta T_{\lambda_i}^{a}(Q_j) = \kappa_{i_1}^{j}(Q_{j_1}-Q_{j\,min}) + \ldots + \kappa_{i_m}^{j}(Q_j - Q_{j\,m-1}) \qquad (1)$$

is used considering the indeterminacy factors indicated in Figure 2b.

It is demonstrated that when using the wave band of $0.8 \leq \lambda \leq 30$ cm, the solution with respect to the parameters T, γ, S in the absence of influence of atmospheric parameters and considering the water reserve of the clouds with an error of 1 to 3% is the most stable in the sections of the spectrum λ_1=5 to 10 cm; λ_2=0.8 to 1.6 cm; λ_3=25 to 30 cm in the intervals of $0 \leq T \leq 30°C$; $0 \leq S \leq 40\%$, $0 \leq \gamma \leq 25$ meter/sec.

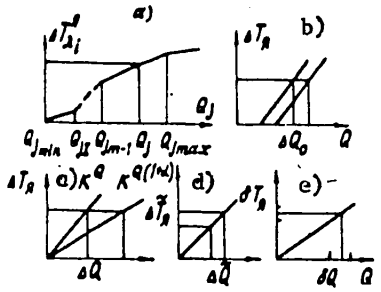

Figure 2. General form of the approximation (a) and error sources: parallel shift (b); variation in curvature (c), random variations in radio brightness (d), fluctuation noise (e)

The approximate expressions (2)-(6) permit estimation of the errors in determining the parameters T, γ, S as a result of the following:

a) Parallel displacement of the radiation functions

$$\Delta T = (Det_{T,\gamma})^{-1}[(\kappa_{1m}^{T}\kappa_{2n}^{\gamma}\Delta T_{0_1} - \kappa_{1p}^{T}\kappa_{1q}^{\gamma}\Delta T_{0_2}) + \kappa_{1q}^{\gamma}\kappa_{2n}^{\gamma}(\Delta\gamma_{0_1} - \Delta\gamma_{0_2})], \qquad (2)$$

$$Det_{T,\gamma} = \kappa_{1m}^{T}\kappa_{2n}^{\gamma} - \kappa_{2p}^{T}\kappa_{1q}^{\gamma}, \qquad (3)$$

b) Variation in steepness

$$\Delta T|_{T} = (Det + \Delta Det)^{-1}[\Delta T_{0_1}'\kappa_{2n}^{\gamma}\alpha_2^{\gamma} - \Delta T_{0_2}'\kappa_{1q}^{\gamma}\alpha_1^{\gamma} - T\Delta Det], \qquad (4)$$

$$\Delta Det = \kappa_{1m}^{T}\kappa_{2n}^{\gamma}(\alpha_1^{T} + \alpha_2^{\gamma}) - \kappa_{2p}^{T}\kappa_{1q}^{\gamma}(\alpha_1^{T} + \alpha_1^{\gamma}), \qquad (5)$$

$$\Delta T'_{\lambda_1} = \delta T_{\theta_1} - \left[T_{i_1 j}\left(\kappa^T_{i_1 j} - \kappa^T_{i_1 l}\right) + \ldots + T_{i_{m-1}}\left(\kappa^T_{i_{m-1}} - \kappa^T_{i_m}\right) + \nu_{i_1}\left(\kappa^\nu_{i_1} - \kappa^\nu_{i_2}\right) + \ldots + \nu_{i_{q-1}}\left(\kappa^\nu_{i_{q-1}} - \kappa^\nu_{i_q}\right)\right] \quad (6)$$

($\Delta T'_{\text{bright}_2}$ is determined analogously),

c) Random variations in radio brightness

$$\tilde{\Delta T} = (Det)^{-1}\left(\Delta \tilde{T}_{\theta_1} \kappa^\nu_{i_n} - \Delta \tilde{T}_{\theta_2} \kappa^\nu_{i_q}\right), \quad (7)$$

d) Fluctuation noise

$$\delta T = |Det|^{-1}\sqrt{\left(\delta T_{\theta_1} \kappa^\nu_{i_n}\right)^2 + \left(\delta T_{\theta_2} \kappa^\nu_{i_q}\right)^2} \quad (8)$$

The errors in the estimates of the parameter γ are determined by analogous relations. The error in determining the salinity is related to the error ΔT by the approximate expression

$$\Delta S / S_{,T} \approx -\left(\kappa^T_{\lambda_p} / \kappa^S_{\lambda_m}\right) \delta T. \quad (9)$$

Variations in steepness of the radiation functions on the wave λ_3 lead to the errors

$$\Delta S \approx \left[\kappa^\delta_{\lambda_m}\left(1 + \alpha^S_\lambda\right)\right]^{-1}\left[\left(\beta \tilde{T}'_{\theta_\lambda}\right)\alpha^\delta_\lambda - \kappa^T_{\lambda_p} T\left(\alpha^T_\lambda - \alpha^\delta_\lambda\right)\right]_0 \quad (10)$$

Key: 1. bright

For random variations of the radio brightness

$$\delta \tilde{S} \approx \left(\kappa^\delta_{\lambda_m}\right)^{-1}\left[\Delta \tilde{T}_{\theta_\lambda} - \kappa^T_{\lambda_p}\, \delta T\left(\Delta \tilde{T}_{\theta_1}, \Delta \tilde{T}_{\theta_2}\right)\right]. \quad (11)$$

The error as a result of fluctuation interference

$$\Delta S \approx \left|\kappa^\delta_{\lambda_m}\right|^{-1}\sqrt{\left(\delta T_{\theta_\lambda}\right)^2 + \left[\kappa^T_{\lambda_p}\, \delta T\left(\delta T_{\theta_1}, \delta T_{\theta_2}\right)\right]^2}. \quad (12)$$

The spectral intervals that are optimal for estimating other hydrophysical parameters in different combinations of them and also the errors in estimating these parameters are defined by the same procedure. For example, for the parameters T and P_ℓ, such sections of the spectrum are λ_1 and λ_2. The relations for estimating the errors are analogous to (2)-(8).

The estimates show that for T=5°C; γ=10 m/sec; S=35‰ and $\partial T_{\text{bright}}$=0.2 K the errors are: ∂T=0.3°C; $\partial\gamma$=0.25 m/sec; ∂S=0.45‰. For $\alpha^T_1=\alpha^T_2=\alpha^T_3=\alpha_3$=3% and $\alpha^\gamma_1=\alpha^\gamma_2$=20% the errors are ΔT=-0.12°C; $\Delta\gamma$=-0.5 m/sec: ΔS=-0.75‰.

The influence of atmospheric parameters is considered approximately by the expressions (7) and (11). In the general case a joint solution with respect to λ, Q_{hydro} and Q_{atm} is necessary with simultaneous consideration of the hydrophysical and atmospheric parameters.

The graphical representation of the system of radiation hydrophysical equations for different pairs of channels (λ_i, λ_ℓ) is the two-dimensional radiobrightness fields $g\{\Delta T^{bright}_{\lambda_1}, \Delta T^{bright}_{\lambda_2}\}$ (Figure 3, 4). The procedure for optimizing λ_1, λ_2 consists in selecting the spectral intervals which insure maximum lengths of the partial vectors $\bar{q}^{Q_j}$ and $\bar{q}^{Q_k}$ and the closest angle between them to 5/2, which fully corresponds to the condition of maximizing the determinant (3).

The inverse problem of determining the nature and intensity of the disturbances Q_j is solved beginning with orientation and extent of the vectors

$$\dot{q}^{Q_j} = Q_j \dot{\xi}^{Q_j} \quad \text{where} \quad |\dot{q}^{Q_j}| = \sqrt{(\Delta T^{Q_j}_{\lambda_i})^2 + (\Delta T^{Q_j}_{\lambda_\ell})^2}.$$

Key: 1. bright

The temperature inside the disturbed region is determined by reducing the values of g from the region $G^{Q_j}_{T,W}$ corresponding to the given region, in the undisturbed reference zone G^{T}_{W} considering the nature of the spectral function characteristic of the given disturbing factor and the values of the optical thickness τ (or the integral water content W) defined by the readings of the shortwave channels for the given region (Figure 4).

In this procedure it is useful to use the measurement data in the infrared band of waves to monitor the state of the atmosphere and the surface temperature in the absence of cloud formations.

The efficiency of the given methods is confirmed experimentally [3-5].

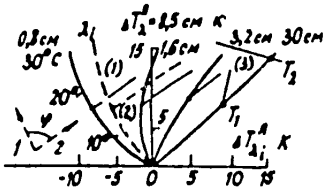

Figure 3. Two dimensional radiobrightness fields for temperature variations $G^{T}_{\lambda_{8.5}\lambda_i}$ (S=0‰; T=0 to 30°C) (1); wave intensity (2) $G^{\nu}_{\lambda_{8.5}\lambda_i}$ ($\gamma=\gamma_1$, $T=T_1$); salinity (3) $G^{S}_{\lambda_{8.5}\lambda_{30}}$ ($T=T_2$, $S=0=S_1$). Partial vectors: I -- $\xi^{T}_{\lambda_{8.5}\lambda_i}$ ($T=T_1$); II -- $\bar{q}_{\lambda_{8.5}\lambda_i}$ ($T=T_1$).

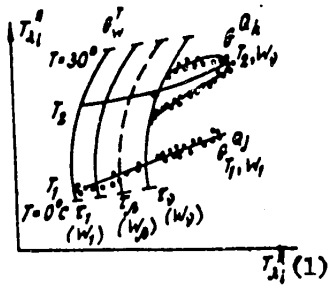

Figure 4. Procedure for estimating hydrophysical parameters considering the influence of atmospheric components
Key:
1. bright

BIBLIOGRAPHY

1. Author's certificate No 319918, A. M. Shutko, "Method of Microwave Radiometric Determination of the Surface State of Bodies of Water," published in RADIOTEKHNIKA I ELEKTRONIKA [Radio Engineering and Electronics], Vol XXIII, No 10, 1978.

2. Author's certificate No 335613, A. M. Shutko, "Method of Determining the Surface Temperature of Bodies of Water from Flight Vehicles," RADIOTEKHNIKA I ELEKTRONIKA, Vol XXIII, No 10, 1978.

3. Shutko, A. M. and Kutuza, B. G., "Radiophysical Studies of the Planets," ITOGI NAUKI SER. RADIOTEKHNIKA [Scientific Results, Radio Engineering Series], No 16, VINITI, Moscow, 1978.

4. Basharinov, A. Ye., et al., in the collection ISSLEDOVANIYA V OBLASTI RADIOTEKHNIKI I ELEKTRONIKI 1954-1974 GG [Research in the Field of Radio Engineering and Electronics, 1954-197], Moscow, Izd. IRE AN SSSR, 1974.

5. Basharinov, A. Ye., Gurvich, A. S. and Yegorov, S. T., RADIOIZLUCHENIYE ZEMLI KAK PLANETY [Radio Emission of the Earth as a Planet], Moscow, Nauka, 1974.

10845
CSO: 8144/1010

UDC 551.46.09

RESULTS OF MICROWAVE RADIOMETRIC SOUNDING OF BODIES OF WATER WITH DIFFERENT TEMPERATURE AND SALINITY

Moscow NEKONTAKTNYYE METODY IZMERENIYA OKEANOGRAFICHESKIKH PARAMETROV in Russian 1981 pp 35-38

[Article by G. I. Chukhray and A. M. Shutko]

[Text] Annotation. Data are presented from experimental studies of the characteristic of microwave radiation of bodies of water with temperature variation within the limits of 10 to 25°C and salinity in the range of 0 to 300 g/liter. The measurements were performed from on board the aircraft laboratories of the IRE Institute of the USSR Academy of Sciences in seven spectral sections in the wave range of 0.8 to 30 cm. The experimental data are compared with the results of model calculations.

The dependence of the characteristic of the natural microwave radiation in the centimeter and decimeter wave range on temperature and salinity gives rise to the possibility of determining the indicated parameters by the methods of microwave radiometry [1].

The radiobrightness temperature is a function of the emissive power and thermodynamic temperature within the limits of the thickness of the effectively emitting layer which, depending on the salinity and temperature of the aqueous medium is (1/10 to 1/3) of the emission wavelength. The radiative characteristics of the water surface in the absence of foam formations are determined by the Fresnel radiation coefficients, the magnitude of which depends on the complex dielectric constant of the medium.

In accordance with the model representations [2], the parameters determining the values of the complex dielectric constant are functions of temperature and salinity, and they also depend on the chemical composition of the aqueous medium.

In order to investigate the influence of temperature and salinity of the water surface on its microwave radiation characteristics, in 1975-1977 the IRE Institute of the USSR Academy of Sciences performed experiments in bodies of water, the salinity of which encompasses the entire concentration range of natural water (0 to 300 grams/liter). The temperature dependence was investigated in experiments performed in the same regions during different seasons of the year. The set of measuring equipment installed on board the laboratory aircraft includes seven

radiometers in the 0.8 to 30 cm range. The fluctuation sensitivity is 0.3 to 1 K.

The investigated bodies of water include the following: a) the Dnestr Liman and the Black Sea (salinity 0 to 15 g/liter), b) the Tatar Strait, the Amur Liman, Sakhalin Bay (salinity 0 to 35 g/liter), c) the Azov Sea, Lake Sivash, the salt lakes on the Arabatskaya Spit (salinity 13 to (80-250) g/liter), d) the Caspian Sea, the Bay of Kara-Bogaz-Gol (salinity 15 to (250-310) grams/liter).

Figure 1 shows an example of recording this signal on a wave length of 18 cm when flying over the Dnestr Liman and Black Sea.

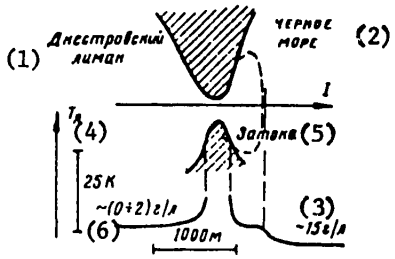

Figure 1. Map of the region of operations (I -- flight path) and example of recording signal while flying on path I; wavelength 18 cm; September 1977

Key:
1. Dnestr Liman
2. Black Sea
3. ~15 g/liter
4. bright
5. Zatoka
6. ~(0 to 2) g/liter

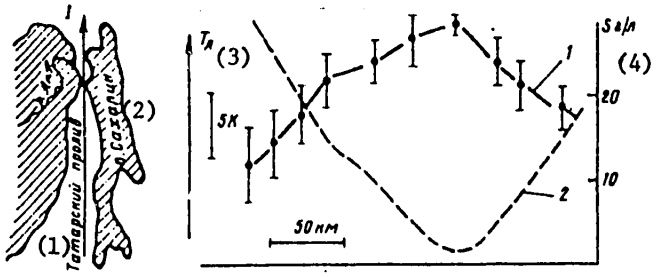

Figure 2. Map of the operation region (I -- flight path) and variations of the radiobrightness intensity during flights along path I; wavelength 30 cm; September 1976 (1); variations in salinity along path I during performance of the experiments (2)

Key:
1. Tatar Strait; 2. Sakhalin Lake; 3. bright; 4. 5 g/liter

From the figure it is obvious that with an increase in salinity the radiobrightness temperature on this wavelength decreases. The region propagated by water from the Dnestr Liman is clearly recorded in the sea.

From Figure 2, in which variations of the radiobrightness intensity on the 30 cm wave are presented for flights over the bodies of water in the Far East and variation of the water salinity along the flight path is also presented, it is obvious that the minimum salinity (the estuary zone of the Amur Liman) correspond to maximum radiobrightness; an increase in salinity (to the south and north of this zone) corresponds to a decrease in radiobrightness.

The dependence of the radiation contrast for a 30 cm wave on the salinity is illustrated in Figure 3. The radiation contrast is the difference in values of the brightness temperatures for current values of the salinity and minimum value of 2 g/liter for this region. In the same figure the calculation relations are presented for a temperature of 10 and 15°C corresponding to the maximum values of the water temperature along the flight path during performance of the experiments. Within the limits of the measurement error, experimental and calculated values agree with each other.

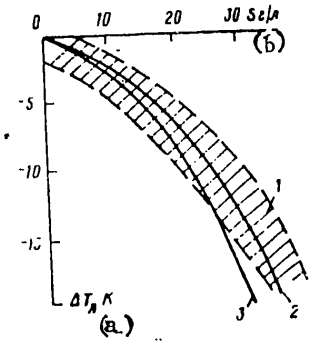

Figure 3. Radiation contrast as a function of salinity; wavelength 30 cm; September 1976. 1 -- experiment; 2, 3 -- calculation for water temperature of 10°C (2) and 15°C (3)

Key:
a. bright
b. 5 grams/liter

As follows from the spectral measurement data, the radiation intensity on wavelengths greater than 10 cm decreases with an increase in salinity; the absolute magnitude of the contrast is greater the longer the wavelength. In the centimeter wave band the variation in radiobrightness is within the limits of error of the experiment.

The steepness of the mineralization relation of the radiation contrast on a 30 cm wave in the range of salinities of 0 to 35 g/liter and temperatures from 10 to 15°C is -0.3 ± 0.07 K/(g-liter^{-1}).

Examples of making a signal recording during flights over a body of water with high salinities are presented in Figures 4 and 5. Here variation in the signal level is also observed with variation in salinity. As follows from Figure 5, an increase in salinity is felt differently in the radiation intensity in the centimeter and decimeter wave bands: on a 2.25 cm wave the signal level increases, and on a 30 cm wave, it decreases with an increase in salinity. The distribution zone and the salt deposits in the dried up part of the bay are recorded.

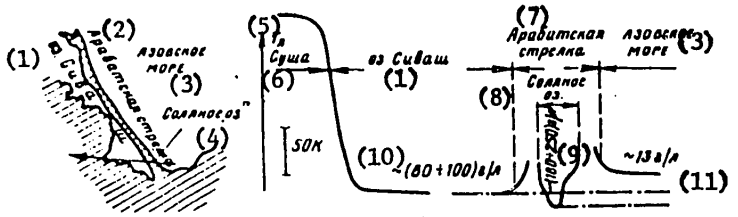

Figure 4. Map of the operation zone (I -- flight path) and example of realizing a signal recording during flights along path I; wavelength 20 cm; July 1975.

Key:

1. Lake Sivash
2. Arabatskaya Spit
3. Azov Sea
4. Solyanoye Lake
5. T_{bright}
6. Dry land
7. Arabatskaya Spit
8. Solyanoye Lake
9. 180 to 250 g/liter
10. ~(80 to 100) g/liter
11. ~13 g/liter

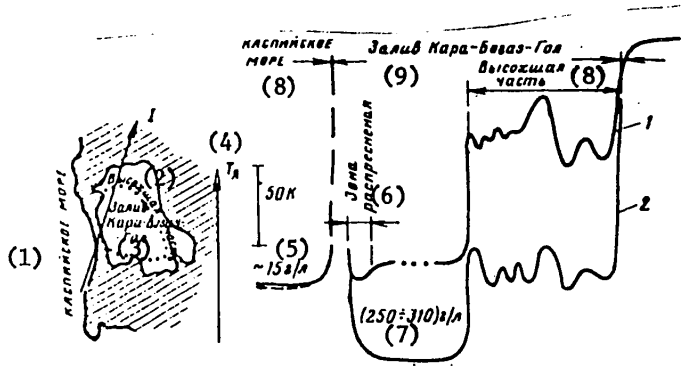

Figure 5. Map of the operations zone (I -- flight path) and example of making a signal recording during flights on path I; wavelength: 1 to 2.25 cm, 2 to 30 cm; May 1977

Key:

1. Caspian Sea
2. Dried up part
3. Kara-Bogaz-Gol Bay
4. T_{bright}
5. ~15 g/liter
6. Fresh water zone
7. (250 to 310) g/liter
8. Caspian Sea
9. Kara-Bogaz-Gol Bay
10. Dried up part

The experimental results were interpreted using published data on the values of the complex dielectric constant of solutions of different salts and mixtures of them contained in the investigated natural bodies of water.

The experimental results confirmed the basic relations calculated on the basis of model representations.

The obtained data indicate the possibility of remote determination of the temperature and salinity of natural bodies of water with respect to the natural emission in the microwave range.

BILIOGRAPHY

1. Basharinov, A. Ye., RADIOIZLUCHENIYE ZEMLI KAK PLANETY [Radio Emission of the Earth as a Planet], Moscow, Nauka, 1974.

2. Debay, P. and Zakk, G., TEORIYA ELEKTRICHESKIKH SVOYSTV MOLEKUL [Theory of Electrical Properties of Molecules], Moscow-Leningrad, GITTL, 1936.

10845
CSO: 8144/1010

UDC 551.46.07/08:537.87

SPECTRAL AND POLARIZATION CHARACTERISTICS OF MICROWAVE RADIATION OF FOAM FORMATIONS

Moscow NEKONTAKTNYYE METODY IZMERENIYA OKEANOGRAFICHESKIKH PARAMETROV in Russian 1981 pp 39-42

[Article by V. Yu. Rayzer and Ye. A. Sharkov]

[Text] Annotation. Results are presented from measurements of the radiation coefficient of a water surface covered with foam formations of different types. An electrodynamic model of the foam medium is proposed in the form of a solid layered-nonuniform structure with effective dielectric parameters.

The possibilities of studying microwave emission of a foam cover under natural conditions are limited in view of its structural variety and dynamic nature. Therefore in order to study the physical mechanism of the phenomenon, laboratory experiments are required. In this paper some results of such research are presented.

The disperse formations -- emulsion multilayer and nonuniform foam layer -- were created on the water surface in a laboratory flume. The thickness of the single layer $h \sim d$, d is the bubble diameter (d=0.2 to 2.0 mm). The nonuniform foam layer consisted of two types of structures--emulsion at the interface with the water surface and polyhedral. Its total thickness was $h \sim 10$ mm.

The measurements were performed using highly sensitive radiometric equipment in the ranges of λ=0.2, 0.8, 2, 8 and 18 cm [1]. The experiments demonstrated the following.

1. The wavelength range of λ=0.8 to 8 cm had the greatest sensitivity to the dynamic structure of the foam layer.

2. The increase in radiobrightness temperature of the surface in the range of λ=0.2 to 2 cm was connected with the presence of an emulsion single layer ($h/\lambda \lesssim 0.1$). In the range of λ=8 to 18 cm the radiobrightness contrasts were observed only on the appearance of a thick layer of foam of polyhedral structure.

3. The roughness of the boundaries of the foam layer was not felt in the qualitative nature of the polarization functions in the millimeter range. The degree of polarization of the radiation decreased with an increase in the layer thickness (Figure 1).

The effort to interpret the experimental data based on a model of the transient dielectric layer with parameters corresponding to the statistical mixture of water and air did not give satisfactory results [2]. The calculated values of the radiation coefficient turned out to be appreciably below the experimental values. A physically more adequate model can be based on individual properties of foam bubbles in the microwave range. The attenuation characteristic σ_e and scattering characteristic σ_s of the bubbles were calculated by the Mie theory for spherical two-layer particles by the author of the procedure of [3]. It was demonstrated, in particular, that in the range of $\lambda \gtrsim 0.8$ cm, $\sigma_s \ll \sigma_e$ ($\delta \ll d$, δ is the thickness of the bubble shell), and the scattering is of a purely dipole nature. These facts permit solution of the problem in the quasistatic approximation and use of the Lorenz-Lorents formula for the effective dielectric constant of a polydisperse medium (the particles are suspended in the air)

$$\varepsilon_\alpha = \frac{1+2X}{1-X}, \quad X = \frac{4}{3}\pi N \int d(r) F(r)\, dr, \tag{1}$$

where N is the particle concentration, d(r) is the polarizability of an individual particle of radius r, F(r) is the normalized distribution function of the particles with respect to sizes ($\int F(r)dr=1$). The polarizability of a hollow spherical shell defined by the first term of the expansion of the Mie series is given by the formula [4]:

$$d = r^3 \frac{(\varepsilon_0-1)(2\varepsilon_0+1)(1-q^3)}{(\varepsilon_0+2)(2\varepsilon_0+1)(1-q^3)+9\varepsilon_0 q^3}, \tag{2}$$

where $q=1-\delta/r$ and ε_0 is the dielectric constant of the shell material (for water $\varepsilon_0=\varepsilon'_0-i\varepsilon''_0$).

The values of ε_α found in this way can be used to construct the electrodynamic model of the "water-foam" system. As the calculations have demonstrated, the presence of sharp boundaries in the two-layer model leads to interference effects in the spectral relations for the radiation coefficient of the system for layers with thicknesses of h=1 to 10 mm, which qualitatively contradicts the experiment. The transient dielectric layer, for example, with parameters that vary by the hyperbolic tangent law, eliminates this deficiency [2].

Figure 2 shows models in which both the dispersion properties of the emulsion structure according to (1)-(2) and the disturbance of integralness of the smooth water surface by its bubbles are illustrated. In the case of a nonuniform foam layer, the role of the polyhedral structure in the formation of radiation reflects the smooth dielectric transition from the emulsion monolayer to the air. Both models correspond well to the experimental data.

The radiation transport theory also gives quite high values of the emissive power of the investigated surface. In the approximation of a nondissipating medium which it is possible to consider a nondisperse layer of bubbles of uniform thickness to be, the radiation coefficient of the system κ_p is defined by the expression

$$\varkappa_p = 1 - r'_p e^{-2\Gamma \sec\theta} \quad (P=B,\Gamma), \tag{3}$$

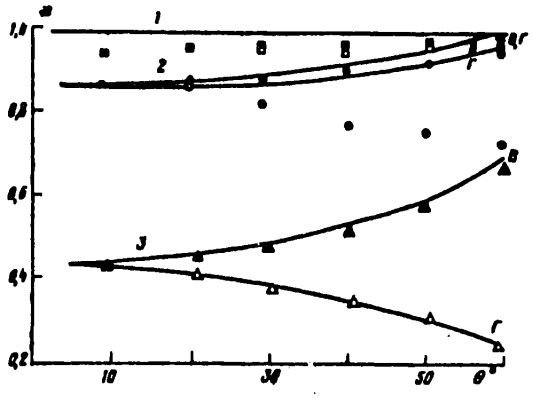

Figure 1. Polarization functions of the radiation coefficient of the water surface covered with foam (λ=0.8 cm; T_0=300 K).
1 — h=10 mm; 2 -- h=1 mm; 3 -- smooth water surface;
Δ, •, ■-r; Δ, o, □-B -- experiments; —— -- calculation by (3);
δ=0.05 mm.

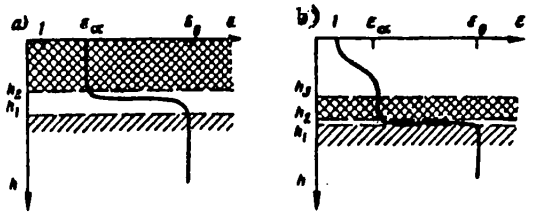

Figure 2. Electrodynamic models of the "water-foam" system:
a -- emulsion structure h_1=1.3 mm; h_2=1 mm;
b -- nonuniform structure h_1=10.3 mm; h_2=10 mm; h_3=8 mm;
the transient layer is given by the hyperbolic tangent law.

where r_p is the Fresnel reflection coefficient of water surface and $\tau=h\int\sigma_e(r)F(r)dr$ is the "optical thickness" of the polydisperse layer. As follows from (3), the equation for τ leads to smoothing of the polarization differences in the angular functions $\kappa_p(\theta)$. In the millimeter range this is manifested much more strongly than the experiment shows (see Figure 1). The spectral functions $\kappa_p(\lambda)$ calculated by (3) coincide well with the experimental functions in the case of an emulsion layer of thickness h~1 to 2 mm.

The authors thank I. B. Vasil'kov for the assistance rendered in performing the computer calculations.

BIBLIOGRAPHY

1. Amirkhanyan, V. R., Bespalova, Ye. A., Bulatov, M. G., et al., TRUDY [Works of the Main Geophysics Observatory], No 371, 1976, p 134.

2. Bordonskiy, G.S., Vasil'kova, I. B., Veselov, V. M., et al., KRATKIYE TEKSTY DOKLADOV NA 7-OM VSESOYUZNOM SIMPOZIUME PO DIFRAKTSII I RASPROSTRANENIYU VOLN. [Brief Texts of Reports at the 7th All-Union Symposium on Wave Diffraction and Propagation], Rostov-na-Donu, Vol 2, 1977, p 272.

3. Dombrovskiy, L. A., IZV. AN SSSR [News of the USSR Academy of Sciences], Physics of the Atmosphere and Ocean, Vol 10, No 7, 1974, p 720.

4. Van de Hulst, G., RASSEYANIYE SVETA MALYMI CHASTITSAMI [Scattering of Light by Small Particles], IL, Moscow, 1961.

10845
CSO: 8144/1010

UDC 551.521

MEASURING SMALL-SCALE ELEMENTS OF WAVES AND FOAM DURING MICROWAVE STUDIES OF THE SEA SURFACE

Moscow NEKONTAKTNYYE METODY IZMERENIYA OKEANOGRAFICHESKIKH PARAMETROV in Russian 1981 pp 43-46

[Article by B. M. Andreyev, V. V. Vinogradov and B. A. Pomytkin]

[Text] Annotation. A study is made of the results of natural studies of foam cover and the gravitational-capillary range of wind waves for ocean and lake conditions.

The emissive power of the water surface in the microwave range varies within broad limits and depends on the state of the sea--the presence of wind waves and foam on its surface. The experimental relations proposed by different authors for the radiobrightness temperature of the surface as a function of the degree of covering of the sea by foam permit estimations of the driving wind velocity.

In order to obtain natural data on this problem, the Leningrad division of the State Oceanographic Institute participated in 1976 in the work of the Soviet-American SAMEX-76 Expedition, during which on board the scientific research ship "Akademik Korolev" comprehensive oceanographic studies were made in the North Pacific. The wind waves and foam were photographed using the AFA-37 camera, which was fastened to a special suspension on the navigating bridge 15 meters above sea level. The pictures were taken from the leeward side of the ship.

The perspective photographs of the sea obtained during this operation offer the possibility of determining the basic elements of wind-driven waves and estimation of the area of the sea surface covered with foam.

However, the processing of perspective images is a complicated and difficult matter in view of variability of the scale of the photographs over the area of the frame. In order to simplify the processing of the photographs, we used a special photogravimetric grid taking into account the scale and magnitude of the perspective distortion of the frame caused by the inclination of the optical axis of the instrument, under the condition of taking the photographs when the ship was on an even keel. The processing reduced to analyzing the foam and the wave elements.

At first, the wave crests were distinguished on the photograph. Depending on the length of the wave crest, the cross section of the profiles was taken in which the wave lengths were measured--the photogravimetric grid was applied to the photographs for the measurements. By using the meter on the photograph, the distance between the wave crestswas determined which was transferred to the graphs on the scale for the given distance from the ship, which made it possible to determine the wavelength. A statistical series was used for the processing.

The sections of the sea covered with foam were determined on the photographs with the help of a master curve. The master curve was applied to the photographs in such a way that the grid lines were parallel to the principal horizontal of the photograph. Then using a measuring rule, the length of the section occupied by the foam or pure water was found on each of the applied lines. Reducing the obtained distances occupied by foam to the total length of all the lines, the amount of foam was found in percentage ratio of the entire section of the body of water.

As a result of processing a large number of wave and foam photographs it is possible to draw the conclusion that the photographs give a distorted picture of the wave situation near the hull of the ship, both with respect to the wave parameters and with respect to the amount of foam. When sighting the camera or microwave radiometers up to angles of 45°, the data correspond to the true picture of the wave field; at sighting angles of more than 45° the data on the amount of foam are low, and the radiometer readings are distorted.

Simultaneously with photographing a wavy sea surface, a visual determination was made of the waves and foam from the direction finding bridge at a height of 15 meters in the parts of the body of water not subjected to the influence of the ship's hull.

The processing and analysis of the obtained materials for the Pacific Ocean during the SAMEX-76 experiments and also analogous data obtained on the "Bering" expedition in 1973, made it possible to establish that there is a relation of the type

$$P = 0.12 \cdot W^2$$

between the area of the sea occupied by the foam and the wind force not exceeding 15 to 20 m/sec, where P is the relative area of the sea surface occupied by foam in percentages; W is the wind velocity, m/sec.

The degree of coverage of the ocean with foam directly connected with the wind velocity offers the possibility of estimating its contribution to the radiobrightness temperature of the water when interpreting microwave measurements.

Analogous work with respect to photographing small-scale characteristics of a disturbed surface was done also in small inland bodies of water such as Krasnoye Lake on the Karelian Isthmus with an area of about 15 km^2. The survey was also made using the AFA-37 camera installed 7 meters above the water surface on a special mast with small support area. The scale of the survey was 1:100.

The best quality photographs of the water surface in the presence of waves were obtained under cloud conditions of force 8. The photographs were taken with surface illumination in the photographed zone by sunlight and inthe shadow of clouds. The

photographs were taken at solar angles of 15 to 20°, with average wind velocity of 4 to 6 m/sec, with gusts up to 10 m/sec, the fetch reached 5 km, and the wave height was up to 30 cm [sic].

On the photographs made in sections illuminated by the sun, in the glare zone, an image of waves in the gravity-capillary range of the spectrum was obtained; the minimum recorded wave lengths were 1 cm. A statistical analysis of the wavelength distribution of the gravity-capillary range of the spectrum demonstrated that the wavelength distribution in this section of the spectrum differs somewhat from the wavelength distribution in the gravity range--less selective variability is observed in one section obtained on the image of one wave of the basic system, and much more selective variability on the cross sections located on the other waves of the basic system. The predominant dimensions of the waves in the gravity-capillary range were in the given case 4 to 5 cm with respect to wavelength.

A characteristic feature of the image of small capillary waves with lengths of 1 to 2 cm is sharp variability of the direction of propagation exceeding 50°, and a partially observed relation of the wave systems of minimum dimensions to the waves of predominant sizes of the gravity-capillary range of the spectrum.

The three-dimensionality index of the capillary-gravity waves is less than the developing and steady-state wind waves of the basic energy bearing region of the gravity range, the crest length of the capillary-gravity waves in individual cases can exceed 10 times the wavelength of this range.

The photographs taken with a wind velocity of 2 to 4 m/sec did not offer the possibility of recording waves in the capillary range as a result of their small dimensions, which is confirmed by the dimensions of the individual hotspot sections. In the photographs obtained for a wind velocity of 5 to 9 m/sec, the dimensions of the individual hotspot sections were less than 0.1 mm on the film, that is, no more than 1 cm in nature; when photographing in calmer weather the average size of individual hotspots was 0.2 mm or more, that is, it exceeded 2 cm in nature. A decrease in surface curvature by more than twofold indicates a significant decrease in the surface slopes, that is, small wave heights in the gravity-capillary range. Their existence is confirmed by the fact that the maximum dimensions of the individual hot spots for small wind velocities are also less than 0.1 mm, but, few of them are observed, and they are arranged randomly, which does not offer the possibility of deciphering the waves in the gravity-capillary range of the spectrum developed in the presence of a weak wind.

Conclusions:

1. Perspective photography of a disturbed surface with small angles of inclination of the optical axis permits us to obtain an image of the characteristic of the state of the sea surface. By the photograph it is possible to determine the amount of foam and the plan characteristics of the waves in the gravity-capillary range of the spectrum. The scale of the photograph is selected insofar as possible within the limits of 1:100 to 1:300. The photographic latitude of the film and its sensitivity must be maximal.

2. According to the data of marine measurements by the authors, the amount of foam on the surface of the sea depends on the square of the wind velocity if the wind velocity does not exceed 15 to 20 m/sec.

3. The characteristic dimensions of the wavelength of the gravity-capillary range with a wind velocity of 5 to 9 m/sec according to the measurement data for a small body of water are 4 to 5 cm and 1 to 2 cm, waves of smaller dimensions are related to larger waves. The variability of the wavelengths in the capillary-gravity range is determined by the gravity waves of the basic energy bearing region of the spectrum --within the limits of one wave the variability is small. For adjacent gravity waves strong variability of the plan characteristics of the capillary-gravity waves is observed.

10845
CSO: 8144/1010

UDC 551.521

PROBLEM OF DETERMINING WIND VELOCITY AT WATER SURFACE BY MEASUREMENTS OF MICROWAVE EMISSION OF EARTH-ATMOSPHERE SYSTEM

Moscow NEKONTAKTNYYE METODY IZMERENIYA OKEANOGRAFICHESKIKH PARAMETROV in Russian 1981 pp 47-50

[Article by P. V. Lyushvin]

[Text] Annotation. A method is proposed for separation of the microwave emission of the atmosphere and the sea surface in the total emission of the earth-atmosphere system by simultaneous measurements of wavelengths of 0.8, 1.35 and 1.6 cm. An example of its use is presented in the experimental data. By the proposed method it is possible better to find the actual values of the microwave emission of the sea surface and the atmosphere; consequently, it is possible more precisely to determine the wind velocity at the surface of the water and the integral characteristics of the atmosphere in storm regions.

1. The determination of the wind velocity at the surface of the water, the total mass of the water vapor in the atmosphere and the water reserve in the clouds is an important problem of satellite hydrometeorology.

At the present time when calculating these characteristics the methods of ground thermo-microwave imaging radar are used [1, 3, 4]. In order to solve these problems from satellites, it is necessary first to separate the contributions of the atmospheric emission and the emission from the sea surface to the total radio emission of the earth-atmosphere system. In the methods with respect to remote determination of the wind velocity at the sea surface, as a rule, the mean statistical distorting influence of the atmosphere is considered or cloudless meteorological situations are selected. When finding the integral characteristics of the atmosphere by microwave radiometric measurements, it is assumed that the ocean emission does not depend on the state of its surface. Such assumptions limit the possibility of the application of these methods and lead to significant errors[1, 4].

In the given case a study is made of the method of separating the microwave contributions of the emission of the atmosphere and the sea surface in the total emission of the earth-atmosphere system with respect to frequently used simultaneous measurements on wavelengths of 0.8, 1.35 and 1.6 cm.

2. For calculation of radiobrightness temperatures (T_{bright}) from artificial earth satellites, we use the simplified solution of the radiation transport equation in the atmosphere from measurements in the nadir of the following type:

$$T_{R,\lambda} = T_0 \varkappa_\lambda \exp(-\tau_\lambda) + T_\lambda + T_\lambda(1-\varkappa_\lambda)\exp(-\tau_\lambda), \quad (1)$$

where T_0 is the temperature of the sea surface, κ_λ is the sea surface emission coefficient on a wavelength λ (for a smooth water surface $\kappa_\lambda = \kappa_{\lambda,\ smooth}$), τ_λ is the optical thickness of the atmosphere, T_λ is the radiobrightness temperature of the atmosphere.

In a system of three equations of the type of (1) for wavelengths of 0.8, 1.35 and 1.6 cm κ_λ and T_λ are known (the temperature of the sea surface will be considered known with accuracy to $\pm$2K; between the optical thickness of the atmosphere and the natural radiation of the atmosphere there is a relation close to functional [1]). In order to solve the system, it is necessary to supplement it by three equations (conditions) relating the system parameters. The conditions of quasiconstancy of the ratios $\Delta\kappa_\lambda$ on pairs wavelengths ($\Delta\kappa_\lambda = \kappa_\lambda - \kappa_{\lambda,\ smooth}$) from references [1, 2] are taken as the two equations:

$$\Delta\varkappa_{0,8} / \Delta\varkappa_{1,35} = 1{,}3 \pm 0{,}2; \quad (2)$$

$$\Delta\varkappa_{1,35} / \Delta\varkappa_{1,6} = 1{,}1 \pm 0{,}1. \quad (3)$$

Let us find the third equation from the condition of equality of the relations between the atmospheric emission on the investigated wavelengths. For individual meteorological situations, for example, in the absence of clouds, the magnitude of the ratio between the radiation of the atmosphere on pairs of waves (especially, for the pair of waves of 0.8 and 1.6 cm) is constant. In the presence of hydrometeors in the atmosphere, constancy of such relations is not maintained [1, 3]. A stable relation between the radiobrightness temperatures of the atmosphere on these wavelengths for any meteorological conditions has been obtained for analysis of the materials of model calculations of the radiothermal emission of the atmosphere by the data of 400 radiosondes of the weather ships of the North Atlantic kindly made available to us by Ye. P. Dombkovskaya [4]:

$$T_{1,6,p} = \frac{0{,}62\, T_{1,35}}{(T_{1,35}/T_{0,8} + 0{,}62)}, \quad (4)$$

where T_λ is the radiobrightness temperature of the atmosphere calculated by the radiosonde data; $T_{\lambda,\ p}$ is the radiobrightness temperature of the atmosphere calculated by this relation.

In a total of 2% of the cases out of 400, $T_{1.6,\ p}$ differed from $T_{1.6}$ by more than 20%. Equation (4) was checked out on independent data on the radiothermal emission of the atmosphere [3]. For model calculations of the radiobrightness temperatures of the atmosphere $T_{1.6,\ p}$ differed from $T_{1.6}$ basically by no more than 10%, and for the experimental data, by 20%.

The equation for the relation between the attenuation of the emission $\exp(-\tau_\lambda)$ by the atmosphere and its natural emission T_λ was obtained by the above-described data [4]:

$$\exp(-\tau_\lambda) = 1 - \beta\ 10^{-3}\ T_\lambda\ , \qquad (5)$$

β is a numerical coefficient equal to 3.5 ± 0.2 for the tropical atmosphere, 3.7 ± 0.2 for the temperate atmosphere and 3.8 ± 0.2 for the polar atmosphere.

When solving a system of equations (1) to (5) for 0.8, 1.35 and 1.6 cm waves, the errors in the determined radiobrightness temperatures of the atmosphere on 1.35 and 1.6 cm waves are 15 to 20%, and the microwave emission of the sea surface, ±3 to 4 K.

3. This method was checked on the materials from the Soviet-American "Bering" experiment. For the measured values of the radiobrightness temperatures on wavelengths of 0.8, 1.35 and 1.6 cm ($T_{bright,\ \lambda}$ are presented in reference [4]), values of the microwave emission of the atmosphere and the sea surface ($\kappa_\lambda T_0$) were calculated by the above-described method. The figure shows the behavior of the microwave emission of the sea surface on a wavelength of 1.35 cm ($\kappa_{1.35}T_0$) along the flight path of a "Convair-990" aircraft from 2 March 1973, and also the behavior of the wind velocity at the water surface (V, m/sec) [2].

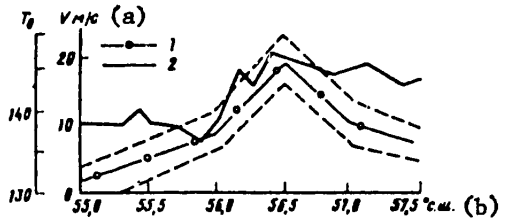

Results of determining the microwave emission of the sea surface ($\kappa_{1.35}T_0$) on a wavelength of 1.35 cm with respect to the path (1), wind velocity (V) and water surface (2)

Key:
a. V, m/sec
b. ° north latitude

From the figure it is obvious that the microwave emission of the sea surface follows the behavior of the wind velocity and assumes a maximum value when the wind velocity reaches 20 m/sec. The dotted line on the figure indicates the extreme possible values of $\kappa_{1.35}T_0$ which can occur during calculations by this procedure. When analyzing the microwave emission data for the sea along the path, it is possible to isolate regions of values of $\kappa_{1.35}T_0$ corresponding to the wind velocities of less than 12 m/sec, from 12 to 18 m/sec and more than 18 m/sec. The obtained increase in the microwave emission of the sea with an increase in wind velocity as a whole coincides with analogous values presented in references [1, 2].

4. The application of this method during microwave measurements will permit better separation of the microwave emission of the atmosphere and the sea surface in the outgoing radiation of the earth-atmosphere systems; consequently, it permits better recognition of the storm wave zones, more precise calculation of the integral atmospheric characteristics, and expansion of the class of solved hydrometeorological problems without creating additional apparatus.

In conclusion, I express my appreciation to Ye. P. Dombkovskaya for constant attention to this work.

BIBLIOGRAPHY

1. Basharinov, A. Ye., Gurvich, A. S. and Yegorov, S. T., RADIOIZLUCHENIYE ZEMLI KAK PLANETY [Radio Emission of the Earth as a Planet], Moscow, Nauka, 1974, 188 pp.

2. Vilkheyt, T., Fowler, M., Stambach, G. and Gloersen, P., "Determination of Atmospheric Parameters by Microwave Measurements During the 'Bering' Expedition," SOVETSKO-AMERIKANSKIY EKSPERIMENT "BERING" [Soviet-American "Bering" Experiment], Leningrad, Gidrometeoizdat, 1975, pp 15-42.

3. Gorelik, A. G., Kalashnikov, V. V., Raykova, L. S. and Frolov, Yu. A., "Radiothermal Measurements of Atmospheric Moisture and the Integral Water Content of Clouds," IZV. AN SSSR. FIZIKA ATMOSFERY I OKEANA [News of the USSR Academy of Sciences, Physics of the Atmosphere and Ocean], Vol 9, No 9, 1973, pp 928-936.

4. Dombkovskaya, Ye. P. and Rabinovich, Yu. I., "Analysis of the Results of Measuring the Radio Wavelength Emission of the Atmosphere during the 'Bering' Experiment (Version A)," SOVETSKO-AMERIKANSKIY EKSPERIMENT "BERING," Leningrad, Gidrometeoizdat, 1975, pp 43-60.

10845
CSO: 8144/1010

UDC 551.321.6:621.384.326

EXPERIMENTAL RESULTS OF JOINT USE OF INFRARED AND MICROWAVE RADIOMETERS FOR REMOTE DETERMINATION OF SEA ICE CHARACTERISTICS

Moscow NEKONTAKTNYYE METODY IZMERENIYA OKEANOGRAFICHESKIKH PARAMETROV in Russian 1981 pp 51-56

[Article by V. V. Bogorodskiy, A. N. Darovskikh, Ye. A. Martynova and V. A. Spitsyn]

[Text] Annotation. A study is made of the results of an experiment to investigate the characteristics of ice by passive methods in the infrared and microwave bands.

In the experimental studies of the drifting snow-ice cover performed in the spring of 1977 in the Arctic, a set of infrared (spectral range 8 to 14 microns) and microwave (wavelength 1.6 cm) equipment was used, supplemented by aircraft actinometric instruments. The goal of the experiment was as follows: 1) the study of the possibility of practical application of the method of infrared radiometery to estimate the thickness of the ice cover; 2) obtaining the characteristics of radiothermal emission of ice of different age gradations; 3) determination of the morphological characteristics of the ice cover.

Remote measurements were accompanied by obtaining monitoring data and other information about the parameters of the snow and ice cover and the distribution of the meteorological elements in the ice layer by contact means when landing the An-2 aircraft on the investigated ice fields. During the period from 19 April to 10 May, 15 ice fields of different age were examined, which were the most uniform with respect to thickness and maximal with respect to extent. Data on the air temperature, wind velocity, radiation budget and temperature of the underlying surface measured by an infrared radiometer was used to estimate the thickness of the ice. The calculation was performed according to the expression obtained from the solution of the equation of thermal conductivity for the uniform steady-state problem [1]. The calculation results are presented in Table 1. As can be seen, in a number of cases the thicknesses of the ice cover determined by its natural infrared radiation agree satisfactorily with the control measurements. At the same time, for points No 3a and No 8 the error in the analysis reaches 65 to 50%. The existing divergences can be explained by a number of causes: namely, the errors in the model of the snow and ice cover used in the calculation, inaccuracies in determining the hydrometeorological parameters and, in particular, determining the radiation budget of the surface of the snow and ice cover, errors in measuring the surface temperature by the infrared radiometer.

Table 1. Estimate of the Thickness of the Snow and Ice Cover by its Natural Infrared Radiation

Дата, № точки (a)	$T_{пов}$ °C (b): радиационная (c)	термодинамическая (d)	$h_{сн}$ см (e)	$\rho_{сн}$ г/см (f)	$T_в$ °C (g)	Температура на границе (h): воздух-снег (i)	снег-лед (j)	v м/с (k)	P мбар (l)	F кал/см²·мин (m)	Q кал/см²·мин (n)	R кал/см²·мин (o)	$H_л$ см (p): измеренная контактно (q)	по данным ИК радиометра (r)
06.05.77 38	-16,1	-15,1	3,4	0,23	-14,6	-14,3	-9,9	5,1	1013,2	-0,052	0,47	0,033	40	66
04.05.77 4	-18,3	-17,3	4,8	-	-18,7	-17,4	-7,1	1,7	1013,2	-0,059	0,64	0,056	30	33
05.05.77 7	-20,8	-19,8	2,8	0,25	-19,4	-19,6	-13,7	1,4	1013,2	-0,055	0,22	-0,015	90	82
06.05.77 8	-15,6	-14,6	5,1	0,22	-15,6	-14,3	-11,7	6,0	1013,2	-0,024	0,37	0,043	93	43
07.05.77 10	-15,5	-14,5	4,2	0,35	-12,8	-11,2	-8,8	1,9	1013,2	-0,056	0,60	0,053	60	60

Key:

a. Date, point No
b. $T_{surface}$, °c
c. Radiation
d. Thermodynamic
e. h_{snow}, cm
f. ρ_{snow}, g/cm
g. T_b, °C
h. Temperature at the interface
i. Air-snow
j. Snow-ice
k. v, m/sec
l. P, mbars
m. F, cal/cm^2-min
n. Q_{cal/cm^2-min}
o. R_{cal/cm^2-min}
p. H_{ice}, cm
q. Contact measured
r. According to the infrared radiometer data

Table 2.

Age characteristics of ice	$\langle T_{bright} \rangle$ K	$\langle \sigma \rangle$
Gray ice (10-15) cm	230	0.93
Gray-white (15-30) cm	239	0.97
Thick first-year white ice (30-70) cm	241	0.98
First-year ice of medium thickness (70-120) cm	239	0.98
Thick first-year (120-200) cm	228	0.95
Multiyear >200 cm	214	0.88

In the centimeter range, as a result of powerful absorption of radiowaves in the body of the ice there is no direct dependence of the radio wavelength emission on its thickness, beginning with gray ice (H=10 to 15 cm). However, as is noted in [3], for the microwave region of the spectrum strong dependence of the radiation coefficient of sea ice on its age gradations is characteristic. Table 2 gives

the average values of the brightness temperatures and radiation coefficients of ice of different age obtained as a result of flights over the investigated ice fields. The first-year white ice has the greatest coefficient of emission. Increasing the brine content in gray ice leads to reduction of $\langle\varepsilon\rangle$ to 0.93. The decrease in the emission coefficient of multiyear ice, in spite of the almost desalinated radiating layer, is caused by scattering of the radio waves on air bubbles in the upper layers of the ice cover.

For statistical estimation of the brightness temperature range characteristic of ice of defined age, an analysis is made of the results of measurements performed during one day of flying over 342 ice fields with a total extent of 120 km. Figure 1 shows the distribution histograms T_{bright} for white ice (a), first-year ice of medium thickness (b) and thick ice (c), multiyear ice (d). Table 3 contains statistical characteristics of the brightness temperatures of various types of ice. It is obvious that for each age gradation of ice there is a characteristic range of values of T_{bright} (for fixed air temperature). However, with great probability (0.92) it is possible to distinguish only thin, first-year ice and first-year ice of medium thickness from multiyear and thick first-year ice. On converting to gray and newly formed ice, a reduction in T_{bright} to the brightness temperature level characteristic of multiyear ice is noted. The indicated ambiguity of the interpretation is eliminated with simultaneous use of the information obtained by the infrared channel. Figure 2 shows a fragment of the synchronous recording of radiation and brightness temperatures illustrating the possibility of estimating the thickness of the floating snow and ice cover by a set of infrared and microwave equipment.

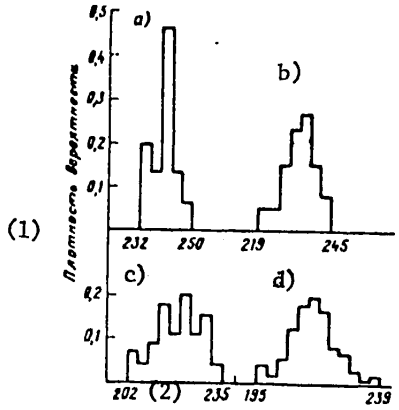

Figure 1

Key:
1. Probability density
2. Brightness temperature, K

Table 3

Age characteristic of the ice	$\langle T_{bright} \rangle$ K	$\sigma_{2\nu}$ °C	Confidence interval Probability 0.8	Probability 0.85	Probability 0.9
Newly formed ice	215	6	-	-	-
Gray ice	222	3	-	-	-
Gray-white ice	241	4	-	-	-
Thin first-year white ice	240	4.3	234-245	234-246	233-246
First-year ice of medium thickness	233	6.1	225-240	224-240	223-242
Thick first-year ice	220	8.6	209-230	208-231	207-233
Multiyear ice	214	9.0	203-224	202-226	200-228

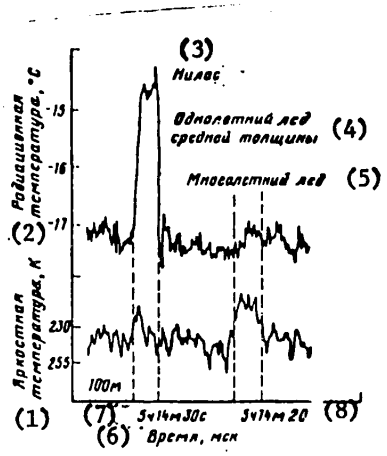

Figure 2

Key:
1. Brightness temperature, K
2. Radiation temperature, °C
3. Newly formed ice
4. First-year ice of medium thickness
5. Multiyear ice
6. time, microseconds
7. 5 hours 14 minutes 30 seconds
8. 5 hours 14 minutes 20 seconds

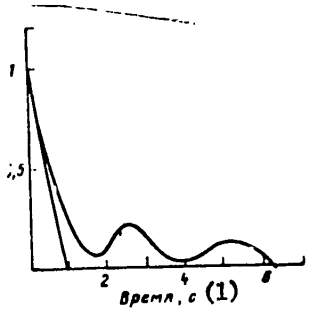

Figure 3

Key: 1. time, seconds

The surface of the ice fields is nonuniform both with respect to its electric characteristics and with respect to geometric characteristics. Therefore, the recorded fluctuations of the thermal emission of the ice fields can be considered as a random process both in time and in space. Since the time interval of recording is significantly less than the time scale of the processes, under the influence of which the thermal emission is formed, the investigated random process can be considered steady-state.

For statistical investigation, measurements were selected which were performed on multiyear and first-year ice extending more than 1000 meters. The discreteness of the readings was 0.5 second. As the basic characteristics, the autocorrelation function $R(\tau)$ and the dispersion σ^2 were selected. The results of the calculation demonstrated that all the autocorrelation functions can be reduced to two types (Figure 3): I -- functions monotonically decreasing with time ($dR/d\tau<0$); II -- functions with oscillatory nature of decrease ($dR/d\tau$--sign variable). The characteristic feature of the autocorrelation functions type II is greater time of complete damping of the correlation. Here the attenuation time τ_1, where $dR/d\tau|_{\tau=\tau_1}=0$, is approximately equal to the time of complete attenuation of the correlation for type I functions. The presence of type II autocorrelation functions permits the assumption of the existence of statistical relations with large and small autocorrelation radii. Small autocorrelation radii (60 meters) of both the radiation and brightness temperatures for first-year ice coincide with the spatial variability of the thicknesses (50 to 70 meters) obtained in reference [2]. The large autocorrelation radii (100 to 300 meters) are obviously related to the spatial distribution of the unevennesses of the upper boundary of the ice, and they require additional experimental refinement.

The performed research permits the following conclusions to be drawn:

1. For the existing level of accuracy of determination of the factors forming the thermal relief of the underlying surface, the method of infrared radiometry is effective only for estimating the thickness of young ice.

2. The complex use of infrared information and microwave channels will permit indexing of the following age groups of sea ice: newly formed ice, first-year white ice of medium thickness, first-year thick and multiyear ice.

3. The application of the apparatus of correlation functions when processing the recorded values of the natural thermal emission of the floating snow and ice cover offers the possibility of determining some of its morphological parameters.

BIBLIOGRAPHY

1. Bogorodskiy, V. V., Martynova, Ye. A. and Spitsyn, V. A., "Study of the Formation of Natural Thermal Emission of Snow and Ice Cover of the Arctic Sea as Applied to the Problems of Infrared Radiometry," TRUDY GGO [Works of the Main Geophysics Observatory], No 399, 1977, pp 87-114.

2. Buzuyev, A. Ya. and Dubovtsev, V. F., "Statistical Characteristics of Some Parameters of the Ice Cover in the Arctic," TRUDY AANII [Works of the Arctic and Antarctic Scientific Research Institute], Vol 303, 1971, pp 166-179.

3. Rabinovich, Yu. I., Loshchidov, V. S. and Shul'gina, Ye. M., "Analysis of the Results of Measuring the Characteristics of the Ice Cover (Version C)," SOVETSKO-AMERIKANSKIY EKSPERIMENT "BERING" [Soviet-American "Bering" Experiment], Leningrad, Gidrometeoizdat, 1975, pp 294-313.

10845
CSO: 8144/1010

UDC 551.521:551.467

MICROWAVE STUDY OF SEA ICE

Moscow NEKONTAKTNYYE METODY IZMERENIYA OKEANOGRAFICHESKIKH PARAMETROV in Russian 1981 pp 57-60

[Article by P. A. Nikitin]

[Text] Annotation. A study is made of the results of model calculations of natural microwave emission of sea ice. A comparison of the calculated data with the experimental data indicates the applicability of a model of thermal radio wavelength emission of random nonuniform layered media with nonuniform temperature profile for description of the investigated phenomenon. The frequency and angular relations are presented for the emissive power of Arctic pack ice. It is demonstrated that the experimentally observed increase in the emissive power of annual ice (by comparison with pack ice) is caused to a higher degree by the temperature distribution with respect to thickness of the ice than by scattering.

For proper interpretation of microwave information obtained using microwave radiometers installed on board an aircraft or artificial satellite, it is necessary to know the radiation characteristics of the sounded surface. Unfortunately, experimental work in studying microwave emission of sea ice is not of a systematic nature, and statistically justifiable relations have still not been obtained. This deficiency can be made up for to some degree by model calculations.

As is known, real sea ice is a nonisothermal layered medium with air, brine inclusions and other nonuniformities. Taking this into account, a model of thermal radio wavelength emission of a randomly nonuniform layered medium with nonuniform temperature profile was selected for performing the calculations. The dielectric constant of this medium can be described as follows:

$$\left.\begin{aligned}\varepsilon &= \varepsilon(z)+\tilde{\varepsilon}(z)\\ \varepsilon(z) &= \varepsilon_1+i\varepsilon_2(z)\end{aligned}\right\}\quad \begin{aligned}&\langle\tilde{\varepsilon}(z)\rangle = 0,\\ &\varepsilon_2(z)\ll\varepsilon_1.\end{aligned}$$

A detailed description of the model with derivation of the basic relations is presented in reference [1]. The output parameters for the calculations are the dielectric constant, the characteristics of its variability and the temperature profile. The scattering coefficients (Kp), phase factors (P) and radiobrightness temperature (T_{bright}) can be calculated by these data for vertical (B) and horizontal (Г) polarizations:

$$K_{pr}=\frac{k^2\Delta l}{\cos\theta}\left[\frac{1+2k^2l^2\cos^2\theta}{1+4k^2l^2\cos^2\theta}\right];$$

$$P_r^{вп}=\left[\frac{1+4k^2l^2\cos^2\theta}{1+2k^2l^2\cos^2\theta}\right],\quad P_r^{н}=[1+2k^2l^2\cos^2\theta]^{-1};$$

$$K_{pв}=\frac{k^2\Delta l}{2\cos\theta}\left[\frac{1+4k^2l^2\cos^2\theta+\cos^22\theta}{1+4k^2l^2\cos^2\theta}\right];$$

$$P_в^{вп}=\frac{2[1+4k^2l^2\cos^2\theta]}{1+4k^2l^2\cos^2\theta+\cos^22\theta},\quad P_в^{н}=\frac{2\cos^22\theta}{1+4k^2l^2\cos^2\theta+\cos^22\theta};$$

$$T_A=\frac{2\gamma(1-R_0^2)}{(\alpha+\gamma)-R_0^2(\alpha-\gamma)}\left[T_z+T'\frac{\alpha}{\alpha+\delta\cos\theta}\right],$$

$$\alpha=[K_p+\gamma]\{(1-A)[1-(\frac{A}{2})P^{вп}+(\frac{A}{2})P^{н}]\}^{1/2},$$

$$A=\frac{K_p}{K_p+\gamma}.$$

Here $k=2\pi/\lambda$ is the wave number, γ is the absorption coefficient, R_0 are the Fresnel coefficients, θ_0 is the sighting angle, $T(z)=T_z+T'\exp(-\delta z)$ is the temperature profile. The correlation function for $\tilde{\varepsilon}(z)$ is $\langle\tilde{\varepsilon}(z_1)\cdot\tilde{\varepsilon}(z_2)\rangle=\Delta\varepsilon^2\exp(-|z_1-z_2|\ell^{-1})$.

The data on the electrophysical characteristics of first-year and multiyear (pack) sea ice obtained under natural conditions by the coworkers of the Arctic and Antarctic Scientific Research Institute are presented in [2]. The values of γ, Δ and ℓ for pack ice were calculated by solving the inverse problem with respect to the experimental data from [3]. The results of calculations of the radiobrightness temperature normalized for the thermodynamic temperature of the ice surface (which is usually recorded by remote measurements) are presented in Figures 1-4.

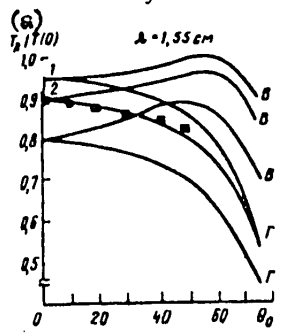

Figure 1. Microwave emission of pack ice for different sighting angle:
1 -- $\Delta=0$; 2 -- $\Delta=0.1$, $\ell=0.01$;
3 -- $\Delta=0.2$, $\ell=0.01$; -- experimental data from [3]; $T(z)=258-14\exp(-0.01\,z)$
Key:
a. $T_{bright}/T(0)$

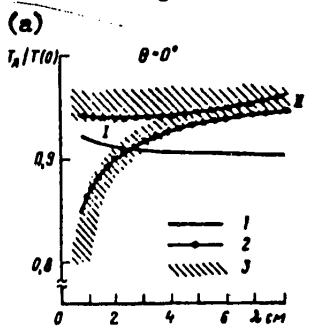

Figure 2. Microwave emission of marine Arctic ice:
I -- first-year ice, II -- pack ice;
1 -- uniform medium, 2 -- considering scattering and distribution T(z),
3 -- experimental data from [4].
Key: a. $T_{bright}/T(0)$

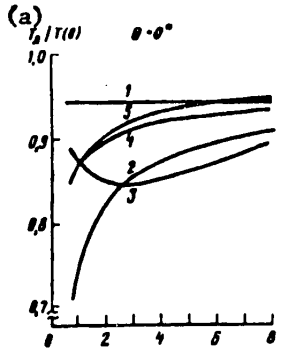

Figure 3. Microwave emission of pack ice with different scattering parameters:
1, 2, 3, 4 -- T(z)=T(0)=258 K,
5-- T(z)=272-14exp(-0.02z);
1 -- Δ=0, 2 -- Δ=0.2, ℓ=0.01,
3 -- Δ=0.01, ℓ=0.1; 4,5 -- Δ=0.1,
ℓ=0.01
Key:
a. $T_{bright}/T(0)$

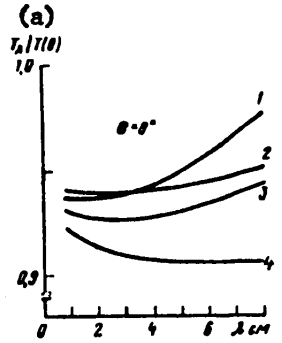

Figure 4. Microwave emission of first-year ice with different internal temperature profiles:
1 -- T(z)=272-25 exp(-0.1z),
2 -- T(z)=272-14 exp(-0.3z),
3 -- T(z)=272-14 exp(-0.1z),
4 -- T(z)=T(0)=258 K
Key:
a. $T_{bright}/T(0)$

Analysis of the obtained variables permits certain conclusions to be drawn:

The selected model of radiation is entirely applicable for calculations of the natural microwave radiation of sea ice, which is confirmed by comparing (see Figure II) the calculated and independent experimental data from [4];

With an increase in the vertical temperature gradient, the value of $T_{bright}/T(0)$ also increases, the more, the longer the emission wavelength (see Figure III-4, 5 and Figure IV). This is entirely legal, for the absorption coefficient in sea ice is inversely proportional to the wavelength and, thus, the long wave emission is formed in a thicker layer, the effective temperature of which is higher than T(0). The increase in effective temperature also explains the fact that T_{bright} of first-year ice turned out to be higher than T_{bright} of multiyear ice even at $\lambda>3$ cm where the scattering is insignificant (for equal T(0)), although the salinity of the multiyear ice is appreciably less and, consequently, the emissive power must be more [3];

In connection with the fact that the scattering is of a selective nature, the position of the minimum on the spectral curve can indicate peculiarities in the internal structure of the ice;

Obtaining the angular and spectral relations of the emissive power of sea ice can be used when developing the corresponding procedure for interpreting the microwave measurements.

BIBLIOGRAPHY

1. Tsang, L. and Kong, J. A., "The Brightness Temperature of a Half-space Random Medium with Nonuniform Temperature Profile," RADIO SCI., Vol 10, No 12, 1975, pp 1025-1033.

2. Bogorodskiy, V. V. and Khokhlov, G. P., "Anisotropy of the Dielectric Constant and Absorption of Arctic Drift Ice in the Microwave Range," ZHURNAL TEKHNICHESKOY FIZIKI [Technical Physics Journal], Vol 47, No 6, 1977, pp 1301-1305.

3. Gloersen, P., Nordberg, W., Schmugge, T. J. and Wilheit, T. T., "Microwave Signatures of First-Year and Multiyear Sea Ice," JOURN. OF GEOPH. RES., Vol 78, No 18, 1973, pp 3564-3572.

4. Gloersen, P., Chang, T. C., Wilheit, T. T. and Campbell, W. J., "Polar Sea Ice Observations by Means of Microwave Radiometry," Doc. X-652-73-341 November 1973, Goddard Space Flight Center, Maryland.

10845
CSO: 8144/1010

UDC 536.521.2:550.46

USE OF METHOD OF INFRARED RADIOMETRY TO STUDY TIME VARIABILITY OF HEAT EXCHANGE OF EASTERN ARCTIC SEAS WITH ATMOSPHERE

Moscow NEKONTAKTNYYE METODY IZMERENIYA OKEANOGRAFICHESKIKH PARAMETROV in Russian 1981 pp 61-66

[Article by A. I. Paramonov]

[Text] Annotation. An analysis is made of the experimental data from measuring the surface temperatures of the Chukchi and Eastern Siberian Seas in September for 4 years obtained by an infrared radiometer installed on an ice reconnaissance aircraft. The spatial distribution of the temperature field is considered to be a random process. The temperatures are interpolated to the nodes of a regular grid at which the heat budget components are calculated. The interyear variations of the heat fluxes are considered as fluctuations around a mean value.

The study of the thermal interaction of the polar seas with the atmosphere is an urgent problem of modern hydrometeorology. The difficulty of such a study is determined by the significant volume of information about the actual distribution of the physical parameters defining the heat exchange process. A variety of causes and interrelations permit consideration of their distribution in space and variability in time a random process. The temperature of the boundary layer or the film is important for calculations of the heat exchange elements of two media. The heat engineering interaction of the water-snow-ice surfaces with the atmosphere creates a complex thermal relief over the entire area of freezing seas. If we limit the investigated process to the time interval during which it is possible to consider the temperature on the average independent of time, then we obtain the three dimensional hydrometeorological temperature field which can be called the temperature surface, thermal relief. For practical construction of the thermal relief, as is shown in references[3-5], it is possible to use the data of infrared radiometry of the underlying surfaces.

In 1973, in the eastern sector of the Arctic, annually during the fall the Arctic Institute takes regular measurements of the surface temperature of the seas by an infrared radiometer installed on an ice reconnaissance aircraft. The work schedule on the aircraft is put together so that each 10-day period of the month studies are made of the same region. However, in the given region there is no repetition or unified scheme for constructing the tacks. Thus, for processing the aerial survey

data there is a set of random routes in a defined research area, along which the random temperature distribution of the underlying surfaces is measured. The methods of objective analysis of hydrometeorological fields are applicable to such data [2].

A ten-day period was selected as the unit time interval. At first, the operation of smoothing of the temperature field was performed, that is, calculation of the weighted mean values and uniform sections of its microscale fluctuations. Here the packing of the ice and number of different age gradations of it in the smoothing section were determined (hereafter these data were used to estimate the surface albedo). The operation of mathematical interpolation of the smoothed experimental values of the temperature was realized by calculating the approximation coefficients a_{pq} of two-dimensional functions by polynomials on the Minsk-32 computer.* At the nodes of the grid the temperatures F(x,y) were restored by the algorithm

$$F(x,y)=\sum_{q=0}^{t}\sum_{p=0}^{m} a_{pq}\,x^p y^q;$$

where m and t, the powers of the polynomials with respect to the arguments x and y, are selected equal to m=t=3, and the new origin of the coordinates (0, 0) was located at the center of a rectangle. The coordinates x, y were found on the parallels and meridians of a Mercator-projection map.

On the basis of analyzing regularity over the course of several years of temperature observations, the research region was defined. Then this region was divided into five rectangles including the western part of the Chukotskoye [Chukchi] Sea (rectangle 4 in Figure 1), Proliv Longa [Longa Strait] (5), the coastal zone of the East Siberian Sea (1) and two regions north of Wrangel Island (2, 3). The separation was made both from geographic and from physical arguments, considering the more uniform structure of the underlying surfaces. The rectangles differed in size (see Figure 1), but they had the same grid spacing (with the exception of the area of Proliv Longa), equal to 75 and 45 km with respect to latitude and longitude, respectively. In Proliv Longa, the grid spacing was half as large. Thus, in the first rectangle there were 75 nodes, in the second rectangle there were 50, in the third, 91, in the fourth 47, and in the fifth, 78 grid nodes. For each rectangle its own approximation coefficients were calculated. By the reproduced temperatures, the thermal relief of the entire region was constructed. Figure 1 shows the temperature surfaces of the second and third 10-day periods of September 1973. Analysis of these data reveals the state of the thermal relief in the temperatures, its configuration and variability in time. Such temperature surfaces were defined by 10-day periods of September and by years. The investigation of the interyear variability shows large temperature fluctuations around the average value in different years. For Proliv Longa, such data are presented in Table 1. The reproduced temperatures at the grid nodes were subjected to statistical processing.

---

*The POLDV program was developed by K. Ye. Chernyy at the Arctic and Antarctic Scientific Research Institute.

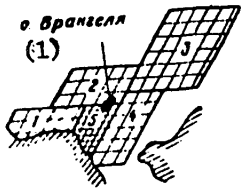

Figure 1. Thermal relief of the entire region in two 10-day periods of September 1973

Key:
1. Wrangel Island

Histograms of the temperature distribution in Proliv Longa on the average for September are presented in Figure 2 for a 4-year period. Analyzing Table 1 and Figure 2, it is possible to draw the following conclusions.

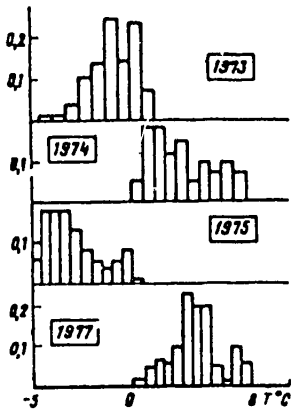

Figure 2. Histograms of average September temperatures (Proliv Longa)

1. Fluctuations of several degrees Kelvin in the mean monthly temperatures for September between different years exist. 2. The average temperature for 4 years of observations in September is close to 0°C (0.61°C). 3. The distribution envelope of the average monthly temperature is the sum of several envelopes subject to a law close to normal distribution. Each such envelope reflects the corresponding quantitative and physical characteristics of the underlying surfaces, for example, the presence of warm water (t>0°C), cold water among the ice of different packing (t<0°C), and residual ice (t<-2°C).

Table 1. Statistical Values of the Mean Monthly Temperature (°C) in September by Years

	1975	1974	1975	1977	(1) Средняя за 4 года
$\bar{a}$	-0,85	2,77	-2,81	3,32	0,61
σ^2	1,35	2,30	1,75	1,41	8,61
σ	1,16	1,52	1,32	1,18	2,93

Key:
1. Average for 4 years

Table 2. Average Thermal Fluxes (kcal/(cm^2-month)) in September

	1973	1974	1975
P	0,02	1,01	0,11
LE	0,51	1,07	0,58
R	1,68	2,11	0,39
q	1,28	0,04	-0,30

By the known values of the underlying surface temperatures, considering the average albedo and the values of the perennial meteorological elements at the grid nodes, the mean monthly values were calculated by the heat balance components of the surface of the turbulent flow P, the latent heat LE, radiation budget R and resultant flow q [1]. Table 2 gives the average values of these flows for Proliv Longa in September.

Analysis of the states and the fluctuations of the thermal processes on the surface of the polar seas by the infrared radiometric data continues.

BIBLIOGRAPHY

1. Budyko, M. I., ATLAS TEPLOVOGO BALANSA ZEMNOGO SHARA [Heat Budget Atlas of the World], Leningrad, Gidrometeoizdat, 1963.

2. Gandin, L. S. and Kagan, R. L., STATISTICHESKIYE METODY INTERPRETATSII METEOROLOGICHESKIKH DANNYKH [Statistical Methods of Interpreting Meteorological Data], Leningrad, Gidrometeoizdat, 1976, 359 pages.

3. Bogorodskiy, V. V. and Martynova, Ye. A., SOBSTVENNOYE TEPLOVOYE IZLUCHENIYE SNEZHNO-LEDYANOGO POKROVA ARKTICHESKIKH MOREY [Natural Heat Emission of the Snow and Ice Cover of the Arctic Sea], Leningrad, Gidrometeoizdat, 1978, 37 pages.

4. Bogorodskiy, V. V. and Paràmonov, A. I., RADIOOKEANOLOGIYA [Radio Oceanology], Leningrad, Gidrometeoizdat, 1976, 24 pages.

5. "Oceanographic Investigations During the AIDJEX Experiment," in AIDJEX BULLETIN, No 27, 1974, pp 125-133.

10845
CSO: 8144/1010

UDC 536.521.2:550.46

APPLICATION OF INFRARED RADIOMETRY IN STUDIES OF FAR EASTERN SEAS

Moscow NEKONTAKTNYYE METODY IZMERENIYA OKEANOGRAFICHESKIKH PARAMETROV in Russian 1981 p 67

[Article by A. A. Visnevskiy]

[Text] Annotation. A discussion is presented of the operating experience using infrared radiometers of different types in the Kolyma Administration of the Hydrometeorological Service during 1967-1977. Undisputed advantages of the Mir-3 infrared radiometer (Leningrad Division of the State Oceanographic Institute--Leningrad Electrotechnical Institute) over its predecessors are noted both with respect to compactness and with respect to operating stability. Nevertheless, the complexity of calibrating the instrument is noted. Operating peculiarities of the Mir-3 radiometer at low temperatures in the fall and winter are discussed. Some results are presented from air observations of temperatures in the Far Eastern seas.

10845
CSO: 8144/1010

UDC 551.46.08

ASYMPTOTIC STUDY OF LASER PULSES REFLECTED FROM SEA SURFACE

Moscow NEKONTAKTNYYE METODY IZMERENIYA OKEANOGRAFICHESKIKH PARAMETROV in Russian 1981 p 68

[Article by V. Ye. Rokotyan]

[Text] Annotation. A theoretical study was made of various sounding conditions of the sea surface by short pulses and narrow light beams. Asymptotic formulas were obtained which relate the shape of the recorded pulse to the shape of the sounded surface.

10845
CSO: 8144/1010

UDC 551.463.5:535.34

POSSIBILITIES OF DETERMINING MARINE HYDROSOL CONCENTRATION BY REMOTE LASER METHODS

Moscow NEKONTAKTNYYE METODY IZMERENIYA OKEANOGRAFICHESKIKH PARAMETROV in Russian 1981 p 68

[Article by S. F. Korchagina, A. L. Kravtsov, A. S. Lezhen and V. I. Khalturin]

[Text] Annotation. A procedure is proposed for determining the marine hydrosol concentration based on recording return light beams during sounding by two lasers.

10845
CSO: 8144/1010

UDC 551.46.08

REMOTE DETECTION AND IDENTIFICATION OF OIL POLLUTION AT SEA BY FLUORESCENT SPECTRA

Moscow NEKONTAKTNYYE METODY IZMERENIYA OKEANOGRAFICHESKIKH PARAMETROV in Russian 1981 pp 69-73

[Article by V. A. Torgovichev, V. F. Krivolapov, T. N. Klimova, V. Yu. Maslov and G. Ye. Nefedov]

[Text] Annotation. A report is presented on the performance of a series of laboratory and natural experiments to study the fluorescence properties of plutonium products and sea water, and also for remote detection and identification of the composition of oil slicks on the sea surface.

At this time there are a number of different methods of remote detection of oil slicks on the sea surface [1]. Microwave radiometers, radar, on-board cameras, infrared thermographs, and so on are used for this purpose. These systems can detect and map oil spills under defined conditions, but none of them are able reliably to classify the type of petroleum product causing the pollution.

The possibility of using the method of laser-radar (lidar) fluorometry for remote detection and identification of oil slicks is based on the known fact of selected absorption (λ=220 to 400 nm) of petroleum hydrocarbons with subsequent powerful Stokes fluorescence (S.F.) in the 300 to 600 nm range. The primary factors limiting the possibility of detection and identification of oil slicks by fluorescent spectra are the great width and variety of the S.F. spectra of petroleum products and also the fluorescence of sea water [2].

The first attempt to use the method of lidar fluorometry for remote monitoring of oil slicks at sea was made by a group of American researchers [3]. On the basis of laboratory analysis of the fluorescence spectra of various types of petroleum and petroleum films on water surfaces, they created the helicopter lidar with nitrogen laser (λ_0=337.1 nm), and they performed a series of full-scale experiments. The results obtained convincingly proved the prospectiveness of this method for detection and mapping of oil spills. However, the S.F. spectra of clean and polluted sea surfaces presented in [3] have noticeable similarity with respect to shape although they differ by two or three times with respect to intensity. The position of the spectral peak (λ_{max}) of the fluorescence of various types of oil films and the S.F. of sea water differs by no more than 10 to 30 nm on excitation by a nitrogen laser.

The intensity of lidar signals depends on the wave state of the sea surface and the sounding angle [1], and λ_{max} of sea water fluorescence can vary by 30 to 50 nm for different bodies of water [2]. Therefore the problem of uniqueness of determining the type of polluting petroleum product from lidar S.F. spectra requires refinement. One of the theoretically possible ways to eliminate the effects of superposition of S.F. spectra of petroleum products and sea water is selection of the optimal sounding wavelength. For this purpose the Central Aerological Observatory of the Main Administration of the Hydrometeorological Service, jointly with the Analytical Laboratory of the Oceanology Institute of the USSR Academy of Sciences, performed a number of laboratory and field experiments.

In the first step of the research, we analyzed the fluorescent spectra of the petroleum solutions of different deposits and their individual fractions in the 300 to 600 nm range on the FICA-58 fluorimeter (France). An analysis of the obtained data demonstrated that the intensity of the S.F. spectra of the petroleum and petroleum product solutions is maximal for excitation in the 330 to 360 nm range for the investigated excitation region. At the same time, just as in [3], great similarity of the S.F. spectra of different petroleum is noted. However, for solutions of products and vapor of volatile fractions the differences in the S.F. spectra are more noticeable and, consequently, the conditions for their identification are more favorable.

The second cycle of laboratory experiments consisted in investigating the frequency dependence of the form and the intensity of the S.F. spectra of the clean surface of the sea water and the surface contaminated by petroleum products. Measurements were performed using the LR-IK lidar developed at the Central Aerological Observatory [4], which is a remote laser spectrometer. For excitation of fluorescence, the emission of the third (λ_0=354.7 nm) and fourth (λ_0=266 nm) harmonics of a 100 kilowatt pulsed Nd:YAG-laser was used. The fluorescence from the investigated surface was gathered by an optical receiving antenna (420 nm in diameter) with subsequent spectral selection by the DMR-4 monochromator and recording in a photoelectronic system operating in the photon counting mode with synchronous range gating. The S.F. spectra were recorded by successive scanning by a monochromator with respect to wavelengths of 270 to 600 nm every $\Delta\lambda$~3 nm with spectral slot width of ~1 nm. The S.F.spectra of sea water samples from the Bay of Biscay and gasoline, oil, diesel fuel and crude oil slicks on the Bay of Biscay 7 microns and 14 microns thick were studied. The normalized fluorescent spectra of some films and water are illustrated in Figure 1. It is obvious that for λ_0=266 nm identification of the petroleum products and their detection are more reliable than for λ_0=355 nm, for the λ_{max} shift for petroleum products is ~90 nm in this case, and the S.F. intensity of sea water decreases by ~3-fold.

We performed a series of full-scale experiments in the port water of the Baltic Shipyard. During spatial scanning of the bay by lidar with λ0=266 nm, we clearly detected and mapped the surfaces polluted by spilled petroleum products (fuel oil, diesel oil) and the petroleum waste usually present in a port to distances up to 250 meters. The fluorescent spectra of these pollutants and the Baltic Sea water are presented in Figure 3. Differences in shape of the petroleum product spectra can be noted well here, which confirms the possibility of identifying them. The repetitiveness of certain spectral fluorescence bands (for example, at λ=390 nm and 470 nm) of different petroleum products is also noted. This is obviously caused by the presence of the same molecular components in them.

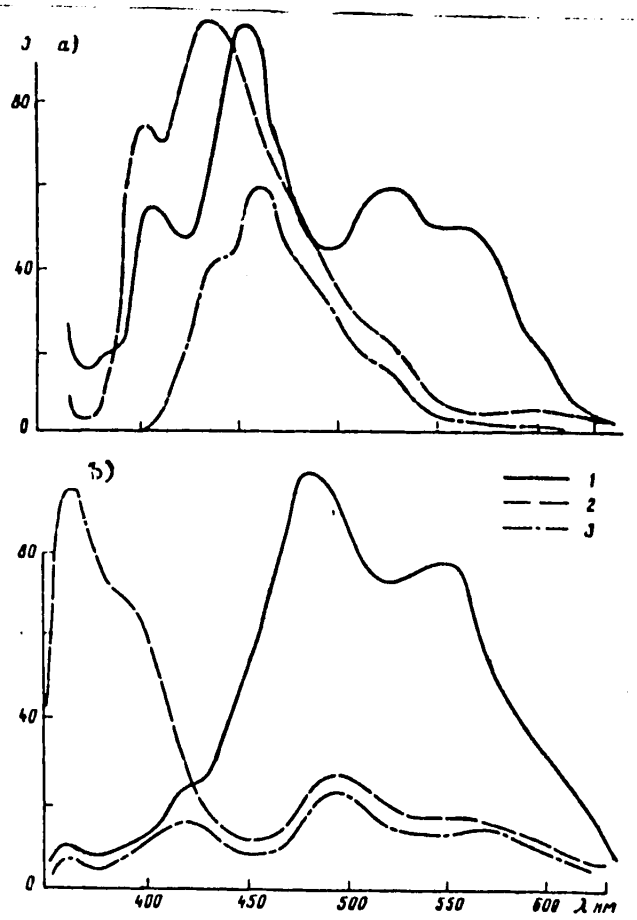

Figure 1. Frequency dependence of the lidar fluorescent spectra of oil slick (7 microns) on the sea surface as a function of radiation excitation wavelength:
a -- λ_0=354.7 nm, b -- λ_0=266 nm; 1 -- oil, 2 -- diesel fuel, 3 -- sea water

The experimental studies that we performed demonstrated that the method of lidar fluorimetry permits remote detection, mapping and identification of oil slicks on the sea surface by lasers with a wavelength of 266 nm.

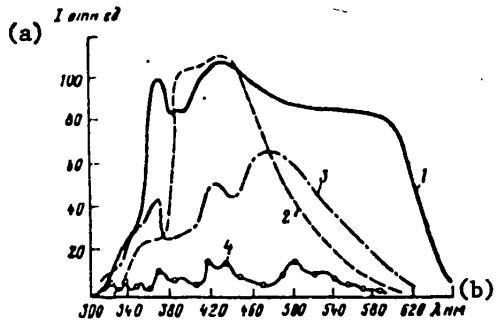

Figure 2. Fluorescent spectra of petroleum products on the sea surface (lidar):
1 -- mazut [fuel oil] (24 hours after the spill), 2 -- diesel oil (fresh spill), 3 -- bilge water, 4 -- "clean water" (after a storm)

Key:
a. Relative units
b. nm

BIBLIOGRAPHY

1. Bogorodskiy, V. V., Kropotkin, M. A. and Sheveleva, T. Yu., METODY I TEKHNIKA OBNARUZHENIYANEFTYANYKH ZAGRYAZNENIY VOD. [Methods and Equipment for Detecting Petroleum Pollutants of Water], Leningrad, Gidrometeoizdat, 1975, p 24.

2. Karabashev, G. S., "Modern Achievements in the Study of the Fluorescence of Materials Dissolved and Suspended in Sea Water," I S"YEZD SOVETSKIKH OKEANOLOGOV [First Congress of Soviet Oceanologists], No 1, FIZIKA OKEANA. MORSKAYA TEKHNIKA [Physics of the Ocean. Marine Equipment], pp 157-158.

3. Fantasia, J. F. and Ingrao, H. C., "Development of an Experimental Airborne Laser Remote Sensing System for Detection and Classification of Oil Spills," PROC. OF THE 9th INTERN. SYMP. ON REMOTE SENSING OF ENVIRONMENT, VIII, 15-19 April 1974, pp 1711-1745.

4. Zakharov, V. M. and Kostko, O. K., METEOROLOGICHESKAYA LAZERNAYA LOKATSIYA [Meteorological Lidar], Leningrad, Gidrometeoizdat, 1977.

10845
CSO: 8144/1010

UDC 551.46.07

APPLICATION OF METHOD OF STATISTICAL TESTS TO CALCULATE OCEAN REFLECTIVITY UNDER LASAR IRRADIATION

Moscow NEKONTAKTNYYE METODY IZMERENIYA OKEANOGRAFICHESKIKH PARAMETROV in Russian 1981 p 74

[Article by A. S. Lezhen and N. V. Urikova]

[Text]. Annotation. A study is made of the application of the Monte Carlo method to study the characteristics of the propagation of laser emission in the marine environment. The probabilities of the transitions of wandering particles in different directions were determined in a model by the scattering indicatrices. A study was made of the penetration of protons into the water and emergence at the surface. A three-dimensional model is reduced to one-dimensional and two-dimensional models considering the probabilities of survival of the protons in the given medium.

The obtained results agree well with the exponential law of intensity damping with depth of penetration. In addition, estimates are presented for the intensity of the radiation emerging at the surface after multiple scattering in the surface layer of the sea.

10845
CSO: 8144/1010

SPACE AND AERIAL SURVEYING IN THE OPTICAL RANGE

UDC 551.465.7

PUSH AND DRIFT OF ICE IN THE HEAD OF GULF OF FINLAND AS APPLIED TO PROBLEMS IN HYDRAULIC ENGINEERING (ACCORDING TO AERIAL PHOTOGRAPHIC SURVEY DATA)

Moscow NEKONTAKTNYYE METODY IZMERENIYA OKEANOGRAFICHESKIKH PARAMETROV in Russian 1981 pp 75-77

[Article by V. V. Drabkin and M. L. Monosov]

[Text] Annotation. Three periods characterized by different effect of the ice cover on hydroengineering structures have been isolated by the results of processing aerial photographic surveying and aerial radiogeodetic data in the head of the Gulf of Finland. In order to calculate the ice loads on the sites of the designed structures, it is recommended that optimal values be selected for the dimensions of the largest pieces of ice and their drift rate.

At the head of the Gulf of Finland in the winter three periods can be isolated which are characterized by different effect of the ice cover on hydroengineering structures:

1. During the growth of the shore ice the ice drift appears to be least dangerous with regard to its effect on hydroengineering structures. The ice is of insignificant thickness and cannot pose a threat to the structures, in particular, if the shore ice sets up in a short period of time, at low temperatures and with little wind.

2. Winter push and drift of the ice during surge. Winter push and drift of the ice occur during the period after final set-up of the shore ice, when the shore ice is broken during surges and high winds, and they are the most dangerous for hydroengineering structures. The thickness of the ice when the shore ice breaks open can vary from 10 to 50 cm. In the entire history of flooding breaking of shore ice more than 60 cm thick has never been observed.

3. Ice drift in the spring. Ice drift in the spring occurs after the shore ice breaks open and before complete disappearance of the ice sheet. During the period the strength of the ice decreases, degradation can reach degree 4 or 5. This drifting of the ice is usually less dangerous for hydrodynamic structures than winter drift because in the spring the ice has less strength.

During set-up of the shore ice loads created by the drift of thin pieces of ice are insignificant.

In the winter, in the presence of pushing storm winds from the western quarter and rises in water level at the head of the Gulf of Finland and in Neva Bay, the shore ice separates from the shore and the entire ice mass is pushed from west to east. During such pushes, ice heaps are formed on the shoals, cribworks, islands and shorelines, and in the open sea, hummocking zones and ice reefs are formed.

In both severe and moderate winters the approach of ice from the direction of the sea has low probability, for stable shore ice is present at the head of the Gulf of Finland.

During mild winters after the shore ice breaks up in the spring, it undergoes partial degradation and is carried away, if there are prolonged winds from the western quarter, drift ice can come in from the sea to the head of the Gulf of Finland and into the vicinity of Yuzhnyye Vorota. The movement of this ice complicates navigation and can cause hummocking and ice heaps on the structures. Drift ice does not reach Severnyye Vorota as a result of the preservation of shore ice north of Kotlin Island. Here the ice sheet primarily thaws out locally and usually disappears only after adjacent regions are clear of ice.

It is known that hydroengineering designers are the most interested in the drift of maximum sized pieces of ice in the vicinity of the structures [1].

One such piece of ice 23.8 km^2 in area was recorded by an aerial photograph on 13 April 1974 as it entered the head of the Gulf of Finland on the phototack from Cape Stirsudden to Cape Shepalevskiy. Three successive drift vectors of the ice field were obtained--26.7, 13.1 and 18.0 cm/sec with directions of 99, 99 and 68°, respectively. The wind was northeasterly, 6-9 m/sec. During the period from 13 to 16 April the average daily drift of this piece of ice was 3.3 cm/sec, and from 16 to 17 April, 7.4 cm/sec.

The largest piece of ice recorded by aerial photography on 20 April 1974 at Yuzhnyye Vorota had an area of 1.5 km^2 (1.8 km×0.8 km), degradation and reefing of degree 1. The ice moved at a speed of about 10 cm/sec under the effect of northerly and northwesterly winds blowing at 8-10 m/sec.

Using the aerial photographic data, V. V. Drabkin and A. S. Kurochkin at the Leningrad Division of the State Oceanographic Institute derived the following formula to calculate the speed of the ice drift at the head of the Gulf of Finland as a function of wind velocity:

$$W = 1.43\ V + 4.40,$$

where W is the ice drift rate, cm/sec;

V is the wind velocity, m/sec.

During the breakup of the head of the Gulf of Finland and Neva Bay, the maximum long-term wind velocity does not exceed 16 m/sec; therefore the maximum drift rate of the ice will not exceed 30 cm/sec according to this formula.

Summing up the results of the discussion, it is possible to draw the following conclusions:

During winter surges the hydroengineering structures can be subjected to static pressure of the entire mass of ice in the head of the Gulf of Finland;

In the vicinity of the designed structures, the dynamic loads from drift ice from the Gulf of Finland and Neva Bay can be expected after the spring debacle;

For calculation of ice loads under the effect of drift ice, it is recommended that the maximum dimensions of the ice field be taken equal to the following: length 2.0 km, width 1.0 km, area 2.0 km^2; with maximum drift rate of 30 cm/sec.

BIBLIOGRAPHY

1. Korzhavin, K. N., VOZDEYSTVIYE L'DA NA INZHENERNYYE SOORUZHENIYA [Effect of Ice on the Engineering Structures], Izd. SO AN SSSR, Novosibirsk, 1962, 198 pages.

10845
CSO: 8144/1010

UDC 551.46:629.786.2:639.2.001.5

EXPERIMENT IN DECIPHERING ZONES OF HIGHEST BIOLOGICAL PRODUCTIVITY WITH RESPECT TO MULTIZONAL SPACE IMAGES OF WATER ENVIRONMENT

Moscow NEKONTAKTNYYE METODY IZMERENIYA OKEANOGRAFICHESKIKH PARAMETROV in Russian 1981 pp 78-82

[Article by G. P. Vanyushin]

[Text] Annotation. The distribution of the phytoplankton concentration can be determined by the image brightness of a body of water in the central range of 0.5 to 0.6 microns inside regions having approximately identical content of inorganic suspension in the surface layer of the water. The boundaries of these regions are established on the basis of image brightness of the water environment in the spectral ranges of 0.6 to 0.7 and 0.7 to 0.8 microns. Results are presented from experimental decoding of the phytoplankton concentration distribution with respect to materials from the space survey and satellite observations of the northwest coast of Africa.

The study of the relations between the brightness (optical density) of multizonal images of the water environment and oceanological characteristics is at the present time one of the procedural problems of studying the ocean from space. Discovery of these laws is necessary, in particular, for interpretation of the remote sounding data in the interests of the fishing industry. The study of zones of increased productivity is directly connected with finding the relation between the optical density of multizonal images of the water environment and the structure of the most important biological element--the phytoplankton. The difficulty of studying phytoplankton concentration by noncontact methods consists in the necessity for exact determination of its contribution to the spectral brightness of the water.

On the basis of an analysis of numerous published data it is possible to propose that the brightness of the water in the spectral range of 0.5 to 0.6 micron depends on the number of particles of phytoplankton and inorganic suspension, and in the spectral zone of 0.6 to 0.7 micron, primarily on the number of particles of inorganic suspension. Separating the investigated body of water into regions having approximately equal inorganic suspension content in the surface layer of the water with respect to brightness values (optical density) of its image in the spectral range of 0.6 to 0.7 (0.7 to 0.8) micron, it is possible to consider that in the spectral range of 0.5 to 0.6 micron the brightness variations of the water in the

central parts of the isolated regions take place as a result of differences in the phytoplankton concentration. This method of discovering the zones of increased productivity was proved when processing the space survey data and the data from satellite observations off the northwest coast of Africa.

The experiment was performed in April 1976 in the region bounded by the coordinates 17 to 24° north and 16 to 22° west. The survey data obtained by the multizonal scanning equipment of an artificial earth satellite were used.

The ships of the USSR Ministry of Fishing (the AtlantNIRO) performed full-scale measurements. The space information was in the form of images of the experimental region in four spectral ranges 0.5 to 0.6, 0.6 to 0.7, 0.7 to 0.8, 0.8 to 1.1 micron in the form of transparent positives. The picture was taken at 1052 hours local time on 30 April 1976.

The ship observations included determination of the following characteristics: depth (meters), color (on the Forel-Wood color scale), relative transparency (meters, by the Secchi disc), the phytoplankton biomass for the 0 to 100 meter layer (g/m^3), the water temperature in the surface layer, the wind direction and velocity, wave direction and height. All the sections were taken in the latitudinal direction with interval between stations of 10 minutes of the grade grid on the average. The distance between sections was also 10 minutes. The hydrologic conditions of the investigated body of water give rise to high biological productivity in the presence of spectral gradients of important oceanographic characteristics (water temperature, color, relative transparency, phytoplankton concentration, inorganic suspension concentration, and so on.

Before comparing the space images of the water surface with the satellite observation data, external conditions of the survey on which the albedo of the ocean depends, were analyzed. Research data were needed to discover whether it is possible to consider the image of the body of water as a united whole or whether it must be analyzed by parts. The influence of the atmosphere on the ocean emission was taken the same for the entire test area, for the experimental region was small (100×160 km), and it was within 280 km of the shore (for the center of the region). The following survey conditions were also analyzed: solar angle, angle of sight, wave height and direction. On the basis of this work, the conclusion was drawn that variations in the values of the optical density of the image of the water in the experimental region primarily reflect the distribution pattern of the oceanographic parameters.

According to the proposed procedure, the investigated body of water was regionalized with respect to relative content of inorganic suspension in the surface layer of the water on the basis of optical density maps in the spectral ranges of 0.6 to 0.7 and 0.7 to 0.8 micron. The maps were constructed on the basis of measuring the optical density of transparent positives using the Gretag densitometer and a multichannel image analysis system ISI-150 [1]. The inorganic suspension is present in the surface water of the experimental region. These are sand and dust particles carried along by the constantly moving air flows from the Sahara Desert.

Four regions were isolated. The correctness of the method was indirectly confirmed by the relative transparency measured at the stations which were located within the parts of the body of water with relatively equal suspension content (see the table).

No of region	1	2	3	3
No of stations	11	9	6	4
Average value of relative transparency, meters	$9.3^{+2.7}_{-1.3}$	8 ± 1.0	$11.2^{+1.8}_{-1.2}$	15 ± 2.0

Some lack of correspondence of the average values of the relative transparency to the quantitative distribution of the inorganic suspension for regions 1 and 2 occurs because the values of the relative transparency are also influenced by the phytoplankton particle concentration. Thus, for region 1, the average plankton biomass is 0.17 g/m^3, and for 2, 0.89 g/m^3. This indicates that with identical relative transparency the part of the water in which there is more inorganic suspension in the surface water will appear brighter on the space image in the spectral range of 0.5 to 0.6 micron. When analyzing variations of the optical density of the image of the water environment from the phytoplankton concentration in the spectral range of 0.5 to 0.6 micron, inside the regions with relatively identical inorganic suspension content, a defined law was discovered which is traced well for all bodies of water (Figure 1).

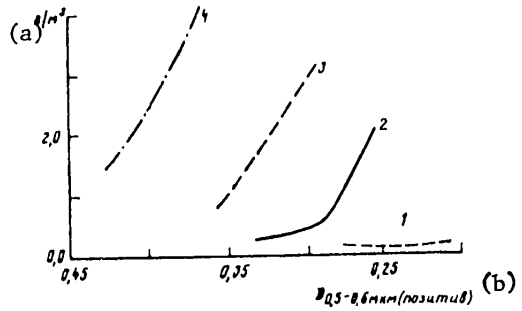

Figure 1. Relation between phytoplankton concentration and optical density of the image of the water in the spectral range of 0.5 to 0.6 micron for bodies of water with approximately the same inorganic suspension content (1, 2, 3, 4, respectively for water with high, medium, "intermediate," and low relative inorganic suspension content)

Key:
a. g/m^3
b. $D_{0.5-0.6}$ micron (positive)

On the basis of the obtained laws, the phytoplankton concentration distribution map constructed initially by the results of the ship observations (Figure 2) was corrected.

Thus, the deciphering of phytoplankton concentrations by the data from multizonal space surveys, in our opinion, must be carried out after the investigated body of water has been regionalized with respect to the amount of inorganic suspension in the surface water. The given method was tested when processing the satellite and ship measurement data in the Atlantic Ocean off the coast of Northwest Africa, and it gave promising results which demonstrated the possibility of discovering zones of increased biological productivity based on the phytoplankton concentration distribution with respect to multizonal space information.

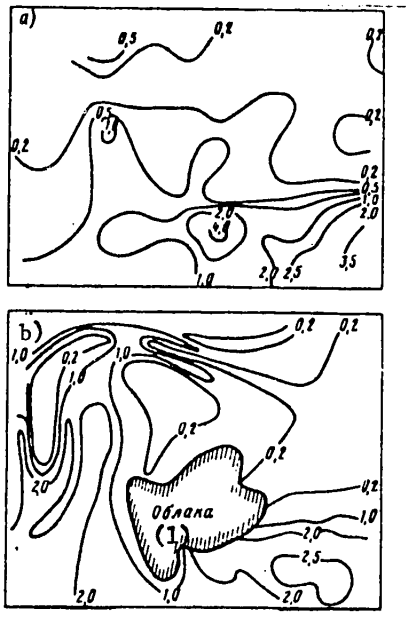

Figure 2. Phytoplankton concentration distribution in the experimental region in g/m^3:
a -- according to the ship observation data, b -- according to the results of analyzing multizonal space images

Key:
1. clouds

BIBLIOGRAPHY

1. Bumblis, V. I., Vanyushin, G. P. and Potaychuk, S. I., "Experience in Studying Water Objects Using Television Systems to Process Multizonal Information," DOKLAD NA I VSESOYUZNOY KONFERENTSII PO OBMENU OPYTOM ISPOL'ZOVANIYA KOSMICHESKOY INFORMATSII [Report at the 1st All-Union Conference on Exchange of Experience in the Use of Space Information], Moscow, 21-24 October 1976.

2. Yerlov, N., OPTICHESKAYA OKEANOGRAFIYA [Optical Oceanography], Moscow, Mir, 1970.

3. Szeklelda, K. H., "Observations of Suspended Material from Spacecraft Altitudes," DEUTSCHES HYDROGRAPHISCHES INSTITUTE, Hamburg, No 4, 1974, pp 159-170

10845
CSO: 8144/1010

UDC 551.46.082:528.7

SOME RESULTS OF AIRCRAFT MEASUREMENTS OF CURRENTS IN LAKES AND RESERVOIRS

Moscow NEKONTAKTNYYE METODY IZMERENIYA OKEANOGRAFICHESKIKH PARAMETROV in Russian 1981 p 83

[Article by Ye. D. Yegorikhin and T. N. Filatova]

[Text] Annotation. Results are presented from measuring currents in Lake Chudsko-Pokovskoye, Narvskoye and Uglegorskoye Reservoirs. On the basis of experience accumulated since 1965, procedural instructions were developed for aerial measurements of currents in lakes and reservoirs.

10845
CSO: 8144/1010

UDC 551.46.08:556

APPLICATION OF ANALOG-DIGITAL DEVICES FOR INTERPRETING AEROSPACE DATA

Moscow NEKONTAKTNYYE METODY IZMERENIYA OKEANOGRAFICHESKIKH PARAMETROV in Russian 1981 pp 84-87

[Article by V. A. Mikhaylov and V. F. Usachev]

[Text] Annotation. When interpreting aerospace data for cases of imaging blurred outlines occurring in oceanographic research, the application of analog-digital devices is urgent. The basic methods of automating the processing of photographic images are investigated. The operating principles of analog-digital devices developed at the State Hydrological Institute for the solution of certain labor-intensive problems of processing aerospace data based on the standard Pallada phototelegraphic unit are presented. A procedure for isolating the given objects and determining their areas is discussed.

In oceanographic research, on the basis of the specific nature of the investigated object, it is impossible to get along without using photographic methods. When investigating bodies of water, the aerial photographic survey data, space photograph data and satellite pictures are used in a wide range. In recent years the flow of photographic information has grown significantly, at the same time as the processing of the images remains quite labor-intensive and little mechanized. It is obvious that automation of these processes is extremely necessary. The most effective are the machine methods of processing [1, 2]. In spite of the broad capabilities of computers, the existing technical difficulties limit the application of such methods. In addition, the cost of processing the images is quite high, and it is expedient to use computer-based devices only to solve highly complex problems. Accordingly, in the organizations which are engaged in processing photographic images, efforts are made to develop simpler analog or analog-digital devices [3]. These devices have also been developed at the GGI [State Hydrological Institute]. The most significant event in the development of analog-digital devices is the creation of equipment which will permit elementary processing based on simple and available means in the network of the Administrations of the Hydrometeorological Service. Therefore, as the basis for the devices, a set of Pallada phototelegraphic units has been adopted. The transmitting equipment converts the image to an electric signal which is subjected to corresponding processing by the analog-digital attachment and the reverse conversion of the processed signal to a photograph image is carried out by means of the receiver.

The analog-digital attachment is a separate module. Simplicity, reliability and quite high parameters of the device are insured by the application of integrated microcircuits in it.

When processing photographic images of the water surface, the most urgent problem is isolation of zones with different optical density of the images, discovery of the causes of the differences and determination of the magnitudes of the areas occupied by each zone. Nonuniformity of the optical density of the photographic image can result from different causes: glare on the water surface, different degree of examination of the bottom for shallow depths, different concentration of suspensions and pollutants, the presence of oil slicks on the surface, a different degree of wave action, and so on. Therefore the first step in the study is recognition and segregation of the objects having even, complex configuration on the outline and also determination of the areas of these objects. The generally accepted method of isolation of objects on the image reduces to quantization of the initial image on two levels. Quantization is done by a precision low-frequency comparator. The "Kvant-1" device permits isolation of objects (or their outlines), the optical density of which is higher than a given value and determination of their area with the help of an electronic counter.

In cases where it is necessary to isolate and determine the area of objects, the optical density of which is within the given limits with upper and lower bound, more complicated equipment is needed. Using the "Kvant-2" device it is possible to isolate various formations on the initial photographic image such as swamps, forests, ice fields with different degree of degradation, and so on. In addition, it is possible to obtain so-called isophotos. Using various light filters, it is possible to process color photographic images and other descriptive information.

In many cases, in order to simplify the analysis of the investigated photographic image it is expedient not to reproduce all parts of the image, but to replace it by a simpler image similar to it, for the reproduction of which a smaller amount of information is needed. In practice, for the solution of many hydrological problems, six quantization levels with variable step size are sufficient. Restriction to six quantization levels arises from the fact that the reproduced quantized image in the black and white version with a large number of levels loses its "cartographic" appearance and requires additional visual deciphering. On the other hand, the possibility of varying the quantization step size makes it possible to obtain high detail of reproduction of the tone fluctuations in the given range of optical densities, redistribution of gradations, enlargement of the optical density range of the investigated section of the image. An analogous "Kvant-3" device permits realization of the described quantization. The most responsible step in processing the image on the "Kvant-2 or 3" devices is choice of the quantization threshold, for it determines the converted image obtained. It is obvious that for every case its own values of the thresholds must be selected as a function of the nature of the image.

Electronic frequency filtration of an image permits significant improvement of the quality of the images having high noise content, defocusing, blurred and uneven outlines. The joint inclusion of an integrator and differentiator permits isolation of low and high frequencies corresponding to the investigated photographic image,

which is required to isolate the oceanological information on low-quality photographs.

In the "Pallada" transmitting phototelegraphic equipment, a balancing modulator is used, the characteristic of which is linear. By varying the balancing of the modulator, it can be made nonlinear. Partial reversal of the photographic image occurs in this case. This method of image conversion permits in some range of densities isolation of nonuniformities poorly visible in the initial photographic image.

An advantage of analog-digital devices is their speed (it is determined by the speed of arrival of the data). The cost of such devices is appreciably lower than that of digital devices, and the image processing is also cheaper. Unconditionally, the developed and used devices for electronic processing of photographic image are still far from perfection. However, the analog-digital devices are simple in operation and can be used for processing images in organizations not having computer centers and also in combination with various computers.

BIBLIOGRAPHY

1. Grishin, M. P., Kurbanov, Sh. M. and Markelov, V. P., AVTOMATICHESKIY VVOD I OBRABOTKA FOTOGRAFICHESKIKH IZOBRAKHENIY NA EVM [Automatic Computer Input and Processing of Photographic Images], Moscow, Energiya, 1976, 145 pages.

2. Rozenfel'd, A., RASPOZNAVANIYE I OBRABOTKA IZOBRAKHENIY S POMOSHCH'YU VYCHISLITEL'NYKH MASHIN [Recognition and Processing of Images Using Computers], Moscow, Mir, 1972, 228 pages.

3. Kersha, V. O., "Image Processing by Electronic Analog Devices," IZV. VUZOV. GEODEZIYA I AEROFOTOS"YEMKA [News of the Institutions of Higher Learning. Geodetics and Aerophotography], No 6, 1974, pp 53-56.

10845
CSO: 8144/1010

ULTRASONIC METHODS

UDC 537.874.2:621.396.96

INFLUENCE OF SPATIAL AVERAGING ON ACCURACY OF LOCATION WAVE RECORDER MEASUREMENT OF WAVE PROFILES

Moscow NEKONTAKTNYYE METODY IZMERENIYA OKEANOGRAFICHESKIKH PARAMETROV in Russian 1981 pp 88-90

[Article by N. I. Seregin and A. A. Kalmykov]

[Text] Annotation. In this paper, on the basis of digital simulation a study is made of the influence of the relation of the dimensions of the irradiated area and wave period on the accuracy of measuring the wave profile by a pulse ultrasonic wave recorder, and models of the meter errors are presented.

One of the basic error components in measuring a wave profile by a location wave recorder is the error caused by the effect of averaging of the measured parameter (in the given case, range) within the limits of the irradiated section of the surface. Averaging leads to the appearance of an error which can be considered as a bias of the measured range relative to the true range combined with filtration of the high-frequency components of the sea wave spectrum. The degree of spatial averaging is conveniently characterized by a relative parameter. As such a parameter it is possible to propose the relation between the wave period and the dimensions of the irradiated area (in the case of vertical sounding, the irradiation spot diameter):

$$\alpha = \lambda_B / D_n . \qquad (1)$$

An estimate of the influence on the wave profile measuring accuracy of a pulse ultrasonic wave recorder was made on the basis of digital simulation of the signal reflected from an elongated rough surface [1]. The experiment was performed for the conditions of moderate wave action (wave height h_B=1 meter, wave length λ_B=20 meters) with meters using differential and integral methods of processing the echo. The basic results of the study are illustrated by the figure in which the relations are presented for the relative measurement error $\delta_{meas}=\sigma_{meas}/h_B$, where δ_{meas} is the mean square error in measuring the wave profile, as a function of the ratio of the wave period and irradiation spot diameter. The results indicate the great advantage of the integral method of signal processing and permit estimation of the parameters of the meter antenna system with given accuracy.

Depending on the variation of the ratio of the irradiation spot dimensions and the wave period, redistribution of the relative contribution of the bias and filtration effects to the total averaging error takes place. The separation of the averaging error into two components manifested for different α served as the basis for constructing two types of models of the meters.

The models of the first type (for the case $\alpha \geq 2$) were obtained on the basis of the method of successive approximations, and they relate the geometric parameters of the wave to its profile measurement error. They have the following form:

$$\Delta i = F(\dot{h}_i, \ddot{h}_i, P); \tag{2}$$

where Δi is the mathematical expectation of the range measurement error to the i-th point of the wave surface;

$\dot{h}_i$, $\ddot{h}_i$ are the values of the first and second derivatives of the wave surface at the i-th point;

P is the meter parameter vector.

For a meter with differential processing of the echo, the model looks like the following:

$$\Delta i = \begin{cases} \Delta_0 + a_1 \dot{h}_i + a_2 \ddot{h}_i & \text{for } \ddot{h}_i \geq 0, \\ \Delta_0 + a_1 \dot{h}_i [1 - \exp(a_2 |\dot{h}_i| / \ddot{h}_i)] & \text{for } \ddot{h} < 0, \end{cases} \tag{3}$$

where each of the α_k (k=1,2,3) is related through the regression equation to the meter parameters.

The accuracy of the models was estimated by averaging the relative error in measuring the wave profile characterizing the accuracy of the meter to the deviation of the output of the model reduced to the wave height from the output of the meter called hereafter the model error (δ_m). For α=2.5 the following results were obtained:

a) For the differential method of processing

$$\delta_{meas}=0.3, \ \delta_m=0.05,$$

b) For the integral method of processing

$$\delta_{meas}=0.043, \ \delta_m=0.018.$$

Models of the second type used in the entire range of variation of α but having higher effectiveness for small values were obtained by the method of identification of linear dynamic systems [2], and they are the difference equations of the following type:

$$y_i = a_1 y_{i-1} + b_1 x_{i-(j-1)} + b_2 x_{i-j} + b_3 x_{i-(j+1)} + b_4 x_{i-(j+2)}, \tag{4}$$

where x_i is the wave height at the i-th point;

y_i is the meter output at the i-th point;

j is the shift parameter which depends on the irradiation spot diameter;

a, b are the coefficients which depend on the meter parameters.

On the basis of the realized nonlinearity of the transformation of the range information by the meter with differential processing of the signal, models of the type of (4) were only obtained for meters with integral processing.

The estimate of the accuracy of the linear model for $\alpha=0.8$ gave the following results: $\delta_{meas}=$ [illegible], $\delta_m=0.13$.

The obtained model can be used to analyze the accuracy characteristics of pulse wave recorders and to compensate for the averaging errors in secondary processing devices. A gross estimate of using first type models to compensate for the meter errors with differential processing of the signal demonstrated that as a result of secondary processing the wave profile measurement error can be reduced by approximately three fold (for $\alpha=2.5$).

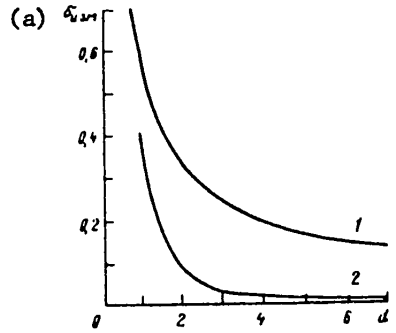

Figure 1. Relative error in measuring the wave profile as a function of the ratio of the wavelength and the irradiation spot diameter:
1 -- for the differential method of signal processing,
2 -- for the integral method of signal processing

Key:
a. δ_{meas}

BIBLIOGRAPHY

1. Zubkovich, S. G., STATISTICHESKIYE KHARAKTERISTIKI RADIOSIGNALOV, OTRAZHENNYKH OT ZEMNOY POVERKHNOSTI [Statistical Characteristics of Radio Signals Reflected from the Earth's Surface], Moscow, Sov. radio, 1968.

2. Box, J. and Jenkins, G. D., ANALIZ VREMENNYKH RYADOV, PROGNOZ I UPRAVLENIYE [Time Series Analysis, Forecasting and Control], Part 2, Moscow, Mir, 1974.

10845
CSO: 8144/1010

UDC 621.396.96+535.853.68

COMPARATIVE ANALYSIS OF USING ELECTROMAGNETIC AND ACOUSTIC VIBRATIONS FOR SHIP LOCATION WAVE RECORDERS

Moscow NEKONTAKTNYYE METODY IZMERENIYA OKEANOGRAFICHESKIKH PARAMETROV in Russian 1981 p 91

[Article by N. A. Nekhonov, A. A. Kalmykov, Yu. I. Kirpa and V. G. Vazenin]

[Text] Annotation. A study is made of the possibility of using location and ranging devices emitting both electromagnetic and acoustic vibrations to measure wave parameters from on board moving ships. The measurement error components are estimated, and the requirements on the basic characteristics of ship location wave recorders are defined.

10845
CSO: 8144/1010

UDC 534.9:551.46.086

SOME RESULTS OF AEROACOUSTIC MEASUREMENTS OF SEA SURFACE TIME-SPACE CHARACTERISTICS

Moscow NEKONTAKTNYYE METODY IZMERENIYA OKEANOGRAFICHESKIKH PARAMETROV in Russian 1981 pp 92-96

[Article by A. P. Aleksandrov, E. S. Vayndruk and G. Yu. Narodnitskiy]

[Text] Annotation. Results are presented from measuring the basic characteristics of sea waves in the coastal zone obtained when testing an aeroacoustic wave meter based on the method of vertical pulse sounding. The synchronous time series of y-axes of the wave oscillations measured at five separate points of the sea surface were used to calculate the frequency spectra of the wave oscillations, the slopes and steepness, the frequency-angular spectra of the surface, and so on. A study was made of the amplitude fluctuations of the signals reflected by the sea surface. Metrologic characteristics of the wave meter and the possibilities of its application for comprehensive studies of the sea surface are discussed.

The wave meter is based on the method of vertical sounding of the sea surface by ultrasonic pulses, during the propagation of which to the surface of the water and back the distance to the water and then the y-axes of the wave oscillations are determined. The wave meter is a system of five independent synchronously operating acoustic wave recorders, the receiving and transmitting antennas of which are arranged in a "cross," that is, at the corners and center of a square with a 2 meter diagonal.

The hardware part of the wave meter is basically described in [1]. Brief technical specifications for the wave meter follow:

Ultrasonic frequency of the sounding pulses 40 kilohertz,

Sounding pulse duration 0.1 to 2 milliseconds,

Sounding frequency 2 to 10 hertz,

Acoustic power of the individual radiator ~0.1 watt,

Irradiation spot diameter (with respect to 0.5 power level) 0.2 meter,

Slope and steepness measurement base 1 or 2 meters,

Hardware error in measuring the y-axes of the wave oscillations $\pm$0.01 meter,

Distance from the receiving-transmitting system to the average water level 5 to 15 m.

When the receiving-transmitting system is installed on a stationary base the wave meter provides synchronous digital measurements at 5 points of the sea surface of the y-axes of the wave oscillations within the limits of $\pm$5 meters in the wave frequency range to 1.5 hertz with mean square error of 4 to 5 cm; measurements of the slopes and steepnesses of the sea surface in two mutually perpendicular directions (determined by the finite difference scheme on a 1 or 2 meter base) in the wave frequency range to 0.5 hertz; the amplitudes of the acoustic echoes; the distribution of the sea wave slopes with respect to directions, and so on. The statistical characteristics of the wave action are calculated by the results of these measurements.

The discussed results are obtained when testing a wave meter near the shore in the presence of the influence of waves reflected from the shore on the overall wave picture.

The operation of the wave meter was monitored by the results of synchronous measurements of the y-axes of the wave oscillations by one of five acoustic wave recorders and the resistive (string) wave recorder designed by Kukulin installed at a distance of 0.15 meter from the irradiation spot center. Figure 1 shows the dispersion spectra of the y-axes of the wave fluctuations on a logarithmic scale for acoustic and string wave recorders (synchronous measurements). On low frequencies the spectra are identical. The "spectral noise" of the acoustic wave recorder on frequencies above 1.5 hertz determines the actual limit of the frequency resolution of the waves of a given version of the wave recorder.

The accuracy of measuring the y-axes of wave oscillations was estimated by the regression equation relating the y-axes of the wave oscillations by the readings of the resistive and acoustic wave recorders. The graph of this equation has the form of a straight line running through 0, which indicates absence of a systematic error in measuring the y-axes by an acoustic wave recorder. The mean square scattering of the readings of the acoustic wave recorder with respect to the readings of the resistive wave recorder does not exceed 4 to 5 cm, which agrees well with the theoretical estimates of the error of the acoustic wave recorder.

In Figure 2, for example, energy spectra of the waves and the slopes (on a logarithmic scale) are presented according to the data from an individual realization ($\bar{h}$=0.42 meter, τ=4 sec, V_B=3.5 m/sec).

In the laws of the decrease in high frequency sections of the spectra of the y-axes (to frequencies of 1.5 to 2 hertz) approximated by a power function $A\omega^{-n}$, the exponent for different realizations varies within the limits of -4 to -5. An analogous law of the decrease of the high frequency spectra of the slopes (considering the filtering function of the slopes measured with respect to a finite base) is characterized by the exponent from -1 and less. The variability of the spectra of the steepness from measurement to measurement is more significant.

The frequency-angular spectra were calculated by the procedure discussed in [2, 3] and providing for approximate representation of the frequency-angular spectrum in the form of its expansions in a Fourier series with respect to angles. The initial calculation data are time series of the y-axes, slopes and steepnesses of the waves in two orthogonal directions. As is known, there are other schemes for calculating the frequency-angular spectra with respect to multipoint measurements of the wave action proposed by Barber, et al. [4], but the advantages of one method of calculation or another have not been analyzed with sufficient clarity in the literature.

Figure 3 shows typical frequency-angular spectra (for three frequencies) for an individual realization (the dotted lines) calculated with respect to five coefficients of the Fourier series using time series of the y-axes and slopes of the waves. Consideration of these spectra reveals the approximate nature of the calculations of the angular distribution of the wave energy, which is the result of expansion in a series of a total of five terms, which explains both the characteristic two-lobed form of the angular distributions on low sea wave frequencies (one of the lobes is "spurious") and the low angular resolution. In the graphs in Figure 3 the solid lines indicate the angular spectra for the same realization calculated by seven terms of the expansion using the time series of the steepnesses of the sea surface. (In order to carry out the expansion in a series of nine terms, it is necessary to consider the mixed spatial derivative $\partial 2z/\partial x\partial y$, but the system of five wave recorders arranged in a "cross" does not permit this to be done.)

AS is obvious, consideration of two more terms of the expansion gives some improvement in the precision of the spectra, in particular, their directionalness is increased, the finer structure appears and also the second (spurious) lobe is diminished.

At the same time, the problem of further improvement of the angular resolution of the frequency-angular spectra remains an urgent problem which, in the given case, requires an increase in the number of wave recorders. It is also necessary to compare different methods of calculating the frequency-angular spectra; other calculation schemes can possibly give better results with a smaller number of primary measurements.

The possibilities of an acoustic wave meter are not exhausted by measuring the mentioned parameters. With respect to the amplitude characteristics of the signals reflected by the sea surface some of the characteristics of high-frequency waves can be measured in the range up to ~10 hertz. Theoretically such characteristics of the sea surface as foam and spray formations, the presence of polluting films, and so on can also be investigated. That is, the aeroacoustic method permits comprehensive studies of important characteristics of the sea surface simultaneously with the basic wave characteristics.

In order to obtain wave characteristics from a ship by an acoustic wave meter, it is necessary to solve the complex technical problem of highly accurate recording of spatial displacements of the receiving-emitting system caused by the movement and rolling of the ship and also the theoretical problem of reproducing true space-frequency characteristics of the waves.

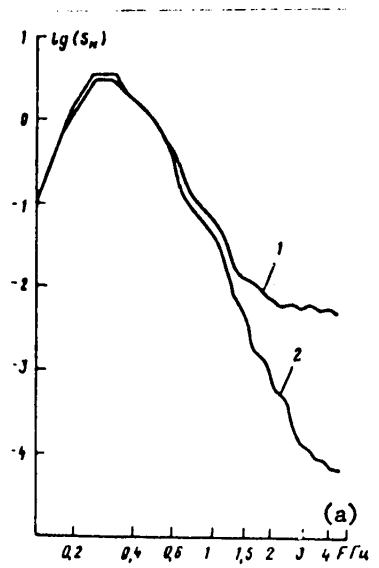

Figure 1. Normalized spectral densities of the dispersions with respect to synchronous measurements by an acoustic wave recorder (1) and a resistive wave recorder (2)

Key:

a. hertz

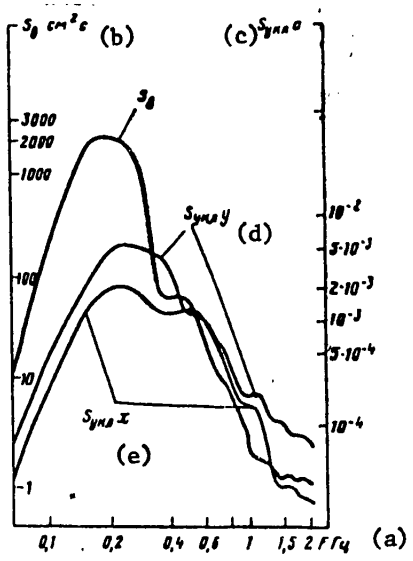

Figure 2. Spectral densities of the dispersions of the y-axes (S_B) and the slopes of the sea surface ($S_{slope}X$ and $S_{slope}Y$) for one realization

Key:

a. hertz
b. S_B, cm^2-sec
c. S_{slope}, sec
d. $S_{slope}Y$
e. $S_{slope}X$

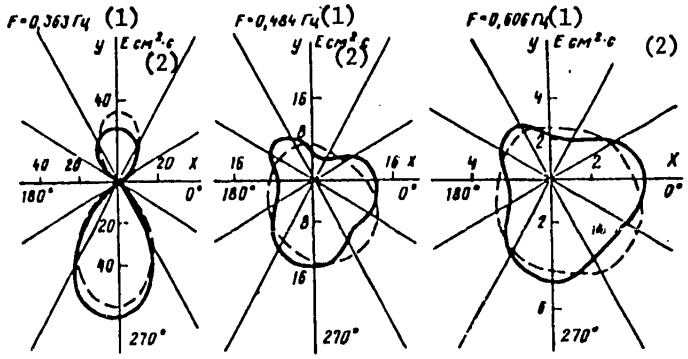

Figure 3. Angular distributions of the spectral density of the dispersions (E) on several frequencies for the realization in Figure 2. The dotted lines are the calculation by five coefficients, and the solid lines, by seven

Key:

1. hertz; 2. cm^2-sec

BIBLIOGRAPHY

1. Aleksandrov , A. P., Vayndruk, E. S., et al., "Hardware Complex for Measuring the Characteristics of the Sea Surface by the Acoustic Sounding Method," NEKONTAKTNYYE METODY IZMERENIYA OKEANOGRAFICHESKIKH PARAMETROV [Noncontact Methods of Measuring Oceanographic Parameters], Moscow, Gidrometeoizdat, 1977, pp 105-108.

2. Krylov, Yu. M., SPEKTRAL'NYYE METODY ISSLEDOVANIYA I RASCHETA VETROVYKH VOLN. [Spectral Methods of Investigation and Calculation of Wind-Driven Waves], Leningrad, Gidrometeoizdat, 1966.

3. Trapeznikov, Yu. A., "Study of the Two-Dimensional Spectral Density of a Wavy Surface at Several Points," TRUDY GOIN [Works of the State Oceanological Institute], No 122, 1974, pp 47-58.

4. Davidan, I. N., METODY RASCHETA SPEKTRA VOLN. SERIYA OKEANOLOGIYA [Methods of Calculating the Wave Spectrum. Oceanology Series], VNIIGMI, Obinsk, 1977.

10845
CSO: 8144/1010

UDC 551.463.26

INFORMATIVENESS OF SEA SURFACE AMPLITUDE SCATTERING CHARACTERISTICS DURING LOCAL IRRADIATION

Moscow NEKONTAKTNYYE METODY IZMERENIYA OKEANOGRAFICHESKIKH PARAMETROV in Russian 1981 pp 97-100

[Article by G. Yu. Narodnitskiy]

[Text] Annotation. A study is made of the possibility of obtaining information on the short wave part of the sea surface spectrum (ripple) by the amplitude characteristics of scattered signals during operation of an ultrasonic wave recorder. It is demonstrated that by the data from measuring the frequency and time correlation intervals of the amplitude fluctuations the mean square values of the y-axes and the vertical velocities of the ripple covering the irradiated section of the sea surface can be obtained, and the mean square slope of the ripple can be found by the regression dependence of the amplitude of the scattered signals on the synchronously measured slopes of large waves. Experimental data are presented from determining the characteristics of ripple obtained using the hardware complex of an aeroacoustic wave recorder.

During operation of the main part of the noncontact meters of sea wave parameters, the measurement results encompass only the long wave part of the surface spectrum (large waves) determined by the spatial resolution of the instruments. Thus, for example, reliable results of measurements taken by the ultrasonic wave recorder under standard operating conditions encompass the frequency range up to approximately 1 hertz. At the same time the information about the higher frequency part of the spectrum (ripple) is needed to study the interaction of the ocean and the atmosphere. This data can be used also for displaying the sections of the sea surface polluted by petroleum products.

The investigation performed in this paper pertains to the conditions of vertical irradiation in the centimeter or millimeter range simultaneously for only a small part of large sea waves (local irradiation) and reception of scattered signals in the return direction. These conditions are characteristic of the ultrasonic wave recorder used experimentally, but the obtained results can be used to expand the possibilities of other instruments.

The method of measuring the mean square slope of the ripple is based on using a natural measurement in time of the slopes of large waves to obtain the regression dependence of the amplitude of the scattered signals on the magnitude of the synchronously measured slopes. The halfwidth of the function on the $e^{-0.25}$ level with respect to the maximum is equal to the mean square slope of the unevennesses of the ripple within the limits of the base of the measured slopes of the large waves. Some results of these measurements are shown in Figure 1 where the regression relations are presented for the signal amplitude as a function of slopes of large waves obtained on a 2-meter base for three values of the wind velocity. Analysis of the measurement process considering the equivalent filtering function demonstrated that the obtained results correspond to the slope spectrum in the wavelength range of approximately from 5 meters to 1 or 2 centimeters. The error caused by the residual influence of larger waves does not exceed units of percentages.

Information about the y-axes and the orbital velocities of the ripple can be obtained by the data from measuring the time and frequency correlation intervals of the fluctuations of the scattered signal amplitude. For this purpose, pairs of emitted pulses are used with variable time interval between them and variable basic frequency of one of the pulses. The time correlation interval is determined by the dispersion of the vertical velocities of the surface elements [1], and the frequency correlation interval, by the dispersion of the y-axes [3]. In the case of local irradiation, these parameters pertain to ripple covering the irradiated section. Figure 2 shows some of the results of measuring the indicated parameters for various values of the wind velocity. The obtained relations as a function of wind velocity obviously are caused both by an increase in energy of the spectral components of the waves and an increase in the upper limiting frequency of the spectrum. The analysis considering the equivalent filtering function demonstrated that for the realized diameter of the irradiated section of 0.2 meter with respect to the halfpower level the presented results correspond to the surface spectrum in the frequency range of (2 to 15) hertz. The error in measuring the vertical velocities caused by the residual influence of the low-frequency components does not exceed 20%. For the process of measuring the y-axes of the ripple, the more expressed influence of the low-frequency components is characteristic.

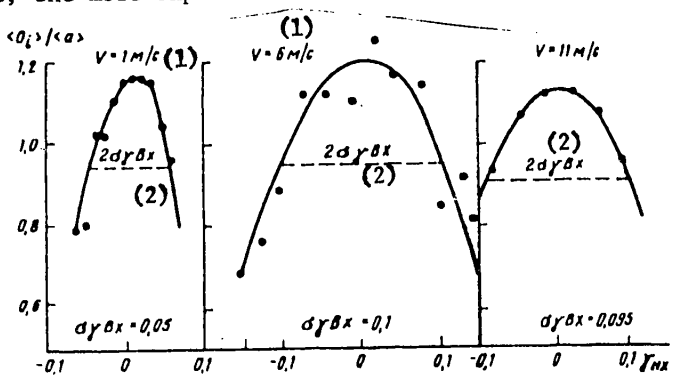

Figure 1. Regression dependence of scattered signal amplitude on slopes γ_{HX} in the x direction, σ_{γ}inp is the mean square slope of the ripple

Key:
1. m/sec
2. inp

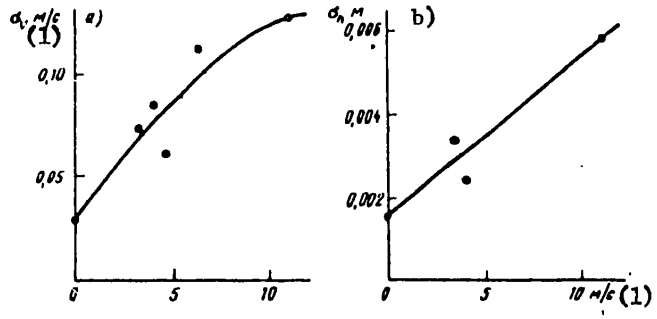

Figure 2. Mean square velocities (a) and y-axes (b) of ripple

Key:
1. m/sec

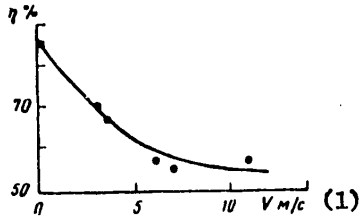

Figure 3. Amplitude variation coefficient

Key:
1. m/sec

For a rough estimate of the ripple state of the sea surface, it is possible to use a simply measured characteristic such as the amplitude variation coefficient of the scattered signals. Thus, for example, in the case of smooth swell, as a result of the departures of the reflecting region of the surface from the axis of the radiator for unfavorable slopes of the swells, very deep amplitude fluctuations are observed (an increase in the variation coefficient to 100% or more). In the presence of quite steep ripple on wind driven waves the slope of the irradiated section does not cause significant variation of the amplitude; therefore the variation coefficient differs little from its value in the absence of large waves (about 52%). In the general case the variation coefficient is determined by the ratio of the dispersions of the ripple slopes and large waves [2]. The experimental dependence of the variation coefficient on the wind velocity is presented in Figure 3.

BIBLIOGRAPHY

1. Bass, F. G. and Fuchs, I. M., RASSEYANIYE VOLN NA STATISTICHESKI NEROVNOY POVERKHNOSTI [Scattering of Waves on a Statistically Uneven Surface], Moscow, Nauka, 1972, 424 pages.

2. Narodnitskiy G. Yu., "Variation Coefficient of the Amplitude of Acoustic Waves Scattered by the Disturbed Water Surface During Local Irradiation," IZV. AN SSSR. FIZIKA ATM. I OKEANA [News of the USSR Academy of Sciences. Physics of the Atmosphere and Ocean], Vol XII, No 10, 1976, pp 1118-1119.

3. Weissman, D. E., "Two Frequency Radar Interferometry Applied to the Measurement of Ocean Wave Height," IEEE TRANS ANTENNAS AND PROPAGATION, AP-21, No 5, 1973, pp 649-656.

10845
CSO: 8144/1010

UDC 551.463.31

OPTIMAL CALIBRATION IN REMOTE SOUNDING OF OCEAN

Moscow NEKONTAKTNYYE METODY IZMERENIYA OKEANOGRAFICHESKIKH PARAMETROV in Russian 1981 pp 101-104

[Article by S. V. Dotsenko, B. A. Nelepo and L. G. Salivon]

[Text] Annotation. A study is made of the optimal method of calibration permitting use of mathematical processing of the time realization of the true field measured by an instrument with a point sensor to significantly increase the accuracy of comparing the results of remote sounding with contact measurements.

The instruments for remote sounding of the ocean average the measured physical field with respect to the resolution element, the dimensions of which are determined by the width of the radiation pattern of its sensor and remoteness of the instrument from the sea surface. In the case of rapid movement of the measuring instrument relative to the field, the field can be considered frozen, and the signal at the input to the measuring receiver has the form

$$Y_\partial = \int X(-\vec{\rho}, 0) h(\vec{\rho}) d\vec{\rho},$$

where $h(\vec{\rho})$ is the hardware function of the remote instrument.

In reality, the value measured by the remote instrument differs from Y_∂ as a result of an entire series of causes (the influence of the atmosphere and additional distorting factors), which forces calibration of the remote instrument by defined regions (test areas), the physical characteristics of which are measured with sufficient accuracy. For this purpose, it is necessary, by measuring the physical characteristics of the sea in the test area, to calculate how they would be reproduced by a remote instrument if the spurious factors were absent, that is, to form the standard value of Y_ε reproducing the value of Y_∂ with the greatest possible accuracy. The difference in scales of averaging of the compared instruments can be decreased if time averaging of the instrument readings with point sensor is used to obtain Y_ε, and a function that minimizes the mean square deviation of Y_ε from Y_∂ is selected as the weight function $U(\tau)$, which insures optimal calibration of the instrument.

It is possible to demonstrate [1,2] that for uniform, isotropic direct measurement of the field which is nonfrozen and stationary with respect to the instrument, the expression for the spectrum of the optimal correction function has the form

$$\widetilde{U}_{(1)}^{opt}(\omega)=\frac{1}{G_1(\frac{\omega\tau_c}{\rho_c})}\int G_k\left[\sqrt{|\vec{\beta}|^2+(\frac{\omega\tau_c}{\rho_c})^2}\right]\widetilde{h}^*(\vec{\beta})\,d\vec{\beta}, \tag{1}$$

Key: 1. opt

where G_1, G_k are the one-dimensional and k-dimensional spectra of the measured field; $\widetilde{h}(\vec{\beta})$ is the spectrum of the hardware function of the remote instrument; ρ_c,τ_c are the characteristic time and space scales of the field; ω is the frequency; $\vec{\beta}$ is the wave vector, and the optimal calibration error is

$$\mathcal{E}^2_{opt(1)}=\frac{\tau_c}{\rho_c}\int G_n\left(\sqrt{|\vec{\alpha}|^2+(\frac{\tau_c\omega}{\rho_c})^2}\right)\left|U_{opt(2)}(\omega)-\widetilde{h}(\vec{\alpha})\right|^2 d\vec{\alpha}\,d\omega, \tag{2}$$

Key: 1. opt; 2. opt

In order to estimate the values found, assumptions were made that the hardware function of the remote instrument has axial symmetry, and its spectrum can be represented in the form

$$\widetilde{h}(\vec{\alpha})=\left[1+\left(\frac{\kappa_x\alpha}{\alpha_{\nu-\frac{1}{2}}}\right)^2\right]^{-(\nu+\frac{1}{2})}, \tag{3}$$

where $\kappa_p=\sqrt{\pi}\Gamma(P+1/2)/\Gamma(P)$; $\Gamma(P)$ is the gamma function; $\nu=n+1/2$, $(n=1,2,3\ldots)$, R_x is the radius of the hardware function, and the k-dimensional spectra of the measured field are defined by the expression

$$G_k(\alpha)=\sigma^2\sqrt{\pi}^{-k/2}\frac{\Gamma(P+\frac{k}{2})}{\Gamma(P)}\left(\frac{\rho_c}{\alpha_P}\right)^k\frac{1}{\left[1+\left(\frac{\alpha\rho_c}{\alpha_P}\right)^2\right]^{P+k/2}}, \tag{4}$$

where k=1,2,3 and P is the parameter defining the degree of decrease in the field spectrum. Here after a number of simplifications expression (1) assumes the form

$$\widetilde{U}_{(1)}^{opt}(\omega)=\frac{2P+1}{2(P+\nu+1)}F\left\{\nu+\frac{1}{2},1;P+\nu+2,1-\left(\frac{z}{z_{rp}}\right)^2\left(\frac{\rho_c d_0}{\alpha_p}\right)^2\right\}, \tag{5}$$

Key: 1. opt

where $Z_{rp}=(\kappa_\nu-1/2)/\kappa_p$; F is the hypergeometric function, $d_0=\omega\tau_c/P_c$; $P=m+1/2$; $\nu=n+1/2$; $(m=0,1,2\ldots,\ n=1,2\ \ldots)$.

Analysis of (5) for the special case where m=0 and n is an arbitrary integer gives a quite awkward expression which can be approximated by the simpler expression

$$\tilde{U}_1(\xi)=\frac{\varkappa_n^2}{\sqrt{\varkappa_n^4+(4n+3)\varkappa_n^2\xi^2+n^2\xi^4}}, \qquad (6)$$

where $\xi=z\sqrt{1+(\omega\tau_c)^2}$ and $z=R_x/\rho_c$, from which it is possible to obtain the expression for calculating the characteristic radius of the correlation function τ_n. The family of functions $\tau_n(z)$ is presented in Figure 1.

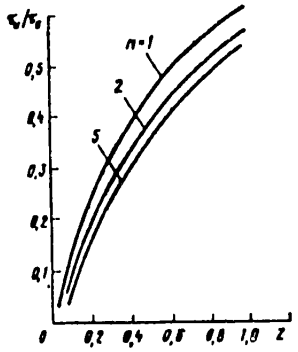

Figure 1. Family of relations for the characteristic radius of the correlation function τ_n/τ_c as a function of z for different n

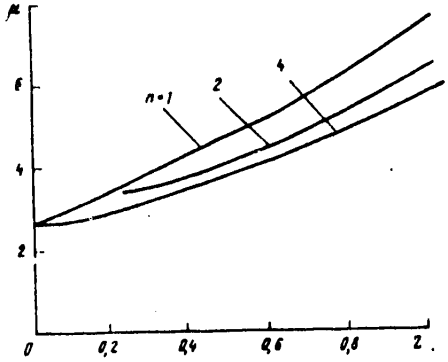

Figure 2. Gain in accuracy of the optimal calibration with respect to the unfrozen, stationary field with a field parameter P=1/2

The results of calculations of the optimal calibration error $(\varepsilon_{opt}/\sigma)^2$ as a function of z for n=1 to 4 were used to construct the graphs in Figure 2, where $\mu=(\varepsilon_1/\sigma)^2/(\varepsilon_{opt}/\sigma)^2$; $(\varepsilon_1/\sigma)^2$ is the calibration error when using a single instantaneous reading of the instrument with point sensor located at the center of the resolution element, μ is the gain in accuracy of the calibration.

As is obvious from Figure 2, the gain is found to be significant in the region of large z, in spite of the fact that, as was pointed out in [2], the investigated case is the least favorable for calibration.

BIBLIOGRAPHY

1. Dotsenko, S. V. and Salivon, L. G., "Optimal Calibration of Remote Instruments with the Application of Time Averaging," MORSKIYE GIDROFIZICHESKIYE ISSLEDOVANIYA [Marine Hydrophysical Research], No 4 (75), Sevastopol', izd. MGI AN USSR, 1976, p 92.

2. Dotsenko, S. V. and Salivon, L. G., "Method of Optimal Calibration of a Remote Instrument," TRUDY I VSESOYUZNOY KONFERENTSII. PROBLEMY NAUCHNOGO ISSLEDOVANIYA V VYSSHEY SHKOLE V OBLASTI IZUCHENIYA I OSVOYENIYA MIROVOGO OKEANA [Works of the 1st All-Union Conference. Problems of Scientific Research in the Higher School in the Field of Study and Exploitation of the World Ocean], 1977, Vladivostok.

10845
CSO: 8144/1010

UDC 551.463:31

REPRODUCTION OF AVERAGED FIELD BY SATELLITE MEASUREMENTS

Moscow NEKONTAKTNYYE METODY IZMERENIYA OKEANOGRAFICHESKIKH PARAMETROV in Russian 1981 pp 105-108

[Article by S. V. Dotsenko and A. N. Nedovesov]

[Text] Annotation. The problem of reproducing a random averaged field by the results of measuring it by a real instrument on several parallel trajectories is solved. The method is illustrated by a specific example.

In space oceanography, the problem arises of reproducing a hydrophysical field by the results of measuring it from a satellite on several trajectories. The solution of this problem is possible with the following assumptions. The remote instrument with given resolution element measures the investigated field on a series of parallel rectilinear trajectories. The element of the field resolution by the instrument sensor is determined by its hardware function $H_p(\vec{\rho}, \tau)$, and the sensor itself is inertialess. The investigated random field $X(\vec{r}; t)$ is uniform, isotropic and steady state. The remote measurement instrument moves at such high speed that the time variation of the field when obtaining the individual realization can be neglected, but this variation takes place from trajectory to trajectory. We shall consider that the instrument moves along the y-axis at different distances r_n from the oy axis after equal time intervals, and the realizations are sufficiently long that it is possible to perform the integration within infinite limits. Then the n-th realization of its output signal is written in the form [1]:

$$Y_n(y) = \iint_{-\infty}^{\infty} X[r_n - \rho_1, y - \rho_2; (n-1)T] H_p(\rho_1, \rho_2) d\rho_1 d\rho_2,$$

where r_n is the radius vector of the displacement of the n-th trajectory with respect to the origin of the coordinates, $y=v_0 t$ is the current coordinate of the trajectory of motion of the instrument, and T is the period of obtaining the realizations. We shall reproduce the field averaged (smoothed) over some region given by the weight function $H_{\text{smoothed}}(\rho_1^0, \rho_2^0)$ with coordinates of the center of averaging $(r_a, 0)$.

The estimate of the reproduced field is equal to

$$Y_a = \int_{-\infty}^{\infty} \sum_{n=1}^{N} Y_n(y) H_n(y)\, dy. \qquad (1)$$

where N is the total number of realizations, $H_n(y)$ is the weight function defining the contribution of each trajectory and the location of the field in the vicinity of the point a. The averaged field in the vicinity of the point a at the time T_a:

$$Y^{(1)}_{cra} = \iint_{-\infty}^{\infty} X(r_a - \rho_1^\circ, -\rho_2^\circ; T_a) f^{(1)}_{cra}(\rho_1^\circ, \rho_2^\circ) d\rho_1^\circ d\rho_2^\circ. \tag{2}$$

Key: 1. smoothed

Then the reproduction error is $\varepsilon = Y_a - Y_{\text{smoothed}}$. The optimalness criterion of the reproduction will be the minimalness of the mean square error.

Let us find the set $H_n(y)$ such that it minimizes the mean square error $\overline{\varepsilon^2}$. Making the transition to the spectra, we obtain

$$\overline{\varepsilon^2} = \int_{-\infty}^{\infty} A(\alpha_2) d\alpha_2 - 2\sum_{n=1}^{N} \int_{-\infty}^{\infty} A_{n,a}(\alpha_2) \tilde{H}_n(\alpha_2) d\alpha_2 + \sum_{n,k=1}^{N} \int_{-\infty}^{\infty} A_{n,k}(\alpha_2) \tilde{H}_n(\alpha_2) H_k(\alpha_2) d\alpha_2, \tag{3}$$

where

$$A(\alpha_2) = \int_{-\infty}^{\infty} S_2(\alpha_1, \alpha_2) \tilde{H}^2_{cra}(\alpha_1, \alpha_2) d\alpha_2,$$

$$A_{n,a}(\alpha_2) = \iint_{-\infty}^{\infty} S_3(\alpha_1, \alpha_2; \omega) \tilde{H}_p(\alpha_1, \alpha_2) \tilde{H}_{cra}(\alpha_1, \alpha_2) e^{j[\alpha_1(r_n - r_a) + (n-1)\eta)\omega]} d\alpha_1 d\omega$$

and

$$A_{n,k}(\alpha_2) = \iint_{-\infty}^{\infty} S_3(\alpha_1, \alpha_2; \omega) \tilde{H}^2_p(\alpha_1, \alpha_2) e^{j[\alpha_1(r_n - r_k) + \omega\tau(n-k)]} d\alpha_1 d\omega$$

characterize the statistical relation between the points of the n-th trajectory and the reproduced point of the field a and the points of the trajectories n and k (n,k=1,2, ..., N), respectively; $\tilde{H}(\vec{\alpha})$ is the frequency-amplitude spectrum of the function $H(\vec{\rho})$; $S_n(\vec{\alpha}; \omega)$ is the time-space energy spectrum of the field.

From (3) we obtain a system of linear equations for determining the spectra of the weight functions

$$\sum_{n=1}^{N} \tilde{H}_n(\alpha_2) A_{n,k}(\alpha_2) = A_{k,a}(\alpha_2), \quad k = 1, 2, \ldots, N. \tag{4}$$

The system (4) has a unique solution, for its determinant, in connection with the proposition of the uniformity and isotropicity of the field, is positively defined [2]. Substituting (4) in (3), we obtain a simpler expression for the mean square reproduction error

$$\overline{\varepsilon^2} = \int_{-\infty}^{\infty} A(\alpha_2) d\alpha_2 - \int_{-\infty}^{\infty} \sum_{n=1}^{N} A_{n,a}(\alpha_2) \tilde{H}_n(\alpha_2) d\alpha_2. \tag{5}$$

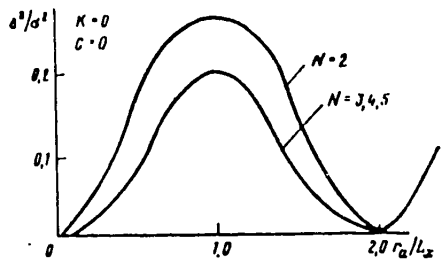

Figure 1. Error in reproducing the random field as a function of the number of trajectories

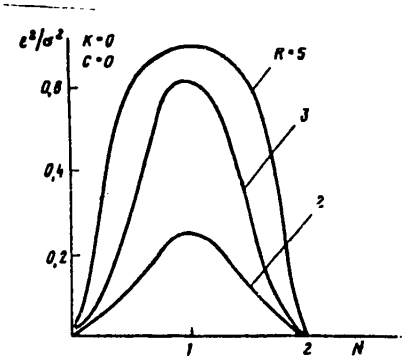

Figure 2. Error in reproducing the random field as a function of the spacing between trajectories

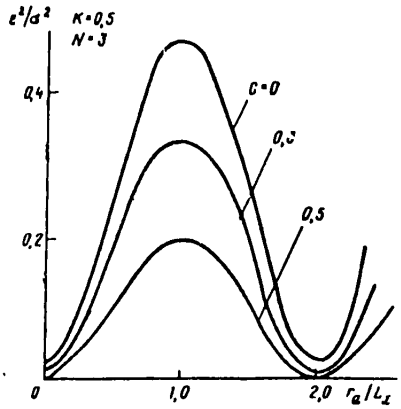

Figure 3. Error in reproducing the random field as a function of the degree of smoothing of the field for a given element of the field resolution by the instrument

Thus, the solution to the problem of optimal reproduction of the averaged hydrophysical field by the results of measuring it by a real instrument on several trajectories is given by expression (1), and expression (5) defines the error occurring in this case. It is easy to demonstrate that the error in reproducing the random field will be minimal when the field resolution element by the instrument is equal to the degree of averaging of this field.

For illustration of the described method and estimation of the field reproduction error, the problem is solved in which the spectra of the field and the bell hardware functions were taken as the mathematical model

$$S_{11}(\vec{\lambda}) = \frac{\sigma^2 L_x^n}{\pi^n} \exp\left(-\frac{L_x^2 |\vec{\alpha}|^2}{\pi}\right), \quad \tilde{H}(\vec{\alpha}) = \exp\left(-\frac{R_0^2 |\vec{\alpha}|^2}{\pi}\right),$$

where L_γ is the characteristic scale of the field, and R_0 is the radius of the resolution element.

As a result, relations were obtained for the mean square error in reproducing the random field as a function of the number of trajectories n, the distance between trajectories N normalized to the characteristic scales, and the degree of smoothing of the field C for the given resolution element of the measured field by the instrument H. C and H denote the ratio of the radii of averaging of the field and the resolution element, respectively, to the characteristic field scale. These relations are illustrated by the presented figures.

The solution of the stated problem permits selection of the optimal distances between trajectories, their number and degree of smoothing of the field for reproduction of it with minimal error.

BIBLIOGRAPHY

1. Dotsenko, S. V., TEORETICHESKIYE OSNOVY IZMERENIYA FIZICHESKIKH POLEY OKEANA [Theoretical Principles of Measuring Physical Fields of the Ocean], Leningrad, Gidrometeoizdat, 1974.

2. Gandin, L. S. and Kagan, R. L., STATISTICHESKIYE METODY INTERPRETATSII METEOROLOGICHESKIKH DANNYKH [Statistical Methods of Interpreting Meteorological Data], Leningrad, Gidrometeoizdat, 1976.

10845
CSO: 8144/1010

UDC 551.521.32:551.526.6

INFLUENCE OF CERTAIN FACTORS ON ACCURACY OF SATELLITE DETERMINATION OF UNDERLYING SURFACE TEMPERATURE

Moscow NEKONTAKTNYYE METODY IZMERENIYA OKEANOGRAFICHESKIKH PARAMETROV in Russian 1981 pp 109-112

[Article by Yu. M. Timofeyev and M. I. Trifonov]

[Text] Annotation. A radiation model of the atmosphere in the window of transparency of 8-12 microns is proposed, and its accuracy is investigated. The influence of the variations of the emissive power on the accuracy of determining T_s is investigated.

I. The problem of determining the temperature of the underlying surface T_s from an artificial earth satellite on the modern level is an extraordinarily urgent problem in connection with the increasing demands of meteorology, oceanology, climatology and a number of branches of the national economy for information on the thermal conditions of the underlying surface. It must be noted that although the problem of determining T_s is a traditional problem of satellite meteorology [1, 2], the high requirements imposed on accuracy of knowing T_s (ΔT_s=-0.1 to 1 K [3]) and not realized in practice at the present time require further investigation of it.

The expression for T_s determined from an artificial earth satellite can be written in the following general form:

$$T_s = B_{\Delta\nu}^{-1}\left\{(J_{\Delta\nu}^{\uparrow}+\delta)\tilde{P}_{\Delta\nu}[T(p), q_i(p), K_{i\Delta\nu}(p), \varepsilon_{\Delta\nu}]\right\}, \quad (1)$$

where $B_{\Delta\nu}^{-1}$ is the inverse Planck function; $\Delta\nu$ is the spectral interval of the measurement; $I_{\Delta\nu}^{\uparrow}$ is the true outgoing radiation; δ is the error in measuring the radiation; $\tilde{p}_{\Delta\nu}$ is the transfer function of the atmosphere which in the general case depends on the temperature profile T(p), the profiles of the content of absorbing components $q_i(p)$, the absorption coefficients of these components $K_{\Delta\nu_i}(p)$, the emissive power of the underlying surface $\varepsilon_{\Delta\nu}$. From expression (1) it follows that the accuracy of determining T_s depends on the following factors:

1. The accuracy of measuring the outgoing thermal emission.

2. Regions of the spectrum and optimalness of the measurement conditions.

3. The accuracy of assignment of the transfer function of the atmosphere which, in turn, is determined by the accuracy of excluding the influence of clouds, the quality of the used radiation model, the quantity and quality of the a priori or independent additional information about the physical state of the atmosphere and the accuracy of knowing the emissive power, and so on.

An analysis of the influence of the series of above-enumerated factors on the accuracy of determining T_s was performed in a large number of papers (see, for example, the monographs [1, 2]). In this article information is presented on the accuracy of the proposed radiation model of the atmosphere in the window transparency of 8-12 microns and the influence of variations of the emissive power on the accuracy of determining T_s.

II. In the radiation model that we used, the absorption caused by water vapor, ozone and carbon dioxide is considered. The transmission function of the atmosphere in the window transparency of 8-12 microns can be described with high accuracy in the following form:

$$P_{\Delta\nu} = P^{E}_{\Delta\nu} \; P^{P}_{\Delta\nu} \; P^{L}_{\Delta\nu}, \qquad (2)$$

where $P^{E}_{\Delta\nu}$ and $P^{P}_{\Delta\nu}$ are defined by various types of continuous water vapor absorption [4], and $P^{L}_{\Delta\nu}$ is defined by the absorption in the spectral lines of various gases. When calculating $P^{L}_{\Delta\nu}$ we used a statistical model of absorption, the parameters of which were calculated on the basis of the data of [5]. The use of this model is justified by the smallness of the contribution to the absorption of the H_2O and CO_2 lines and good approximation of the O_3 absorption by this model [6].

III. The quality of the radiation model used to a significant degree determines the accuracy of giving the transfer function $P_{\Delta\nu}$ and, consequently, the errors in defining T_s. In particular, our estimates demonstrated that in a wide range of states of the atmosphere, in order to determine T_s with an error of ~1K it is necessary to know the transmission functions with an accuracy of 2 to 4%. Accordingly, the problem of checking the adequacy of the proposed radiation model acquires special significance. This checking was done in our paper on the basis of comparing the experimental $P^{exp}_{\Delta\nu}$ and calculated $P^{calc}_{\Delta\nu}$ spectra of the transparency of the atmosphere in the range of 770 to 1250 cm^{-1}. (The experimental data accompanied by the corresponding radio sounding data were provided to us by A. M. Brounshteyn (Main Geophysical Observatory)).

In the figure cases of comparison of $P^{exp}_{\Delta\nu}$ and $P^{calc}_{\Delta\nu}$ are presented. An analysis of the comparison data permits the following conclusions to be drawn:

1. In the greater part of the investigated spectral range the radiation model used describes the results of the observations within the limits of error of the measurements (~5 to 7%).

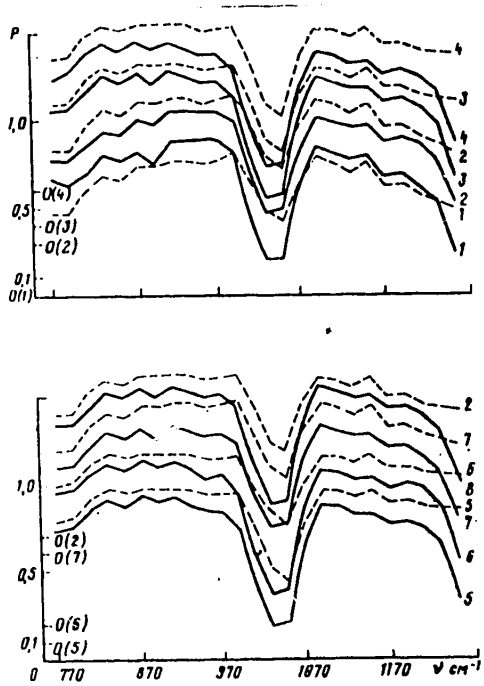

Comparison of the calculated (dotted line) and experimental (solid line) transmission functions (O(i) is the origin of the coordinates for the i-th spectrum)

2. The divergences between the experiment and the calculation exceeding the experimental errors are observed in the range of 1160-1250 cm^{-1}, where the CH_4 and N_2O absorption is not considered in the model, and in the region of the O_3 absorption band 9.6 microns, which is connected primarily with absence of data on the actual ozone content in the atmosphere.

Thus, it is possible to draw the preliminary conclusion that the proposed radiation model agrees well with the variations in transparency of the atmosphere.

3. When interpreting the satellite measurements to obtain information about T_s usually it is proposed that the emissive power is equal to 1. In reality, noticeable variations of $\varepsilon_{\Delta\nu}$ are observed even for the water surface. Inexact knowledge of the emissive power leads to errors in determining T_s. Calculations of the outgoing radiation for various models of the atmosphere and different values of $\varepsilon_{\Delta\nu}$ demonstrated that the errors in $\Delta\varepsilon_{\Delta\nu}=0.01$ lead to errors in $\Delta T_s \approx 0.6$ to 0.7 K. The presented figures illustrate the importance of knowing the actual values of the emissive power of natural underlying surfaces.

BIBLIOGRAPHY

1. Kondrat'yev, K. Ya. and Timofeyev, Yu. M., TERMICHESKOYE ZONDIROVANIYE ATMOSFERY SO SPUTNIKOV [Thermal Sounding of the Atmosphere from Satellites], Leningrad, Gidrometeoizdat, 1970, 410 pages.

2. Malkevich, M. S., OPTICHESKIYE ISSLEDOVANIYA ATMOSFERY SO SPUTNIKOV [Optical Studies of the Atmosphere from Satellites], Moscow, Nauka, 1973.

3. Ivanov, G. S., "Basic Requirements on Mass Oceanographic Information," NEKONTAKTNYYE METODY IZMERENIYA OKEANOGRAFICHESKIKH PARAMETROV [Noncontact Methods of Measuring Oceanographic Parameters], Leningrad, Gidrometeoizdat, 1977, pp 4-10.

4. Roberts, R. E., Selby, J. E. A. and Biberman, L. M., "Infrared Continuum Absorption by Atmospheric Water Vapor in the 8-13 μ Window," APPL. OPT., Vol 15, No 9, 1976, pp 2085-2090.

5. McClatchey, R. A., et al., "AFCRL Atmospheric Absorption Line Parameters Compilation," ENV. RES. PAPER, 434, 1973.

6. Goldman, A. and Kyle, T. G., "A Comparison Between Statistical Model and Line by Line Calculation with Application to the 9.6 μ Ozone and 2.7 μ Water Vapor Bands," APPL. OPT., Vol 17, No 6, 1968, pp 1167-1177.

10845
CSO: 8144/1010

UDX 551.466.326

REPRODUCTION OF SEA WAVE SPECTRA BY MEASUREMENTS BY MOVING SENSORS

Moscow NEKONTAKTNYYE METODY IZMERENIYA OKEANOGRAFICHESKIKH PARAMETROV in Russian 1981 pp 113-116

[Article by A. V. Kats and I . S. Spevak]

[Text] Annotation. A theoretical study is made of the problem of determining the two-dimensional spectra of sea waves undistorted by movement of the sensor system. The relation of the frequency-angular spectra in a moving and stationary coordinate system is established, and the conditions of unique reproduction are analyzed. Explicit analytical expressions of the two-dimensional spectrum in terms of the measurement data of a small number of sensors were obtained in limiting cases of a narrow angular spectrum and low velocity.

For measurements of sea waves by a moving sensor the measured value, for example, the rise of the surface $\zeta(\vec{r},t)$ contains information both about the wave field itself and movement of the sensor. An important problem having great applied significance is the problem of reproduction by the data of such measurements of the true wave spectrum. In the model case of one-dimensional waves, this problem was investigated in [1]. In the present paper a study is made of the case of two-dimensional waves which is of interest for full-scale measurements.

The statistically uniform and steady state rise field is completely characterized by the space-frequency spectrum [2]

$$X(\vec{k},\omega) = (2\pi)^{-3}\int d\vec{r}dt\ exp(i\omega t - i\vec{k}\vec{r})Z(\vec{r},t), \quad (1)$$

where $Z(\vec{r},t)$ is the correlation function. The spectrum $X_u(\vec{k},\omega)$ measured in the coordinate system moving with the velocity $\vec{U}$ is related to $X(\vec{k},\omega)$ by the doppler frequency transformation

$$X_u(\vec{k},\omega) = X(\vec{k},\ \omega + \vec{k}\vec{U}). \quad (2)$$

For the wave field with dispersion law $\omega=\omega_k(\omega_k=\sqrt{kg})$ the following representation occurs

$$X(\vec{k},\omega) = \sum_{p=\pm 1} X(p\vec{k})\,\delta(\omega - p\omega_k), \quad (3)$$

that is, the total information about the statistical characteristics of the waves is contained in the function $Z(\vec{k})$. In particular, the spatial spectrum is equal to

$$\Psi(\vec{r}) = \int_{-\infty}^{\infty} d\omega\, \chi(\vec{r},\omega) = \chi(\vec{r}) + \chi(-\vec{r}). \qquad (4)$$

In the majority of experiments, the frequency spectrum is measured

$$\Phi(\omega) = \int d\vec{k}\, \chi(\vec{k},\omega) \qquad (5)$$

or the frequency-angular spectrum

$$E(\omega,\theta) = \int_{0}^{\infty} dk\, k\, \chi(\vec{k},\omega). \qquad (6)$$

The relations (2), (3), (6) make it possible to find the relation of the frequency-angular spectra in the moving and stationary coordinate systems

$$E_u(\omega,\theta) = \eta(-U_k) \sum_{i} E(\omega_i', \theta + \tfrac{1-\rho}{2}\pi) \Big/ \Big|1 + \rho\, \frac{\omega_i'}{2\Omega}\Big| + \\ + \eta(\Omega-\omega)\,\eta(U_k) \sum_{i} E(\omega_i', \theta) \Big/ \Big|1 - \frac{\omega_i'}{2\Omega}\Big|, \quad \omega > 0. \qquad (7)$$

Here $\omega_i' = \rho g/2U_k + \sigma\sqrt{g^2/4U_k^2 - g\omega/U_k}$ are the roots of the dispersion equation in the moving coordinate system, $\sigma = \pm 1$, $\Omega = g/4|U_k|$, $U_k = \vec{k}\vec{U}/k$, $\eta(x)$ is the Heviside function. The spectrum $E_u(\omega,\theta)$ is defined by the spectrum $E(\omega', \theta')$ at several points, which is caused by nonmonotonicity of the dependence of the doppler shifted frequency $\omega_k^u = |\omega_k - \vec{k}\vec{U}|$ on the wave vector for a following sea ($\vec{k}\vec{U} > 0$, $\omega > 0$) (Figure 1). Therefore the unique reproduction of the undistorted spectrum $E(\omega', \theta')$ is possible only in the absence of spectral components of the waves corresponding to nonmonotonic sections of the dispersion curve.

In particular, if the following sea does not exist in the spectrum (Figure 2), then from (7) we obtain

$$E(\omega,\theta) = \left(1 + \frac{\omega}{2\Omega}\right) E_u\left(\omega + \frac{\omega^2}{4\Omega}, \theta\right), \quad \omega > 0, \; U_k < 0. \qquad (8)$$

For uniform wave action hence we have

$$\Phi(\omega) = \left(1 + \frac{\omega}{2\Omega_0}\right) \Phi_u\left(\omega + \frac{\omega^2}{4\Omega_0}\right), \quad \Omega_0 = \frac{g}{4U|\cos\varphi|}. \qquad (9)$$

The reproduction of the frequency spectrum of one-dimensional waves was considered earlier in [1], but in the presented frequency spectrum relation there is an error--the result differs from (9) by the absence of the factor $(1+\omega/2\Omega_0)$. The presence of the factor $(1+\omega/2\Omega_0)$ in (9) insures satisfaction of the equality $\int d\omega \phi(\omega) = \int d\omega' \phi_u(\omega')$, which is a corollary of the identity $Z(0,0) = Z_u(0,0)$.

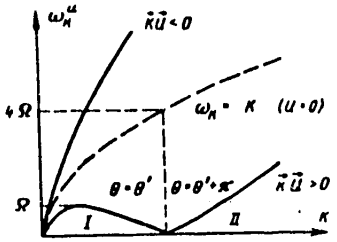

Figure 1. Wave dispersion law. Section II corresponds to waves that change direction of propagation on transition to a moving coordinate system

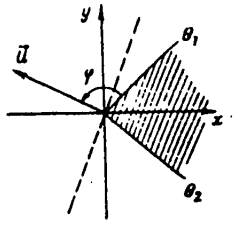

Figure 2. Example of the wave spectrum permitting unique reproduction

Thus, if the frequency-angular spectrum in a moving coordinate system is known, the problem of reproduction of the true wave spectrum in the absence of following seas is solved by expression (8). However, in practice such complete information about waves is absent (see, for example [3]). The derivatives of the correlation function are determined by the measurements at several points

$$Z^{(n)}(t) = \left(\frac{\partial}{\partial x} + i\frac{\partial}{\partial y}\right)^n Z(\bar{r}, t)\Big|_{r=0}, \tag{10}$$

in terms of which the coefficients $C_n(\omega)$ of the expansion of the frequency-angular spectrum in a Fourier series are expressed [3]:

$$E(\omega,\theta) = \sum_{-\infty}^{\infty} C_n(\omega)\, e^{-in\theta}, \quad C_n(\omega) = \frac{1}{2\pi i^n}\left(\frac{g}{\omega^2}\right)^n Z^{(n)}(\omega),$$
$$Z^{(n)}(\omega) = \frac{1}{2\pi}\int dt\, e^{i\omega t} Z^{(n)}(t). \tag{11}$$

If the measuring system moves, then the functions constructed analogously

$$\mathcal{E}_n(\omega) = \frac{1}{2\pi i^n}\left(\frac{g}{\omega^2}\right)^n Z_u^{(n)}(\omega) \tag{12}$$

are not equal to the coefficients $C_n^u(\omega)$. However, using expressions (1), (2), (6), (11), it is possible to express the experimental data of $\varepsilon_n(\omega)$ in terms of the desired coefficients $C_n(\omega)$. The complex system of linear integral equations obtained in this way with respect to $C_n(\omega)$ cannot be solved in general form.

Let us present the solution in the limiting cases.

a) Small velocities: $\omega U/g \ll 1$

$$C_n(\omega) = \mathcal{E}_n(\omega) - \frac{U}{2g}\hat{L}_1\left[e^{i\varphi}\mathcal{E}_{n+1}(\omega) + e^{-i\varphi}\mathcal{E}_{n-1}(\omega)\right] +$$
$$+ \frac{1}{2}\left(\frac{U}{2g}\right)^2\hat{L}_2\left[e^{i2\varphi}\mathcal{E}_{n+2}(\omega) - e^{-i2\varphi}\mathcal{E}_{n-2}(\omega)\right] +$$
$$+ \left(\frac{U}{2g}\right)^3\hat{L}_3\left[\mathcal{E}_n(\omega) + e^{-i2\varphi}\mathcal{E}_{n-2}(\omega)\right] + O\left[\left(\frac{\omega U}{g}\right)^4\right], \tag{13}$$
$$\hat{L}_1 = \frac{1}{\omega^{2n}}\frac{\partial}{\partial\omega}\omega^{2n+2}, \quad \hat{L}_2 = \frac{1}{\omega^{2n}}\frac{\partial^2}{\partial\omega^2}\omega^{2n+4}, \quad \hat{L}_3 = \frac{1}{\omega^{2n}}\frac{\partial}{\partial\omega}\omega^4\frac{\partial}{\partial\omega}\omega^{2n}.$$

For large velocities $\omega U/g>>1$ (large frequencies), using the expansion with respect to U^{-1} it is possible to reproduce the spatial spectrum $\Psi(\vec{k})$. The results obtained for this case will not be presented because of insufficient space.

b) A narrow angular spectrum: $E(\omega,\theta)\neq 0$ for $|\theta|<\Delta\theta<<1$.

For countermotion, the system of integral equations reduces to differential with respect to moments

$$M_n(\omega) = \frac{1}{2\pi}\oint d\theta\, \theta^n E(\omega,\theta) \sim (\Delta\theta)^n, \qquad (14)$$

which permits determination of the first ℓ moments with respect to ℓ known functions $\varepsilon_n(\omega)$ with an absolute error $o((\Delta\theta)^{\ell+1})$. In particular, the zero moment $M_0(\omega)=(2\pi)^{-1}\phi(\omega)$ is

$$M_0(\omega) = \frac{(1+4/2\Omega_0)}{\ell}\sum_0^{\ell-1} Re\left\{\left(1+\frac{\omega}{4\Omega_0}\right)\varepsilon_n\left(\omega+\frac{\omega^2}{4\Omega_0}\right)\right\} + o(\Delta\theta). \qquad (15)$$

The remaining relations have more awkward form.

BIBLIOGRAPHY

1. Zaslavskiy, M. M., Kestner, A. P. and Filippov, I. A., TROPEKS-72 [TROPEX-72], Leningrad, Gidrometeoizdat, 1974, 641 pages.

2. Phillips O., DINAMIKA VERKHNEGO SLOYA OKEANA [Dynamics of the Upper Layer of the Ocean], Moscow, Mir, 1969.

3. Krylov, Yu. M., SPEKTRAL'NYYE METODY ISSLEDOVANIYA I RASCHETA VETROVYKH VOLN. [Spectral Methods of Investigation and Calculation of Wind-Driven Waves], Leningrad, Gidrometeoizdat, 1966.

10845
CSO: 8144/1010

UDC 53.085.4:681.3

PROBLEMS OF COMPRESSING OCEANOGRAPHIC INFORMATION DURING REMOTE MEASUREMENTS

Moscow NEKONTAKTNYYE METODY IZMERENIYA OKEANOGRAFICHESKIKH PARAMETROV in Russian
1981 pp 117-119

[Article by N. N. Volynskaya and I. F. Kon'kov]

[Text] Annotation. A discussion is presented of ways to compress information based on adaptive digitalization of the information received from one sensor, and the possibility of reducing the mutual redundancy of the information received from several sensors of oceanographic parameters.

The problem of compressing oceanographic information has arisen recently in connection with development of methods and means of remote measurement of ocean parameters. Since almost all remote measurement means involve the application of previously known methods for oceanographic purposes, their time-space resolution, dynamic range and accuracy are not matched to the variability of the ocean characteristic. This explains the high degree of informative redundancy of remote meters. In addition, oceanographic parameters, as a rule, are nonsteady; therefore the sensor characteristics are determined beginning with the requirements of sufficient resolution in the highest frequency regions of the spectra of the investigated processes, as a result of which additional redundancy of the received information occurs. On combining informatively redundant means into a unified system, the total volume of information exceeds the possibilities of real devices for processing and recording measurement results. Thus, for example, the volume of information received on a 10-hour aircraft flight with continuous operation of all of the sensors is about 1200 megabits. For satellite systems to study the oceanographic parameters, the problem of information compression is still more urgent. At the present time there are no other recommendations with respect to processing and storing information except recommendations to average the oceanographic information with respect to areas, as a result of which the meaningfulness of using systems with high resolution is lost.

At the present time information compression procedures have been developed which consist in adaptive-time digitalization of the investigated process [1]. As applied to the study of ocean characteristics it is possible to propose more specialized methods. Since the number of types of sensors used exceeds the number of independent oceanographic parameters, the output signals of a number of sensors are in a statistical and possibly functional relationship to each other. This relation can be detected and considered both by investigating the properties of the current

information itself and by a priori determination of the contribution of each independent oceanographic parameter to the signal of each sensor. The first path leads to factorization of the space of the sensor signals, that is, compression of the information consists in conversion of the signals of n sensors to values of k factors for n>k. A second means provides for taking the physical parameters of the ocean as the primary parameters, conversion of the results to primary parameters and recording them. The difference in the second path consists in the fact that the factors acquire physical meaning.

In conclusion, let us present preliminary results from estimating the effectiveness of information compression in the example of processing the recordings of an infrared radiometer installed on the Il-14 aircraft. The measurements were performed in the summer and fall of 1977 in the Caspian Sea, and also in the winter of 1977 in the Baltic Sea. The total length of the fixed profile of the surface temperature was 3000 km, which corresponds to 832 minutes of flight time. Digitalization was carried out under the condition of the possibility of reproducing the temperature profile with an error not exceeding 2.5 σ (the mean square value of the fluctuation error of the initial realization). A study was made of three types of approximations: a stepped broken line with fixed quantization levels, a stepped broken line with adaptive levels and a broken line with adaptive values of the gradient. The total number of readings was found to be equal to 260, 181 and 152 respectively. In the handbook [2] it is recommended that a digitalization interval be selected which does not exceed 3 to 5 minutes. If we take an interval equal to 1 minute, the effectiveness of the information compression will be, in accordance with the adopted form of the approximation, 3.2, 4.6 and 5.4 times.

In the figure we see the distribution of the lengths of the sections of the realization approximated by a stepped broken line. The distribution approximately follows Poisson's law. From the distribution it is obvious that for a nonadaptive sample with an interval of one minute about 20% of the fixed nonuniformities are lost, that is, the information loss is significant.

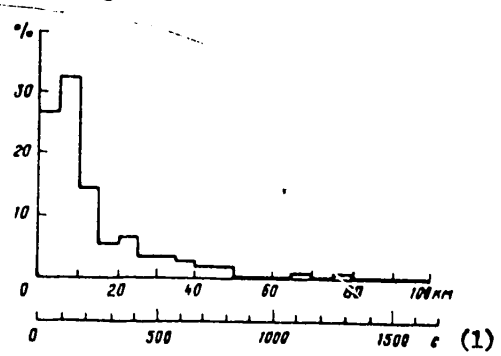

Distribution of lengths of the sections of the realization

Key:

1. seconds

The recommended preliminary processing of the information must precede recording it on the technical carrier. The requirements on the system following from the adopted information compression algorithms must be considered when developing it.

BIBLIOGRAPHY

1. Avdeyev, B. Ya. and Antonyuk,Ye. M., "Reduction of Redundant Information in Information Measuring Systems," IZVESTIYA VUZOV SSSR, PRIBOROSTROYENIYE [News of the Institutions of Higher Learning of the USSR, Instrument Making], Vol II, No 4, 1969.

2. RUKOVODSTVO PO PRIMENENIYU AEROMETODOV V OKEANOGRAFII [Handbook on the Application of Aerial Methods in Oceanography], Part II, Leningrad, Gidrometeoizdat, 1971.

10845
CSO: 8144/1010

- END -